UNIVERSITÀ DEGLI STUDI DI MILANO

Corso di dottorato
Medicina Traslazionale

Dipartimento di Scienze Biomediche per la Salute

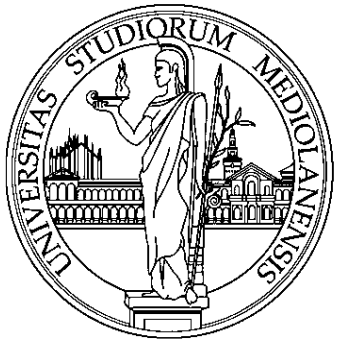

Lipid-based approaches to optimize the effectiveness of innovative drug modulators in Cystic Fibrosis

BIO/10

DOTTORANDA
Dorina DOBI
Matricola: R12988

TUTOR: Prof. Massimo AURELI

COORDINATORE DEL DOTTORATO: Prof.ssa Chiarella SFORZA

Anno academico: 2022-2023

INDEX

SUMMARY

Cystic Fibrosis (CF), a life-threatening hereditary disease prevalent among Caucasians, results from mutations in the Cystic Fibrosis Transmembrane Conductance Regulator (CFTR) gene. This gene encodes a chloride-conducting transmembrane channel crucial for ion transport across epithelial cells. CFTR mutations lead to impaired expression and function of the channel, causing disrupted chloride ion transport in secretory epithelia. Severe manifestations affect many organs, primarily the respiratory system, with impaired mucociliary clearance and airway surface liquid dehydration, leading to recurrent infections and high morbidity. The most common mutation, the deletion of phenylalanine at position 508 (F508del), induces misfolding and retention of CFTR in the endoplasmic reticulum, causing premature degradation. In airway epithelial cells, CFTR associates with proteins in a macromolecular complex, and its channel activity and surface expression are regulated by local signaling and recycling through endosomal compartments. The CFTR interactome also includes lipids, such as cholesterol and sphingolipids, that play a significant role in stabilizing CFTR within the cell membrane, particularly in specialized regions known as lipid rafts. In fact, the ganglioside GM1 is an important bioactive sphingolipid that has been reported to play a crucial role in the control of several plasma membrane (PM) proteins and its correlation with CFTR prompts speculations about its possible role in the CFTR interactome. Despite therapeutic improvements that extended CF patients' life expectancy, a cure remains elusive. Promising strategies involve CFTR-modulators, such as correctors, enhancing CFTR biosynthesis and trafficking, and potentiators, ameliorating mutated channel function. Treatment of patients having F508del mutation requires a combination of correctors and potentiators. Indeed, recent advancements in therapy encompass the triple combination Kaftrio (comprising two correctors, VX-661, VX-445, and a potentiator, VX-770) as a pharmacological intervention for CF patients who have at least one F508del mutation in the CFTR gene.

In my PhD project, I explored the impact of Kaftrio on the lipid composition of bronchial epithelial cells expressing WT and F508del-CFTR. I found that it induced significant changes reducing LacCer levels and increasing the content of GM1 and GD1a, respectively. The modifications were attributed to the effect of Kaftrio on the activity of some enzymes related to sphingolipid metabolism, specially the GM3 synthase and sialidase. Additionally, the administration of GM1, previously noted for improving the rescue of F508del-CFTR with Orkambi (consisting of the corrector VX-809 and potentiator VX-770), has also shown effectiveness with Kaftrio, mitigating the side effect of VX-770 on the stability of F508del-CFTR rescued at the cell surface by the correctors. This additive effect of GM1 to Kaftrio was maintained also in the presence of *Pseudomonas Aeruginosa* infection. On the other hand, I demonstrated that Kaftrio induces a further decrease of already reduced levels of cholesterol in F508del-CFTR mutated cells. However, exogenously administering cholesterol, in

particular with low-density-lipoprotein, I observed a cumulative effect of this lipid to the triple drug combination on CFTR correction at the PM.

Understanding the CFTR interactome, including its interactions with lipids, is important for unraveling the molecular mechanisms of cystic fibrosis and may provide insights into possible therapeutic strategies given the ongoing challenge of developing new correctors and potentiators. These findings highlight the potential of exogenous GM1 and cholesterol administration in restoring plasma membrane properties conducive to CFTR correction, suggesting novel therapeutic approaches to enhance the effectiveness of CFTR modulators in the treatment of the disease.

INTRODUCTION

Cystic Fibrosis

Cystic fibrosis (CF) is the most common inherited, life-limiting disorder in Caucasian population, affecting approximately 1 in 2500-3500 newborns. It is an autosomal recessive disease, caused by mutations in a gene which encodes for a transmembrane channel called cystic fibrosis Transmembrane Conductance Regulator (CFTR). CFTR functions mainly as a chloride-ion channel expressed across the apical membrane of epithelial cells of different organs. In CF, mutations in the CFTR gene lead to reduced expression of the functional CFTR channels resulting in an impaired chloride ion transport of secretory epithelia. Although CF is considered a multi-system disease, influencing several areas of the body, for example airway, intestines, pancreas, kidney, and sex organs, the most severe manifestations occur in the respiratory system [1]. The defective chloride and bicarbonate secretion, together with enhanced sodium absorption and mucus secretion, cause insufficient osmotic pressure, increased absorption of water followed by dehydration of the airway surface liquid, and diminished mucociliary clearance. Consequently, mucus accumulates on the bronchial surface of epithelial cells promoting bacterial infections, inflammation, and impairment of lung function, as forced expiratory volume in 1 second (FEV1) in CF patients is below 2,5 l (normal range is between 2,5-4,5 l). In CF the main cause of morbidity and mortality is due to respiratory failure and pulmonary insufficiency [2].

Despite the major improvements in the therapy of cystic fibrosis patients, which have extended progressively life expectancy up to 50 years in developed countries, CF remains a major and challenging health problem [3].

CFTR genetics

The first genetic analysis for cystic fibrosis dates back to 1946 when a recessive mutation was first proposed as the cause of the disease, however, genetic linkage analysis for disease gene identification was not broadly widespread until the early 1980s. In fact, early CF linkage and association studies were conducted with polymorphic biochemical markers, like immunoglobulins, protein markers and serum enzyme markers for genetic mapping and the gene responsible for the onset of CF was identified in 1989 by positional cloning [4,5]. The number of sequence variants identified in the CFTR gene has now exceeded 2100, although less than 200 have been definitively proven to cause the disease.

Belonging to the long arm of chromosome 7 (7q31.3) and composed by 27 exons, the full-length human CFTR gene consists of a 6129-base pair transcript, that encodes for a 1480-aa protein [4,6]. The total size of the CFTR transcription unit is ~216.7 kb. The predominant CFTR transcription start site is as described in the original study by Rommens et al. [7], saying that CFTR transcription mechanisms start from the same site, from the key promoter. However, there are also mechanisms of alternative splicing that lead to the omission of certain exons. Some of these alternatively spliced variants can give rise to a truncated CFTR protein with partial functionality [4,8].

Regarding the expression of CFTR, it was deeply analyzed both in humans and mice [6]. Of primary importance, CFTR mRNA is constitutively expressed in the epithelia of the airway, sweat glands for example in the pancreatic duct epithelium, and gastrointestinal tract starting from early development, and it is maintained for the adult life [9]. However, the gene is also expressed in a wide range of other cell types, such as in hypothalamic neurons, mucin secretory cells, gallbladder epithelia and Brunner glands. Measurable levels of CFTR were detected in female and male reproductive tissues and organs as well, like cervix, endometrium, and ovary, or epididymis and testis. Low and intermediate levels of CFTR transcripts can also be found in the kidney, thyroid, and salivary glands [10]. The majority of these sites of CFTR expression in the fetus are similar to those seen in adult tissues, with the exception of the respiratory system. Although high levels of CFTR expression are found in the epithelium of the airways in the fetal lung, epithelia of the lung contain relatively little CFTR mRNA in the adults [9, 11]. On the contrary, CFTR expression in the submucosal gland becomes apparent only after birth, making it undetectable in the fetus. In adult respiratory tissues, CFTR is primarily expressed in the serous submucosal gland, emphasizing its crucial role in regulating mucus production and fluid balance within the airways [11, 12].

The mechanisms controlling the complex expression pattern of CFTR are not completely understood. Although the promoter plays a crucial role in the basal expression of CFTR by binding to transcription factors, it alone cannot explain the tissue-specific regulation of its expression. Indeed, there are distal cis or trans-acting regulatory elements which are critical regulators of this process. The CFTR promoter is a housekeeping-type promoter; it is rich in CpG, without TATA box, and possesses several putative Sp1 (specificity protein 1) and putative AP-1 (activator protein 1) binding sites, for different transcription factors [13,14]. In addition, expression of CFTR appears to be dependent on cellular oxygenation since it exhibits transcriptional repression during hypoxia, and it is regulated by hormonal stimuli both in males and females. Also, several enhancers were characterized in the CFTR locus that help transcription, for example the intron 1 enhancer is specific to the intestine and genital duct [13].

CFTR structure

CFTR, an integral membrane protein functioning as a phosphorylation- and nucleotide- regulated conductance chloride channel, belongs to the family of ABC (ATP-binding cassette) transporters [15]. It has the typical ABC transporter structure composed of two membrane spanning domains (MSDs), each containing six transmembrane segments (TM1-6 and 7-12), four intracellular linkers (ICL1-ICL4), two nucleotide binding domains (NBDs), and a regulatory domain (RD), as well as long amino-terminal and carboxy-terminal extensions of about 80 and 30 residues in length [15,16].

In certain human ABC transporters, including CFTR, both MSDs and both NBDs are fused within a single polypeptide chain, which spans at least 1100 amino acids in length, resulting in an effectively heterodimeric functional organization. Whereas, the regulatory domain is approximately 240 residues in length and inserted between NBD1 and MSD2. MSDs are composed of six transmembrane α-helices, forming the channel pore for ions transport. Instead, NBD1 and NBD2 gate the chloride flow across the channel through cycles of ATP binding and hydrolysis. NBD1 has an extra 35-residue insertion, and NBD2 has an 80-residue extension at its end. These additional peptides may regulate CFTR channel interaction with other cellular molecules. The four intra-cellular loops are predicted to interact and transduce information between MSDs and NBDs. Regarding the regulatory domain, it plays a central role in mediating the activation of CFTR by protein kinase A (PKA) regulation. It is characterized by a series of phosphorylation sites (12 serine and 8 threonine) and is believed to act as an integrator of PKA signaling and also signaling from some other physiological systems [17, 18].

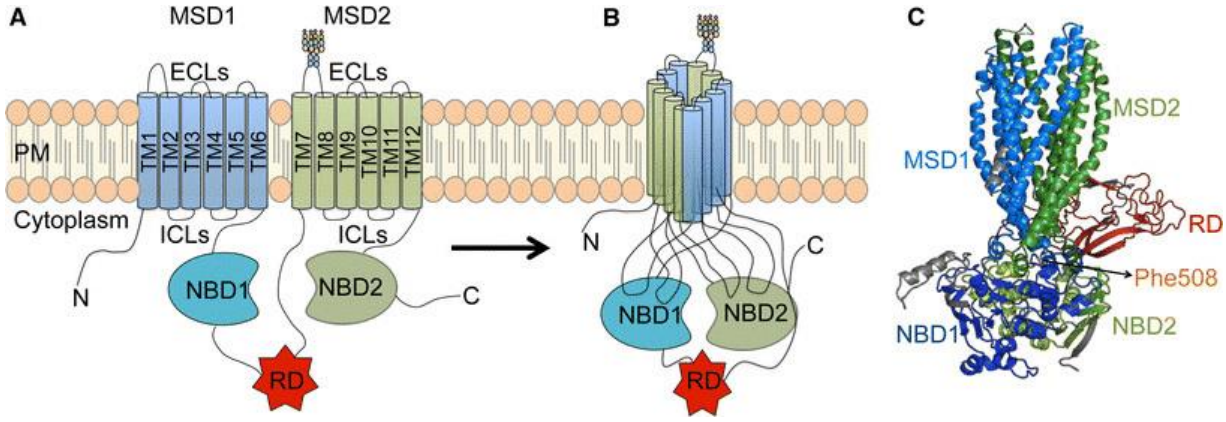

Figure 1. CFTR protein structure.

A) CFTR protein composed of five domains, arranged from N- to C-terminus: MSD1-NBD1-R-MSD2-NBD2; two membrane spanning domains (MSD1, MSD2) containing six-six transmembrane segments (TM1-12), two nucleotide binding domains (NBD1, NBD2), four intracellular linkers (ICL1-ICL4), regulatory domain (RD). B) Five domains packed together to form the channel pore. C) structural model for CFTR. Figure from [19].

In contrast to the vast majority of members of the ABC family that function as ATP-dependent active transporters, the main function of CFTR is to regulate a passive flux of anions, mainly chloride and bicarbonate, throughout the plasma membrane (PM) [20]. Indeed, CFTR is positioned on the apical surface of epithelial cells and serves as a pivotal element in a macromolecular signaling complex that includes sodium and potassium channels, anion exchangers, transporters, as well as other regulator proteins and molecules. As other chloride channels, CFTR plays a crucial role in the regulation of the secretion of fluids and electrolytes across the epithelia. Upon activation, it allows chloride (Cl^-) to exit passively from the cells [21]. Furthermore, CFTR has the capability to transport bicarbonate (HCO^-_3), with HCO^-_3 transport being facilitated through a coupled Cl^--dependent process [22, 23].

CFTR in the PM is present in three different possible status; open, closed, and open-ready. The open-ready conformation does not permit chloride flux; nevertheless, it is poised for a rapid transition into the open state in response to specific stimuli. CFTR activation by the cAMP pathway is well established in the literature. Activation of the channel depends on PKA-dependent phosphorylation of the RD, and intracellular availability of ATP [24]. The ATP switch model [25] can be described in 4 steps; (1) The transport cycle is triggered by the binding of a substrate to its site on the MSDs, which then promotes ATP-binding at the NBDs, leading to the formation of a closed, head-to-tail sandwich heterodimer. (2) ATP-dependent dimerization of the NBDs induces conformational changes in the MSDs via NBD-MSD coupling helices that open the channel gate to release the bound substrate. (3) ATP hydrolysis undermines the NBD closed dimer and leads to the closing of the channel. (4) Sequential release of inorganic phosphate and ADP from the NBDs restore the protein to its basic, inward-facing conformation, and the non-phosphorylated RD inhibits again CFTR channel activity by blocking heterodimerization. The duration of the CFTR gating cycle, approximately 1 second, closely aligns with the ATP turnover rate. However, non-hydrolysable ATP analogues have been shown to prolong channel openings [24, 25].

CFTR activity can also be regulated by protein kinase C (PKC) as consensus sites for PKC-phosphorylation on CFTR were observed [26]. PKC facilitate PKA stimulation of open probability of the channel without increasing the number of functional channels [27]. Moreover, cGMP-dependent protein kinases (PKG or cGK) were also shown to phosphorylate CFTR [28]. More recently, evidence has proved that CFTR can be activated also in the absence of PKA stimulation, by increasing the intracellular calcium levels [29]. Indeed, calmodulin, the major calcium signaling molecule, was found to bind to the non-phosphorylated RD's α-helices leading to channel activation. Nevertheless, calmodulin binding inhibits phosphorylation by PKA and PKA phosphorylation inhibits calmodulin binding. This results in a complex interconnection in which PKA phosphorylation can synergize with the activating effects of calcium on CFTR or separate CFTR from calcium

activation [30]. In addition, CFTR activity is likely regulated by a large number of other proteins, including PDZ-interacting proteins and STAS (antisigma factor antagonist) domain interactors [31].

CFTR biosynthesis

CFTR is a multi-domain glycoprotein of which biosynthesis, maturation and function as a chloride ion channel involve multi-level post-translational modifications and complex folding processes to reach its native, tertiary conformation [32].

CFTR biosynthesis begins in the endoplasmic reticulum (ER) with the folding of the cytosolic domains, towards the acquisition of a fully folded native structure. CFTR folding is presumed to be co-translational, with individual domains folding independently before forming inter-domain interactions during synthesis. This process leads to the creation of a fully functional chloride channel. [33]. Folding of the protein starts early during its translation in the ER, however, takes place in multiple cellular compartments along the secretory pathway (Figure 2). The ER quality control system assesses this process, permitting the exit of correctly folded proteins while targeting unfolded or misfolded CFTR to ER-associated degradation (ERAD). A mere 20–40% of nascent chains successfully attain a folded conformation, with the remaining molecules being directed for degradation, either through the endoplasmic reticulum, lysosomes, or autophagy [32]. In the ER and cytoplasm, chaperons control the folding of CFTR, such as Calnexin, Aha, and HSP40/70/90. For the protein to leave the ER, both inter, and intra-domain foldings are required [24].

After proper folding, CFTR can move from the ER to the Golgi-apparatus via COPII vesicles where the glycan moieties are processed. Mature CFTR remains stable for 16-24 hours in post-Golgi compartments before undergoing further trafficking to the PM, where its level is determined by a dynamic equilibrium involving membrane delivery, endocytosis, and recycling processes. Indeed, the PM provides the final stages of CFTR maturation, as the protein takes part in an interactome, together with members of Rab and Rho families, or GTPase and cytoskeleton proteins, such as the PDZ-interacting NHERF-1 [34, 35].

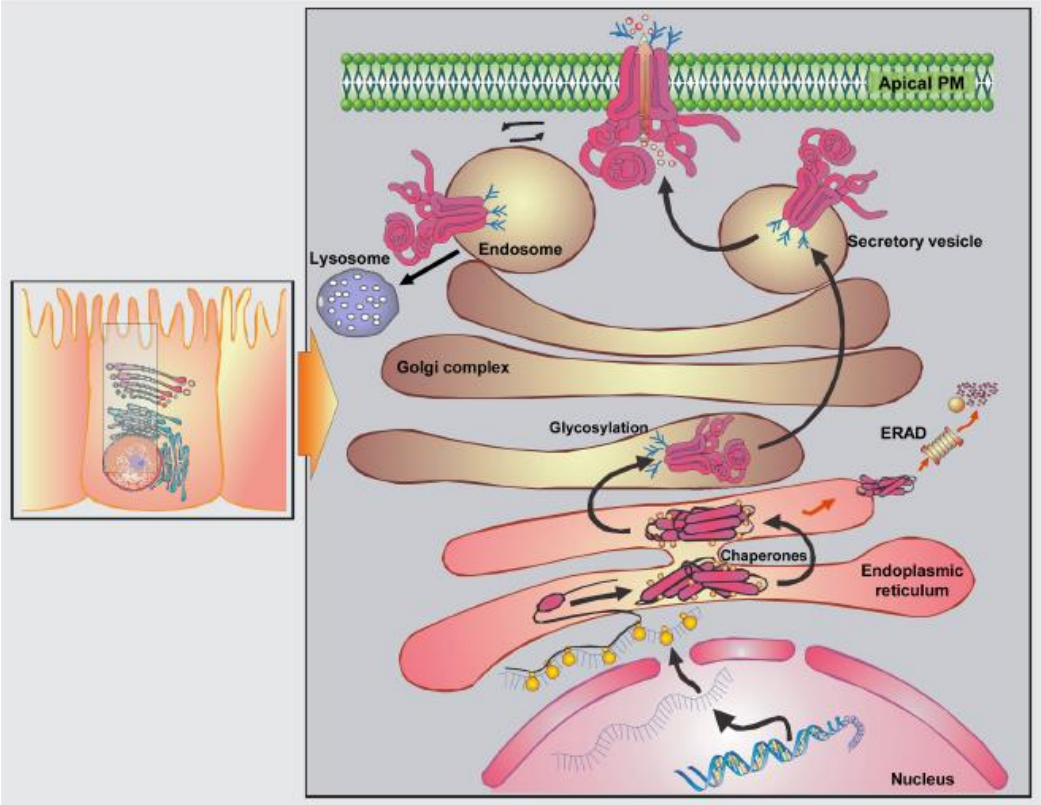

Figure 2. Successive steps of CFTR biosynthesis, trafficking, and degradation.

Figure adapted from [32].

The N-linked glycosylations in the 4th extracellular linker (ECL) at residues 894 and 900, recognized by calnexin which is part of the checkpoint that allows CFTR to proceed to the Golgi, serve as markers for the correct and mature form of CFTR. Complete glycosylation is considered an indicator of the folded state of CFTR, although it has been demonstrated to be unnecessary for plasma membrane localization or channel function [24]. In fact, CFTR undergoes post-translational modifications, like glycosylation, palmitoylation, methylation and phosphorylation, that are important for its correct folding, stability, and biological activity [36, 37].

CFTR interactors and microenvironment

CFTR at the apical surface of the plasma membrane is associated not just with proteins, but also with lipids in a macromolecular complex (Figure 3), and its channel activity and surface expression are regulated by local signaling and recycling through endosomal compartments.

However, regulation of CFTR at the PM is a complex process that involves, on one side the modulation of CFTR Cl^- channel activity, and on the other, the CFTR membrane levels. Channel activity is regulated both at N- and C-terminus of CFTR by PDZ proteins, such as NHERF-1 and CAL (CFTR associated ligand), by protein kinases, and by the other scaffolding protein of CFTR, Ezrin. Indeed, Ezrin, an A-kinase anchoring protein, tethers PKA in the proximity of CFTR allowing cAMP-dependent control of chloride efflux [38]. Instead, level of CFTR at the PM is regulated by endocytosis in clathrin-coated vesicles, followed by either recycling to the PM or targeting for lysosomal degradation. These trafficking events at the PM are controlled by multiple protein interactors, including Rab GTPases, Rme-1 and myosins, as well as some protein kinases, like spleen tyrosine kinase or lemur tyrosine kinase 2 [39].

Moreover, several papers reported that the second messenger cAMP has a role in regulating CFTR PM stability. Intracellular cAMP impact is mediated by cAMP dependent PKA, which directly phosphorylates CFTR's R domain. Interestingly, a family of guanine nucleotide-exchange factors, called EPACs, have also been discovered to respond to cAMP levels, however, they do not lead to PKA activation [39]. On the other hand, EPAC1 activation is reported to stabilize CFTR at the PM, therefore, these data indicate that cAMP signaling regulates CFTR through two different but complementary pathways, mediated by PKA and EPAC1 [40].

Interactions with other proteins are fundamental for CFTR function and channel activity, nevertheless, also membrane lipids are crucial in regulating CFTR's life cycle. In particular, a bioactive group of lipids, the sphingolipids, and cholesterol are important for the stabilization of CFTR in highly restricted membrane domains, called lipid rafts [41,42]. It has been proved that in bronchial epithelial cells the lack of CFTR in the PM, such as in the case of the patients carrying the mutation F508del (the mutation with highest frequency), is associated with a decreased content of the sphingolipid monosialo-ganglioside GM1 [43], suggesting a direct correlation between CFTR expression and this ganglioside. Indeed, CFTR was reported to reside in the same PM microenvironment as the GM1, making this ganglioside its interactor [41,42]. Another important lipid in the CFTR microenvironment is the cholesterol. Recent works indicate a dependence of CFTR dynamics and distribution on cholesterol levels [44], describing how its reduction induces an increased mobility of CFTR at the PM with a consequent negative effect on the stability of the channel. On the contrary, increasing the cholesterol content at the PM ameliorates the activity of CFTR and increases its confinement in membrane domains [45, 46]. Moreover, an important role of sphingomyelin for the regulation of CFTR activity was also suggested [39].

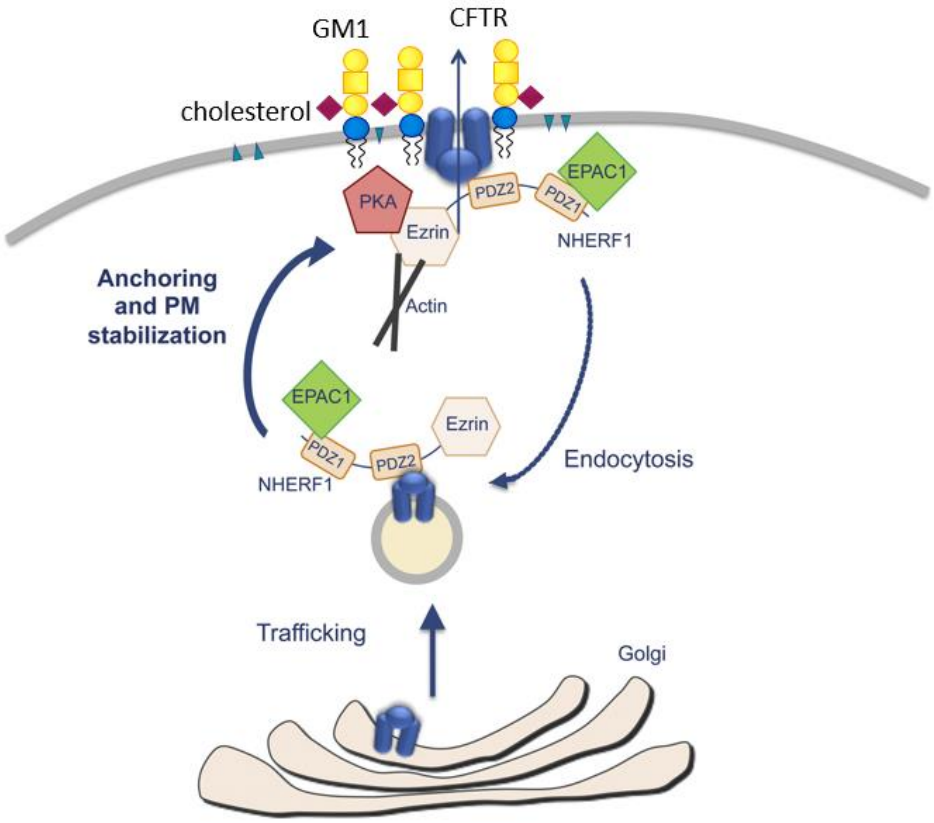

Figure 3. CFTR regulation and interactions.

Figure modified from [19].

Cystic Fibrosis epidemiology

Cystic fibrosis is categorized as a rare disease, nonetheless, it is the most common life-threatening autosomal recessive disorder, and despite its highest prevalence among Caucasians, it is considered a pan-ethnic condition. The estimated incidence rate of CF varies between countries and territories; in the U.S. it is approximately 1 in 1000, data similar also in the U.K. and Canada, whereas, it is lower across the European Union, 1 in 2000/3000, and it is thought to be under-diagnosed, due to a lack of registries and newborn screening programs, for example in Latin-America, Asia and Africa [47].

More than 160,000 people were estimated to be living with CF globally, exhibiting geographical heterogeneity [48], with the highest prevalence observed in Europe, North America, and Australia. Nevertheless, epidemiological changes have occurred both in the incidence of CF, which seems to be decreasing in most countries, and in the survival of CF patients, which has greatly improved [49].

Given that the disease has a genetic nature, cystic fibrosis epidemiology is specific to a wide range of factors, like race, gender, and age. Despite affecting both male and female individuals equally, female patients with CF generally exhibit a shorter life expectancy than their male counterparts, often attributed to an earlier onset of respiratory infections. Nonetheless, because of the implementation of newborn screening, most of the CF diagnoses occur before a child reaches 2 years of age. Indeed, age at diagnosis has an impact on disease outcomes, with earlier diagnoses resulting in improved survival rates. Moreover, nowadays, the estimated median age of survival is close to 50 years [47, 49, 50].

Apart from the heterogeneity in the landscape distribution, there is a great variability in the clinical manifestations of CF as well. Some patients may have all the classical features of CF from infancy and have a relatively poor prognosis, while others have much milder or even atypical disease manifestations and still carry mutations on each of the CFTR genes. The majority of patients experience classic or typical CF, marked by one or more phenotypic features and a sweat chloride concentration exceeding 60 mmol/L. They may exhibit either exocrine pancreatic insufficiency or sufficiency. The disease can present as severe with a rapid progression of symptoms or as milder with less deterioration over time. Mortality in classic CF patients is primarily attributed to progressive respiratory disease. Whereas non-classic or atypical CF encompasses individuals with at least one CF phenotypic characteristic and a sweat chloride level that is either normal (< 30 mmol/L) or borderline (30–60 mmol/L). These patients may have both multi- and/or single-organ involvement, with most having exocrine pancreatic sufficiency and a less severe lung disease [51].

CFTR mutations

Although more than 2100 mutations have been described in the CFTR gene with a wide range of biological and functional phenotypes, not all of them cause CF [11]. Mutations include missense, frameshift, splicing and nonsense mutations, in-frame deletions, and insertions. On the basis of the effect on CFTR function, the mutations are classified into seven major classes (Figure 4): class I, II, III and VII mutations are linked to the absence of residual CFTR function and are correlated with a severe phenotype in patients, demonstrating a pronounced clinical manifestation. On the contrary, patients with mutations belonging to class IV, V and VI show some residual CFTR function with mild lung disease and pancreatic sufficiency [52].

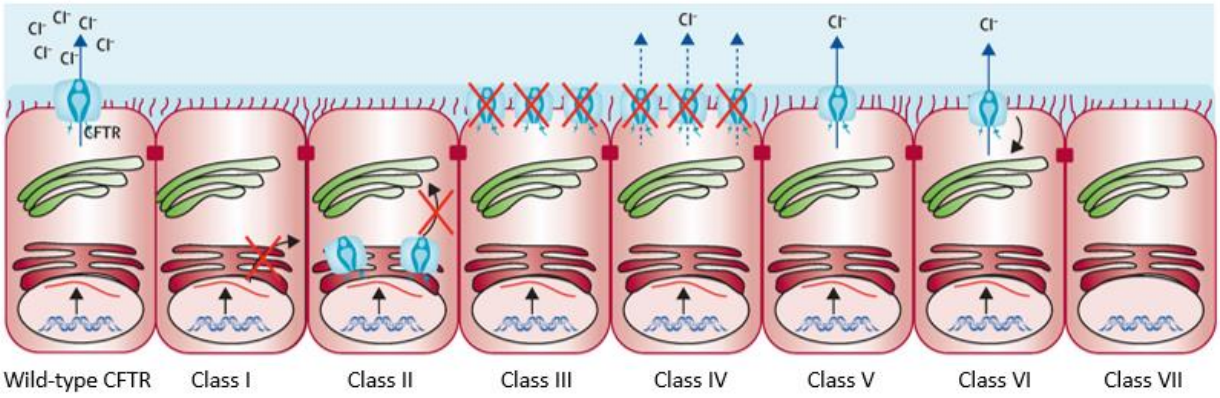

Figure 4. Classification of CFTR mutations.

Figure modified from [52].

Class I: protein synthesis defect

Class I mutations result in a severely reduced or absent expression of a functional CFTR protein. Such mutations may be due to a nucleotide substitution which introduces an in-frame premature termination codon (like W1282X, G542X and R1162X), frame-shifting insertions or deletions, and a complete or partial deletion of the CFTR gene or a rearrangement in the gene which can alter the exon sequence. G542X is the most frequent mutation of this class and leads to a reduced steady state level of mRNA, caused by the presence of a premature stop codon in its sequence [52, 53].

Class II: maturation defect

Class II mutations are associated with a defective processing and trafficking of the CFTR protein due to misfolding, severely reducing the number of CFTR molecules that reach the cell surface. Even if it is translated into full-length polypeptide, the misfolded protein is retained into the ER, targeted to degradation by the ubiquitin/proteasome pathway, rather than trafficked to the PM. The most frequent CF mutation, the deletion of a phenylalanine at position 508 (F508del), belongs to this class leading to energetic and kinetic instability of the NBD1 domain due to improper folding [53, 54].

Class III: channel regulation defect

Mutations of the third class are frequently located in the ATP binding domains (NBD1 and NBD2) and are mainly composed of missense mutations. They are referred to as gating mutations, as the produced CFTR can reach the PM, but the regulation of the channel is impaired with decreased channel opening time and chloride flux. Class III mutations are caused by resistance to activation by protein kinase A. The most described mutation of this class is G551D [21, 52, 54].

Class IV: conductance defect

Class IV mutations influence mainly the membrane spanning domains (MSD1 and MSD2) implicated in the constitution of the channel pore. The missense mutations located in these regions produce a protein which is inserted in the membrane, but with a reduced channel conductance with fewer ions passing through the open channel pore [52,53]. The R117H mutation is the best-characterized class IV mutation. Recently, the subclass IV.b has been identified in relation to mutations regarding only defect in CFTR bicarbonate conductance [54].

Class V: reduced protein synthesis

Class V mutations are often alternative splice mutations that reduce the total amount of CFTR protein by affecting pre-mRNA splicing. These splice site mutations can induce complete or partial exclusion of an exon. As result, CFTR is fully functional in the PM but with lower content. The most frequent and well-studied is the skipping of exon 10 [54].

Class VI: reduced protein stability

Class VI mutations include those ones which can destabilize CFTR in the post-ER compartments or at the PM, by reducing its conformational stability [55] and/or generating additional internalization signals [56]. Therefore, these mutations can accelerate PM turnover and reduce apical PM expression. Class VI has recently been combined with class V, as mutations leading to a reduced amount of functional CFTR protein.

Class VII: non rescuable mutations

Since the CFTR modulator era, a seventh class has been added. These mutations are called the irrecoverable mutations, because they cannot be pharmacologically rescued per se, such as large deletions (dele2,3(21kb) mutation) and frameshift mutations [57].

Clinical features of Cystic Fibrosis

The progression of cystic fibrosis displays significant variability, influenced not only by the specific CFTR mutation but also by other genetic and environmental factors. Onset can occur anywhere from a few months to several decades after birth, and numerous patients may present with mild or atypical symptoms [58].

The primary challenge in individuals with CF arises from the impaired secretion of chloride, sodium, and water, leading to the formation of thick mucus in the respiratory, digestive, and reproductive

systems. Conversely, the inadequacy in ion reabsorption at the sweat glands holds lesser significance in the overall pathology. Accordingly, abnormally viscous secretions within the airways of the lungs and the ducts of the pancreas in individuals with CF result in obstructions, leading to inflammation, tissue damage, and destruction in both organ systems. The most common symptoms occur in the respiratory tracts, featuring pertussis-like cough, several bronchiolitis or obstructive bronchitis, and are present in more than 90% of CF patients. On the other hand, loss of pancreatic exocrine function results in malnutrition and poor growth, which can lead to death in the first decade of life for most untreated individuals [59]. Other organ systems containing epithelia, such as sweat glands, biliary duct of the liver, male and female reproductive tract, and intestines are also affected. Indeed, CF liver disease is the third cause of mortality in CF [60].

Cystic Fibrosis lung disease

CF lung disease is the major cause of mortality and morbidity in CF patients. While primarily characterized as an infectious disorder, the consequent and associated inflammation in CF is both intense and ineffective in eliminating pathogens. Continued and intense inflammation contributes to structural damage in the airways, leading to impaired lung function that may result in respiratory failure and eventual death [58]. CFTR deficiency has been associated with multiple faulty inflammatory responses, including dysregulation in both innate and acquired immunity, abnormalities in cell membrane lipids, heightened production of pro-inflammatory mediators, and various defects in transcription factor signaling [61, 62]. The prevalent pathological observations include bronchiectasis, airway obstruction and chronic infection driven by different bacteria, with *Pseudomonas aeruginosa* (PA) being the most frequent [58,62]. Persistent bronchopulmonary infections can be caused by other pathogens as well, like *Staphylococcus aureus* (SA), *Burkholderia cepacia* and *Mycobacterium abscessus* (MA) [61].

Numerous studies highlight a multitude of defects in CF lung disease and inflammation that are directly or indirectly associated with the CFTR protein. These include reduced airway surface liquid and mucociliary clearance, hypoxia in the mucus layer, lower pH of airway surface liquid, and even abnormalities in sphingolipids [61, 63, 64]. The airway mucus is a dynamic, intricate, and viscous colloid that can undergo continuous modifications in response to various signals. It is a gel-like aqueous solution that contains different molecules like antibacterial defensins, immunoglobulins, glycoproteins, enzymes, lipids, inorganic salts, and protein mucins. Due to these components, airway mucus serves various functions, such as forming a protective barrier against harmful substances and

facilitating the clearance of pathogens. However, the mucus must be sufficiently fluid to allow the elimination of particles and pathogens [65]. The presence of the CFTR protein influences the characteristics of the airway surface liquid and mucus layer by regulating water content through its capacity to secrete chloride ions and control sodium absorption [66]. Indeed, dysregulated regulation of sodium and chloride content in CF results in defective osmotic pressure, heightened water absorption, and, consequently, dehydration of the airway surface liquid [64, 67]. As a result, very thick and viscous mucus is formed, unable to eliminate bacteria, leading to a chronic retention of pathogens and a strong inflammatory response [61, 68].

Another important parameter of CF is pH, which is eight times more acidic in CF airway surface fluid than in non-CF individuals [70]. In fact, low pH at the airway surface results in the inactivation of antimicrobial peptides thus creating a host defense defect [61]. Local pH is essential also to the correct function of several proteins, in particular the mucins, principally MUC5A, MUC5B, and MUC2, which are able to impart viscoelastic and adhesive properties of respiratory mucus [66]. In addition, CFTR is required for normal bicarbonate secretion too [71, 72, 73]. Recent findings indicate that CFTR-dependent bicarbonate plays a crucial role in determining the expansion and solubilization of mucin granules, as well as the density of airway mucus. Actually, the absence of bicarbonate leads to the formation of a dense layer of mucins tightly adherent to the epithelial surface [61, 67, 74].

Regarding the lipid abnormalities, it was observed in several papers [63, 75, 76] that ceramide plays an important role in the pathogenesis of cystic fibrosis because of its accumulation in lung epithelia. High cellular concentrations of ceramide have been suggested to increase cell death, stimulate release of DNA, increase bacterial binding to extracellular DNA, and initiate IL-1ß and chemokine discharge.

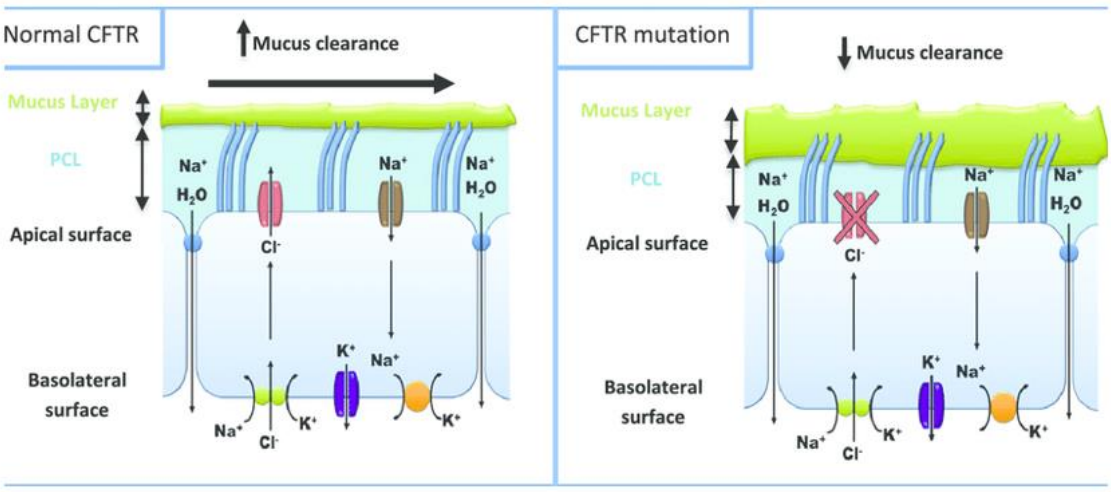

Figure 5. Defect in Cystic Fibrosis.

Mutations in the CFTR gene inhibit the secretion of Cl^-, resulting in uncontrolled absorption of Na^+ and impaired mucus clearance. Image from [77].

Therapeutic options in CF

Although there is not yet a definitive cure for cystic fibrosis, advances in treatment are helping many people have longer life expectancy. In the current treatment profile for CF patients, novel challenges have emerged: targeting the molecular defects in CFTR to restore the function of the mutated channel. However, none of the new therapies are sufficiently effective to serve as standalone treatments at present, emphasizing the equally crucial concurrent utilization of standard symptomatic treatments for individuals with CF. Standard symptomatic treatments consist of several therapeutic approaches to relieve patients' symptoms, including medications to help thin and clear the thick mucus from the airways, enzymes to help absorb fat and nutrients, and antibiotics to treat chronic lung infections [78].

Treatment of CF lung disease

Treatment of lung disease in CF is central, fundamental to improve the quality-of-life of CF patients, but is also complex, and can be approached by several ways. The hallmark of cystic fibrosis lung disease is infection by bacteria and other pathogens. Antibiotics have a role in treating acute pulmonary exacerbations and chronic respiratory infections, and they can be administered both by orally and intravenously, depending mainly on the targeted pathogen and on the severity of the symptoms [79]. The most prevalent bacteria amongst CF patients treated with antibiotics are *Staphylococcus aureus,* followed by *Methicillin-resistant staphylococcus aeurus* (MRSA), *Pseudomonas aeruginosa,* and *Haemophilus influenzae* [80, 81].

Pulmonary exacerbations and airway obstructions can be treated also by the restoration of airway surface liquid and mucociliary clearance using mucolytics, like Dornase alfa [82], or inhaling hypertonic saline and mannitol [79, 83].

In addition to these therapies, patients with CF have to take anti-inflammatory drugs too as the associated inflammation is increased but is still ineffective to clear pathogens from the lungs [84]. Both non-steroidal anti-inflammatory drugs (NSAIDs), like Ibuprofen, and steroidal anti-inflammatory drugs, such as corticosteroids, are used. As pulmonary damage in CF may occur as a consequence of inflammation, it has been hypothesized that prolonged use of NSAIDs may prevent progressive pulmonary deterioration and respiratory morbidity [85]. Furthermore, inhaled corticosteroids are often used to treat children and adults with CF, as they have the potential to mitigate lung damage caused by inflammation, along with their impact on alleviating symptomatic wheezing [86].

To ameliorate the breathing conditions, physiotherapy plays an important role in the management of CF, as well as daily airway clearance techniques, oxygen therapy and ventilator support [78].

Intensive use of oral, inhaled, and systemic antibiotics has undoubtedly improved survival of patients with cystic fibrosis and is still one of the mainstay therapies. However, the need for innovative antimicrobial treatments is on the rise due to the escalating prevalence of multi-drug resistant (MDR) bacteria in individuals with CF, especially in the context of an aging patient population [79]. For this reason, interest in treatment with bacteriophages is increasing [87, 88]. Bacteriophages are viruses that infect and replicate in specific strains of bacteria, lysing the host bacteria and killing it. The use of single or multiple bacteriophages in combination with antibiotics is also of enquiry, as they may have synergistic advantages in treatment. Phage therapy is currently being studied in preclinical studies for CF patients infected with SA, PA, MRSA and MA [89, 90]. Moreover, lung transplantation, a complex and high-risk yet potentially life-saving therapy, may be considered as an option for CF patients in the end-stage of lung disease [91].

Treatment of pancreatic, biliary, and liver disease

The continuous pursuit of optimal nutritional status is a major treatment goal in every CF individual, since they are characterized by pancreatic insufficiency, occurring in 85% of patients, or even biliary obstruction, occurring though in less than 10% of patients. Pancreatic insufficiency and biliary disfunction can be treated with pancreatic enzyme replacement therapy [92, 93]. More commonly, people with CF have heterogenous abnormal liver function, such as hepatic steatosis or fibrosis, but just a small group of these patients develop cirrhosis or portal hypertension, whose unique treatment is liver transplantation [94, 95].

Gene and molecular therapies

The primary objective of CF treatment is gradually transitioning from symptomatic management to addressing the underlying CFTR defect, aiming to stop disease progression and prevent the onset of complications. One of these approaches is gene therapy focusing on encompassing the CFTR protein repair and CFTR gene correction by introducing exogenous CFTR gene into the airways of CF patients via viral or non-viral vectors [96]. After cloning the CFTR gene, gene therapy was originally the priority for therapy of CF individuals, but gene transfer into lung cells *in vivo* soon proved more challenging than anticipated because of the innate barriers of airway epithelia and the thick, sticky mucus of CF patients [84]. Nevertheless, in 2012/13, a randomized, double-blind, placebo-controlled phase 2b clinical trial involving 140 patients was conducted for a DNA plasmid introduction, that contained the CFTR cDNA complexed with cationic liposomes. This major study of lung delivery has shown some promising effects on important clinical parameters of FEV1 but suggested also that substantially more efficient vectors and delivery systems are required to achieve sufficient expression of CFTR [97].

Other options as targeted therapies for the treatment of CF patients consist in promoting CFTR mRNA readthrough technology (for example non-antibiotic glycosides) [98, 99], or introducing new, wild-type RNA into the cells to be utilized in the production of complete CFTR protein [100], also by lipid nanoparticles [79]. Moreover, genome editing mechanisms are promising as well, like zinc-finger nucleases (ZFNs), transcription activator-like effector nucleases (TALENS), and clustered regularly interspersed palindromic repeats (CRISPR) or CRISPR-associated nuclease 9 (CAS9), that aim to repair the host DNA [101].

The restoration of reduced Cl^- secretion can also be accomplished by influencing other ion channels, the activity of which is dependent on or can substitute for CFTR, such as through the control of amiloride-sensitive epithelial Na^+ channel (ENaC). When activated through the PKA-dependent pathway, it is theorized that CFTR inhibits ENaC, thereby decreasing Na^+ absorption [102]. Hence, in CF, the absence of CFTR results in increased Na^+ conductance, making the modulation of ENaC activity a significant therapeutic target in CF [102, 104]. Additionally, recent attention has also been given to the activation of alternative Cl^- channels, specifically Ca^{2+}-activated Cl^- channels (CaCCs), like anoctamins (TMEM16A) [105] and SLC26A9 [106]. Support for alternative strategies targeting other membrane transporters is derived from evidence indicating that the presence of CFTR, even in its mutant form, at the PM appears to be sufficient to influence the activity of these other proteins.

CFTR Modulator Therapy

Defining the cellular and molecular pathology associated with CFTR mutations has proven to be invaluable in the development of small-molecule compounds aimed at addressing the fundamental defects in CF. These compounds are the CFTR modulators, the latest and most promising therapeutic options designed to enhance the function of the mutated channel. They are divided into two groups based on their function as chaperons; correctors, capable of improving the biosynthesis and trafficking of CFTR towards the PM, and potentiators, enhancing the probability of the CFTR channel opening once the protein reached the PM [107]. There are four CFTR modulators that have successfully progressed through clinical trials and are currently used in the therapy of CF.

The first proposed modulator was a potentiator, N-(2,4-di-tert-butyl-5-hydroxyphenyl)-4-oxo-1,4-dihydroquinoline-3-carboxamide (Ivacaftor, VX-770), approved in 2012 by the U.S. Food and Drug Administration (FDA), and soon afterwards by the European Medicines Agency (EMA), in children ages 6 years and older [108]. Ivacaftor was identified via high throughput screening and subsequently modified to optimize its therapeutic effect. It binds to the defective protein at the cell surface (to MSDs) and induces channel opening in a PKA phosphorylation dependent way, independent of ATP [109]. It was initially administered to CF patients who have the G551D CFTR gating mutation [110],

however, in other class III and IV mutations Ivacaftor has shown to correct CFTR-mediated chloride transport [111, 112], and now is administrable also in children of younger age, as young as 1 months old [113]. Until now, Ivacaftor is the only molecule approved to be used as a monotherapy treatment for CF patients with gating mutations, known under the commercial name Kalydeco by Vertex Pharmaceuticals.

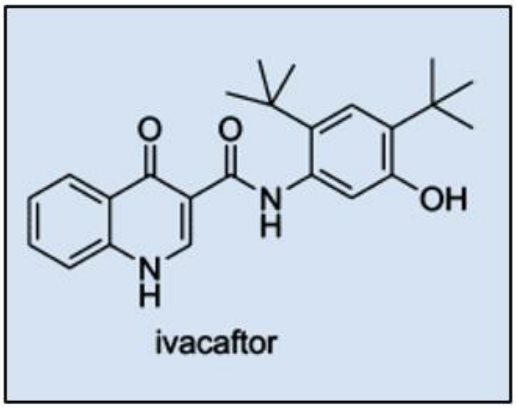

Figure 6. Structure of Ivacaftor

Unfortunately, gating mutations represent only one class of CFTR mutations, and therefore, additional therapies have been developed to target the pathophysiologic diversity. The most common mutation, the F508del, apart from its instability at the PM, results in misfolding and retention of the CFTR in the ER, and has reduced trafficking to the cell surface and, thus posing a challenge that is not entirely resolved by potentiators [114]. For this reason, correctors were developed to target this deficiency in folding and to increase the amount of CFTR protein produced and transported to the cell surface. The first corrector that has been approved by the FDA is Lumacaftor, VX-809. VX-809, functioning as a type-1 corrector, intervenes early in CFTR biosynthesis to adjust the conformation of MSD1. Consequently, it mitigates folding defects by strengthening interactions among NBD1, MSD1, and MSD2 domains in F508del-CFTR and similar MSD1 mutants [115, 116]. It is used only in combination with Ivacaftor in CF patients ages 1 and older with homozygous F508del mutations, and it was introduced in 2015 under the trade name Orkambi by Vertex Pharmaceuticals [113, 117].

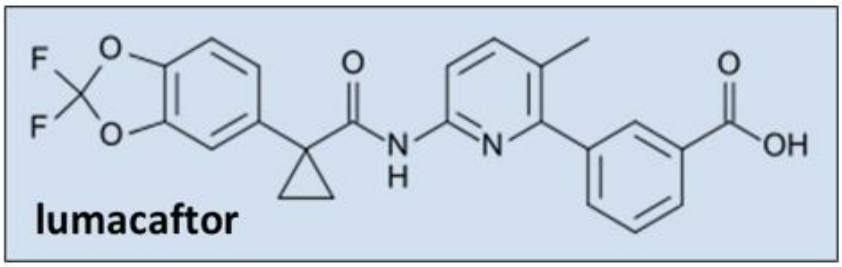

Figure 7. Structure of Lumacaftor

Lumacaftor, serving as a corrector, enhances the trafficking of CFTR protein to the outer cell membrane, while Ivacaftor, acting as a potentiator, facilitates the opening of an otherwise dysfunctional chloride channel. The safety and efficacy of the drug have been assessed in global studies carried out by the CF Therapeutics Development Network. These include two Phase III multinational, double-blind, placebo-controlled studies named TRAFFIC and TRANSPORT, published in 2015 [118], followed by an open-label trial known as PROGRESS in 2017 [119]. Treating patients with Orkambi formulation, symptoms have showed improvements, such as lower rate of pulmonary exacerbations and sweat chloride levels, but significant increase in FEV1, as well as in quality of life [119]. Nevertheless, clinical studies have shown that the long-term impact of Orkambi on lung function is modest and constrained [121, 122]. It was proposed that this modest effect could be attributed to a negative impact of VX-770 on the stability of F508del-CFTR at the PM [43]. A recent study indicates the potential for non-specific effects of VX-770 on the lipid bilayer, since as a small, lipophilic molecule, the potentiator has been found to accumulate and enhance the fluidity of the PM leading to its reorganization. This effect may be held accountable for inhibiting the VX-809-mediated correction of the interface between MSD2 and NBD1, and thus the folding efficacy of F508del-CFTR [122, 123].

Vertex continues the production of Orkambi; nevertheless, its diminished long-term effects underscore the necessity for the development of additional modulators to optimize the clinical benefits of corrector-potentiator therapy in CF. Another combinatory therapy has been approved in 2018 by the FDA consisting in Tezacaftor, VX-661, as the corrector, and VX-770, as the potentiator, licensed as Symdeko by Vertex Pharmaceuticals [113]. This drug is allowed for people ages 6 and older, both for those who are homozygous, and for those who are heterozygous for the F508del mutation and have another CFTR mutation that is responsive to this treatment, expanding the number of individuals who could benefit from CFTR-modulator therapy [124].

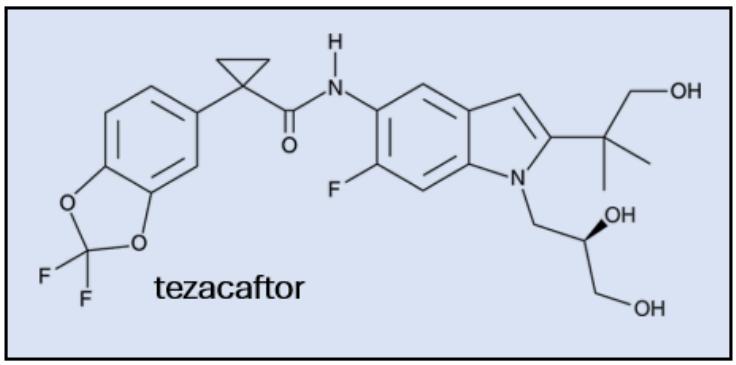

Figure 8. Structure of Tezacaftor

Lumacaftor and Tezacaftor belong to the same cluster, type I correctors. They are structural analogs and have a similar mechanism of action sharing an overlapping binding site of CFTR, the hydrophobic pocket of MSD1 [114]. While this drug combination demonstrates similar efficacy to Orkambi, it appears to be better tolerated and has fewer problematic drug interactions [125, 126].

Following the success of dual combination therapies, a triple therapy with ETI, or trade names Trikafta (USA) or Kaftrio (EU), was developed and approved by the FDA in 2019, consisting of two correctors, Elexacaftor (VX-445) and Tezacaftor, combined with the potentiator Ivacaftor. This combinatory therapy is now in use to treat patients ages 2 and older who have at least one F508del mutation in the CFTR gene, making the CFTR-modulators a possible therapeutic option for an even greater number of people with CF [113].

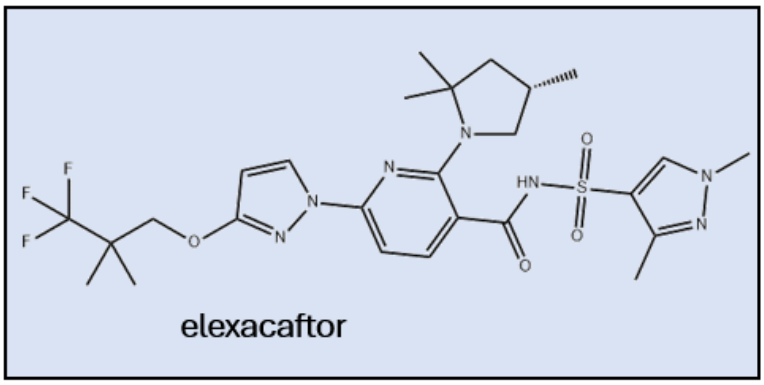

Figure 9. Structure of Elexacaftor

Elexacaftor is a molecule belonging to the type-3 correctors, binding to NBD1 and stabilizing it [127]. However, additional studies have demonstrated that VX-445 is effective in correcting rare class II mutations located in various domains of the CFTR, supporting, therefore, the idea that VX-445 has the capability to facilitate the multi-domain assembly of the CFTR protein [128, 129], interacting also with MSD2 [130]. It has been also postulated that VX-445 possesses dual activity, functioning both as a defective CFTR corrector and a potentiator [131], and its effect is synergic either with type-1 or with type-2 correctors.

Indeed, *in vitro*, Elexacaftor-Tezacaftor-Ivacaftor considerably improved F508del-CFTR protein processing, trafficking, and chloride transport to a greater extent than any two of these agents in dual combination. Moreover, recent phase 2 trials showed a further improvement in lung function, namely a 10% improvement in FEV1, as well as in general life quality, when the second corrector Elexacaftor was added to the Tezacaftor-Ivacaftor combination in homozygous F508del subjects [133], and also in individuals heterozygous for the F508del mutation and a minimal function mutation [134].

Altogether, Kaftrio seems to be a transformative therapeutic approach for the vast majority of individuals with CF globally. [135]. These influential medications fall under the category of highly effective modulator therapy (HEMT) and have played a role in enhancing lung function as assessed by FEV1, body mass index (BMI), respiratory symptoms (according to the CFQ-R respiratory domains), while decreasing pulmonary exacerbations [79, 135]. Indeed, due to HEMT, life expectancy is experiencing a significant improvement; as per the 2021 United States Cystic Fibrosis Patient Registry, the median predicted age of individuals with CF is now over 52 years [136].

Although the follow up of CF patients undergoing treatment with CFTR-modulators indicates an important improvement of the clinical symptoms and life expectancy, the necessity of developing new modulators and potentiators remains a crucial challenge in CF. This is particularly significant for approximately 30% of patients who bear either minimal function mutations not recognized to be responsive to HEMT, known as orphan mutations, or have unknown genotypes [79, 137].

Sphingolipids

CFTR protein forms connections with other proteins in a large molecular complex at the PM level. The activity of its channel and its presence on the cell surface are controlled by localized signaling and recycling processes within endosomal compartments. These processes appear to depend on the compartmentalization and lateral mobility of CFTR and its interactome. While the majority of research has concentrated on protein-protein interactions, there is currently emerging evidence highlighting the significance of lipids in compartmentalizing CFTR. Specifically, lipid rafts containing sphingolipids and cholesterol on the plasma membrane play a crucial role in organizing the proper microenvironment for various proteins, including CFTR. Indeed, lipids impact both the activity and stabilization of the CFTR channel, but on the contrary, CFTR loss of function can also influence lipid metabolism [137].

Structure and chemical properties

The lipid composition of the cellular plasma membrane is highly intricate, encompassing glycerophospholipids, cholesterol, and sphingolipids. [138]. Although glycerophospholipids and cholesterol are the main lipids that make up eukaryotic cell membranes, nowadays, unfolding data support the important role of sphingolipids (SLs) [139]. Indeed, SLs define the structure, integrity, and fluidity of the phospholipid bilayer, and many of them are considered also as bioactive molecules directly involved in cell development, signaling, cell-to-cell or cell-to-matrix adhesion, proliferation,

and apoptosis [140, 141]. Sphingolipids (SLs) are mainly linked to the outer layer of the plasma membrane (PM), where they are confined to distinct membrane regions known as lipid rafts or detergent-resistant membrane domains (DRMs). These domains serve as organizing platforms, segregating specific proteins responsible for mediating signaling processes across the plasma membrane [142].

All SLs are amphipathic molecules characterized by a hydrophobic group inserted in the lipid bilayer, called ceramide, and by a hydrophilic head of different complexity protruding toward the extracellular environment. They share a common structure consisting of a "long chain" backbone or “sphingoid” base, which is formed by a 2-amino-1,3-dihydroxy-octadec-4-ene, an amino alcohol called sphingosine. Sphingosine has four different chemical configurations, but only the 2S, and 3R are found in nature. Through an amide-bound sphingosine is linked with a long or very long fatty acid-chain, predominantly composed of 14 to 36 carbon atoms in length [143]. The N-acylated form of sphingosine is called ceramide (Cer), the hydrophobic lipid moiety of SLs, which is the starting point for the biosynthesis of more complex phosphosphingolipids (PSLs) and glycosphingolipids (GSLs) (Figure 10) [144].

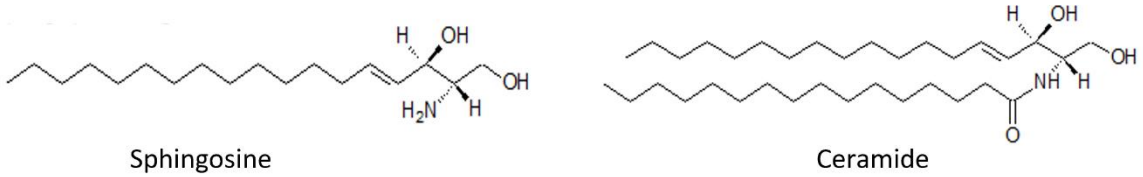

Figure 10. Chemical structure of sphingosine and ceramide

The ceramide backbone exhibits variation in length depending on the carbon chain; however, it is a fundamental component present in all SLs. In turn, the polar segment differs among various classes of SLs: in case of sphingomyelin (SM), it is composed of phosphocholine, regarding glycosphingolipids, it is a saccharide moiety, which can either be a monosaccharide or a polysaccharide generating more complex GSLs (Figure 11). In all cases, the polar head group is bound to the first hydroxy group of the ceramide backbone through a β- glycosidic linkage [143, 144].

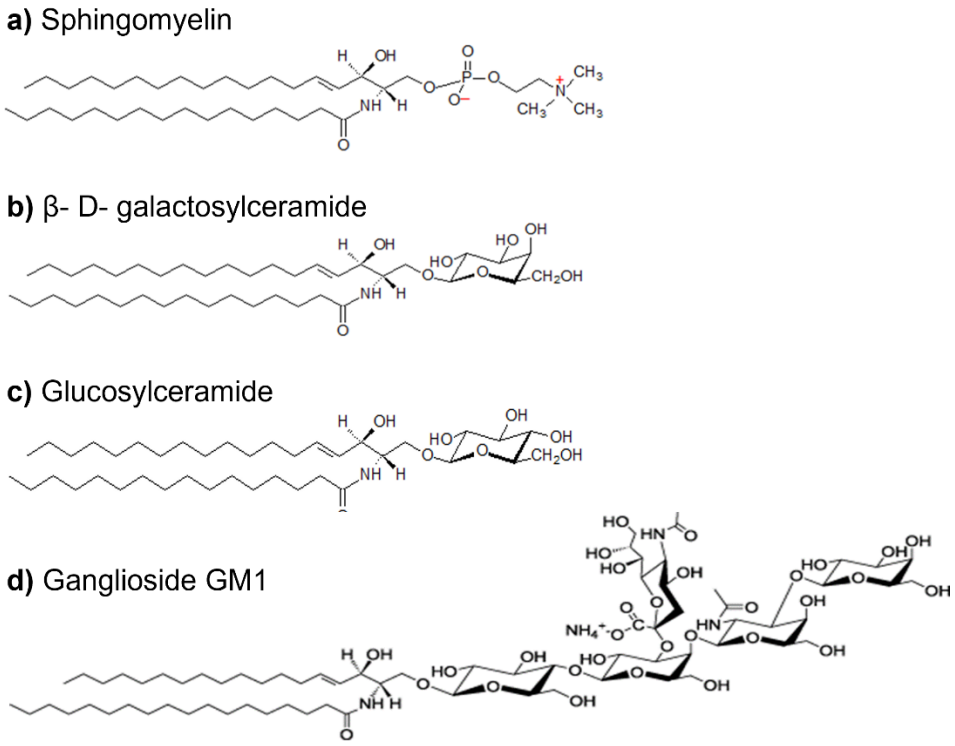

Figure 11. Chemical structure of principle sphingolipids

As a monosaccharide, both glucose and galactose could be added to the ceramide portion forming either the glucosylceramide (GlcCer) or galactosylceramide (GalCer), known also as cerebrosides. They represent the most basic GSLs and, along with globosides—sphingolipids containing two or more sugar moieties like glucose, galactose, and N-acetyl-galactosamine—they collectively make up the neutral glycolipids class. Cerebrosides are prevalently located at encephalic level and in the peripheral nervous tissue [144]. Instead, the gangliosides are a particular class of complex GSLs, whose oligosaccharide portion consist of at least 3 monosaccharides, such as D- glucose, D-galactose, N- acetylglucosamine, N- acetylgalactosamine, containing also one or more sialic acid residues through an α- glycosidic linkage. They are classified according to the amount and position of the hexoses and sialic acid residues, following the IUPAC nomenclature [145]. They are mainly located in ganglion cells of the central nervous system. The polar head of gangliosides extrudes from the outer layer of the cell membranes, where it can work as a receptor, or it can be involved in cell-to- cell or cell- to- substrate recognition as it occurs during cell growth [146].

Sulfatides represent another class of SLs. They are esters of sulfuric acid with GalCer inserted in the outer leaflet of the membrane and are particularly abundant in the kidney, gastrointestinal tract,

erythrocytes, as well as in the nervous tissue where they contribute to the proper structuring and functioning of myelin. Moreover, they are also involved in cell recognition and adhesion processes [147].

Sphingolipids' metabolism

The metabolism of SLs is a complex process involving the collaboration of numerous enzymes operating in distinct subcellular compartments, as illustrated in Figure 12. These processes are intricately linked and regulated by intracellular and extracellular signaling pathways, with the primary objective of defining the SL pattern that governs biosynthesis, trafficking, catabolism, and recycling of SLs. In the different cell types, the composition of SLs can be largely attributed to the combination of enzymes with transferase activities, depending on the cell function and pathological conditions [148, 149].

Sphingolipids' biosynthesis

SLs biosynthesis in mammals requires the intracellular formation of the membrane anchor, the ceramide [148]. Cer plays a pivotal role in SL metabolism as it serves as the shared intermediary in both the biosynthetic and catabolic pathways of SLs. Its production occurs through three different metabolic ways: de novo biosynthesis, complex SL catabolism and sphingosine recycling/salvage pathway. Instead, the oligosaccharide chain of GSLs is constructed by the sequential addition of monosaccharides either to the ceramide backbone or to the expanding saccharide chain [150]. Both events are coupled to intracellular movement of metabolic intermediates and final products to the PM [151].

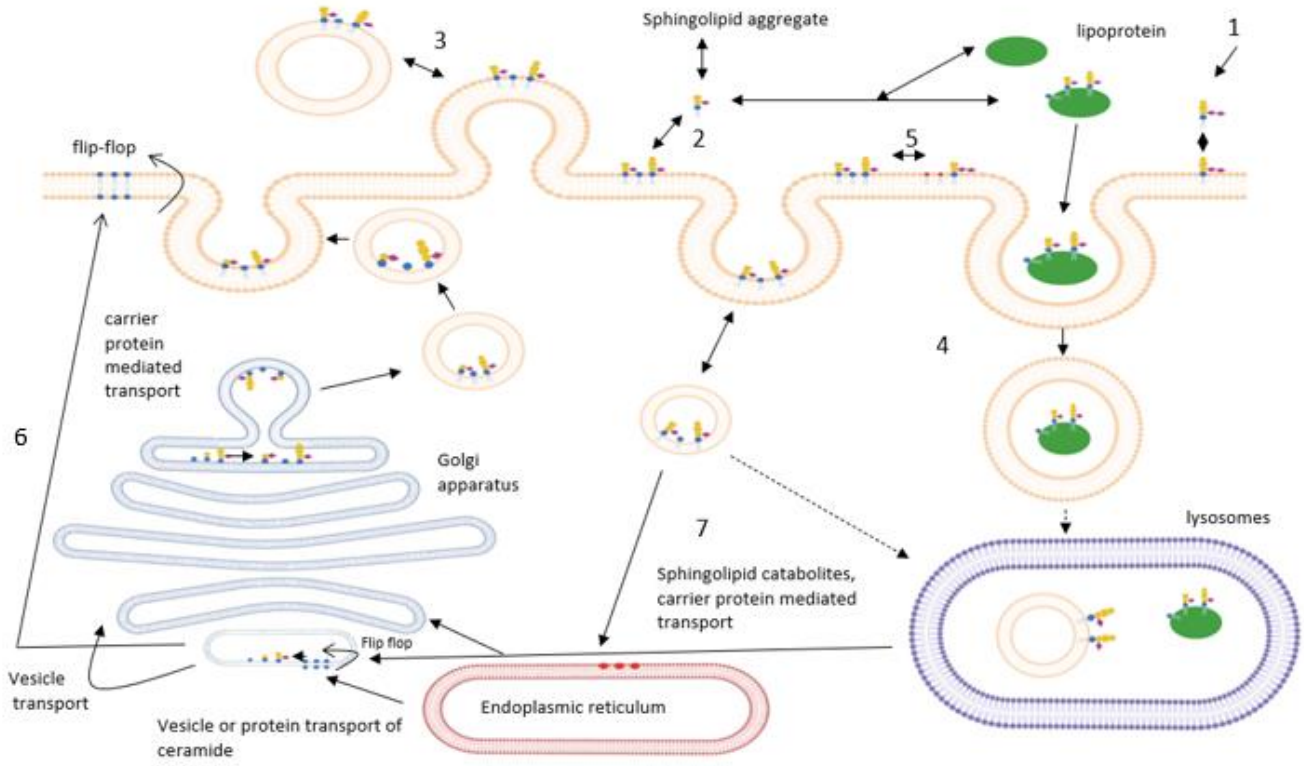

Figure 12. Scheme depicting glycosphingolipid metabolism.

Various metabolic pathways contribute to alterations in the composition of GSLs in the plasma membrane. These pathways include: 1. Uptake of extracellular glycolipids shed by neighbouring cells into the plasma membrane, 2. Shedding of glycolipid monomers, which can fuse directly with the membrane or interact with extracellular proteins or lipoproteins, subsequently taken up by cells and catabolized in lysosomes, 3. Release of vesicles containing glycolipids from the plasma membrane, 4. Membrane endocytosis, followed by sorting to lysosomes and catabolism within lysosomes, 5. Biosynthetic modifications carried out by PM associated glycosyltransferases and glycosidases, 6. Neobiosynthesis of glycosphingolipids and their transport to the cell surface, 7. Recycling in the biosynthetic pathway of partially catabolized molecules. Figure from [148].

Biosynthesis of ceramide

De novo biosynthesis of Cer takes place in the ER starting with the condensation of the amino acid L-serine with palmitoyl coenzyme A (CoA), catalyzed by serine palmitoyl transferase, forming 3-ketosphinganine [152, 153]. Afterwards, 3-ketosphinganine is reduced to d-erythro-sphinganine by 3-ketosphinganine reductase in a NADPH-dependent reaction [154]. Subsequently, sphinganine is acylated by the addition of a fatty acid in position 2 by N-acyltransferase (ceramide synthase), leading to the formation of dihydroceramide [155]. A major part of dihydroceramide is then desaturated in position 4,5 to Cer by the dihydroceramide desaturase (DES) enzyme [156].

Cer is also generated during either the catabolism of complex sphingolipids or the hydrolysis of sphingomyelin. SLs degradation occurs in the lysosomes by the action of specific glycohydrolases

which sequentially cleave off the sugar residues from the non-reducing extremity of the oligosaccharides, resulting in the formation of also Cer. Whereas, SM hydrolysis is catalyzed by the action of sphingomyelinases (SMases), directly into Cer [157].

Ceramide synthase can use with similar affinity both sphingosine and sphinganine [158], thus Cer can also be formed through a salvage pathway by the direct N-acylation of sphingosine produced by the catabolism of complex SLs and SM. Since this pathway doesn't need the action of ceramide desaturases, it is responsible for a massive production of cell SLs [159]. The synthesized ceramide can be transported to the PM to synthetize complex SLs, or it can be used to synthesize SM [160].

Biosynthesis of sphingomyelin

Regarding the SM biosynthesis, it occurs either at the luminal part of Golgi membranes or at the plasma membrane, by SM synthase 1 and 2 (SMS). Both isoforms transfer phosphorylcholine from phosphatidylcholine onto the 1-hydroxyl group of Cer, resulting in the release of diacylglycerol [161].

Biosynthesis of complex GSLs

GSLs biosynthesis is facilitated by a multienzyme system of glycosyltransferases found in both the Golgi cisterns and at the plasma membrane level. Glycosyltransferases catalyze the transfer reaction of a carbohydrate from the sugar nucleotide (UDP-Glucose or UDP-Galactose) to a specific type of acceptor, like ceramide or the non-reducing end of a carbohydrate chain linked to Cer [162].

The first step of the process happens at the cytosolic side of early Golgi membranes and starts with the glycosylation of Cer to glucosylceramide by a ceramide glucosyltransferase, called GlcCer synthase [163]. The neo-synthetized GlcCer can either be transported to the PM or it can be shifted to the luminal side of the Golgi, where it undergoes further glycosylation by various glycosyltransferase to form more complex SLs [164]. For instance, the addition of a galactose residue from UDP-Gal to GlcCer, facilitated by a galactosyltransferase, leads to the creation of Lactosylceramide (LacCer), which is the intermediate of complex GSLs [165].

One of the main branches of LacCer metabolism is the formation of ganglio- series. Biosynthesis of gangliosides occurs in the lumen of the Golgi apparatus by different glycosyltransferases, with the addition of neutral sugars and sialic acids [145]. The GM3 synthase or sialyl-transferase (SAT1) is responsible for the sialylation of LacCer to form the GM3 ganglioside by the transfer of a sialic acid residue. The other downstream metabolites in this pathway are formed by similar reactions; GM3 is converted to GM2 by GM2 synthase or β-galactosaminyl transferase, which transfers an N-acetylgalactosamine to GM3, and GM2 is converted to GM1 by GM1 synthase. Consequently, neo-synthetized GSLs reach the PM through exocytotic vesicular traffic [148].

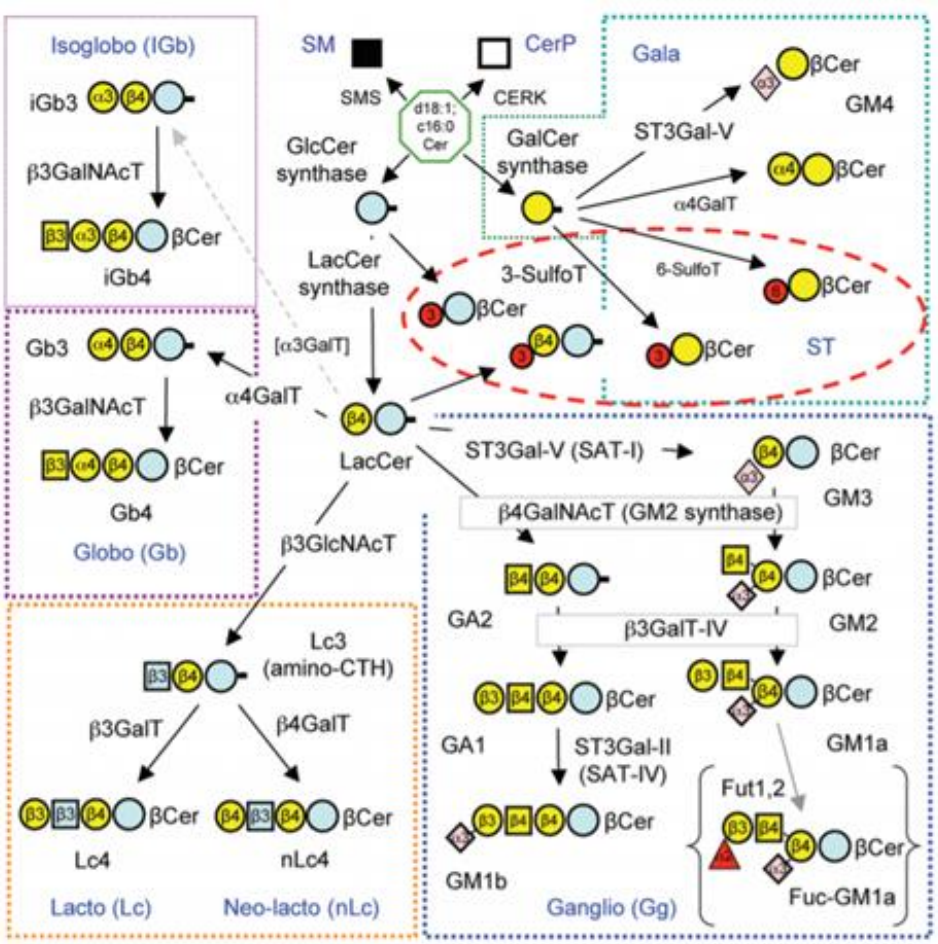

Figure 13. Biosynthesis of sphingolipids.

Scheme illustrating the principal headgroup additions in the Golgi apparatus during the biosynthesis of complex SLs. Each segment corresponds to a specific GSL category. Green dotted area: ala- series; red dotted area: sulfatides; blu dotted area: gangliosides; orange dotted area: lactosides and neolactosides; purple dotted area: globo and isoglobo series. Abbreviations: Cer=ceramide; LacCer=lactosylceramide, GalCer=galactosylceramide; GlcCer=glucosylceramide; GalNAc=N-acetylgalactosamine; Fuc=fucosyl; T=transferase. Figure from [144].

Trafficking of sphingolipids

Complex SLs are transported via vesicle- dependent or protein- dependent pathways from their site of synthesis, the ER, to the Golgi apparatus, the PM, and the endo-lysosomal system (Figure 12). Another mean of transportation is called “flip- flop”, helped by proteins known as flippases, when lipids can move from one membrane leaflet to the other, allowing the generation of specific lipid profiles in cell membranes. Moreover, lipoproteins or extracellular vesicles can exchange SLs with the PM. They can be internalized and directed to the endolysosomal system for their complete degradation or recycling. On the contrary, vesicles can be shred from the endolysosomal compartment and merge with the plasma membrane, a phenomenon referred to as lysosomal exocytosis [166].

Catabolism of sphingolipids

Lysosomal Glycolipid Degradation

Metabolic turnover and constitutive glycolipid degradation of PM sphingolipids takes place in the acidic compartments of cells, the endosomes and the lysosomes. Indeed, PM portions containing GSLs intended to degradation are internalized via endocytosis and the vesicles pass through endosomal compartments to the lysosomes [167]. The degradation process consists in the remodeling of the hydrophilic head of SLs as lysosomal glycosidases sequentially remove saccharides from the non-reducing end of their glycolipid substrates. The resulting molecules from the catabolism, such as monosaccharides, sialic acids, fatty acids and sphingoid bases, can either be further degraded or they can leave the lysosome to be recycled within salvage processes [168].

During the catabolism of sphingosine, it is first phosphorylated to sphingosine-1-phosphate (S1P) by sphingosine kinases and then sphingosine-1-phosphate lyase degrades it to phosphoethanolamine (PE) and hexadecanal [169]. Regarding the ganglioside catabolism, GM1 is cleaved to GM2 by β-galactosidase, removing the galactose. The produced GM2 is then degraded to GM3 and N-acetyl-galactosamine through the action of β-hexosaminidase A (Hex A), in the presence of GM2 activator protein. The enzyme is also responsible for the formation of GD1a by removing the N-acetyl-galactosamine from GalNAc-GD1a [148]. β-hexosaminidases are dimeric enzymes composed of two diverse subunits, α and β. The different possible dimerization of their subunits leads to three different isoforms of the enzymes in human cells: Hex A (α+ β), Hex B (β + β) and Hex S (α+ α) [170]. GM3 is a substrate of sialidase Neu1 and Neu3, which leads to the formation of LacCer and sialic acid. These enzymes are responsible also for the formation of GM1, removing a sialic acid from the ganglioside GD1a. Sialidases or neuraminidases are glycohydrolases that catalyze the removal of α-glycosidically linked sialic acid from the oligosaccharide chains of GSLs to form less complex SLs. Four different isoforms have been isolated from four different genes: Neu1, Neu2, Neu3 and Neu4. Neu1 and Neu2 are predominantly localized in the lysosomes and cytosol, Neu3 is found at the PM level, while Neu4 is present in mitochondria and ER [171]. The degradation of LacCer is driven by β- galactocerebrosidase, which removes the galactose obtaining GlcCer [172]. The GlcCer obtained by this reaction is further degraded by the action of β-glucocerebrosidase (GCase), a lysosome associated enzyme that hydrolyze the β-glycosidic linkage of GlcCer producing ceramide and glucose [173]. At the end, ceramide is catabolized into sphingosine and a fatty acid by acid ceramidase. On the other hand, SM is hydrolyzed to Cer by sphingomyelinase (SMase). Different forms of SMase are known, and are characterized by specific optimum pH, subcellular localization, or cation dependence, such as acid sphingomyelinase (aSMase) and neutral sphingomyelinase (nSMase). The acid one is principally located in lysosomes [174].

Plasma membrane sphingolipid metabolism

Several processes are responsible for the construction of the cell membrane sphingolipid pattern and content. The main ones are neo-biosynthesis of SLs in the ER and Golgi apparatus, the membrane turnover with final lysosomal catabolism, and vesicles shedding. Some data reported that enzymes involved in the metabolism of sphingolipids can directly modify the SL head groups at the PM level [175]. In fact, some of the same enzymes of SL biosynthesis and catabolism have been found not only in the lysosomes, but also associated with the cell surface [176], including sialidase and sialyl transferase, SMase and SMS, β-hexosaminidase, β-galactosidase and β-glucosidases, ceramidase and two glycosyltransferases: GalNAc transferase and sialyl tranferase 2 (Figure 14). These enzymes are frequently observed to occur as pairs, catalyzing the same reaction in opposite directions, thus contributing to the *in-situ* modifications of SL composition. The process by which enzymes working in the lysosomes are found also at the PM is a result of lysosomal exocytosis. This process involves the fusion of the lysosomal membrane with the PM, resulting in the secretion of the lysosomal content into the extracellular environment, and the association of lysosomal enzymes with the outer surface of the PM [148]. These phenomena have very important biological consequences, considering that they can affect cell function without involving the complex intracellular metabolic machinery.

The presence of active Hex A in the outer membrane layer of the PM was demonstrated in cultured fibroblasts [177], illustrating by immunological and biochemical characterization that it has the same structure of the lysosomal isoform. Regarding the neuraminidases, Neu2 and Neu3 are also present at the cell surface having a crucial role in transmembrane signalling [178]. β-galactosidase activity associated with the cell surface has been measured in several cell lines. Nevertheless, the identity of the proteins responsible for the enzyme activity at PM level is unknown so far [173]. In case of the β- glucosidase, at least two different enzymes had been detected with β- glucocerebrosidase activity capable of catalyzing the conversion of glucosylceramide into glucose and ceramide; β-glucocerebrosidase (GCase) which works in the lysosomes and a non-lysosomal β-glucocerebrosidase (NLGase), residing at the PM level [173]. Nevertheless, GCase was found to be present also at the PM level, and NLGase also within the ER and endosomal vesicles. They are considered central enzymes in the GSLs homeostasis, and, in addition, studies have shown that an increase in PM β- glucosidase activity (β-Glc TOT= GCase and NLGase) is accountable for inducing cell cycle arrest and apoptosis [179, 180]. With regards to the sphingomyelin synthase 2, the PM-associated one is genetically distinct from the Golgi's one. SMS2, at the PM, is present in combination with a particular isoform of neutral SMase, the nSMase2 [174].

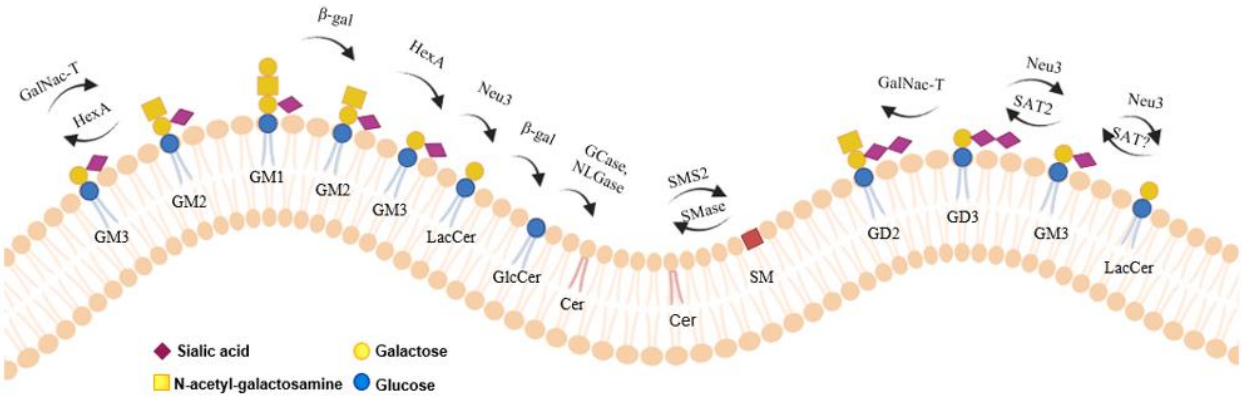

Figure 14. Image illustrating the glycosyltransferases and glycohydrolases linked to the cell surface.

β-glucocerebrosidase (Gcase); non-lysosomal β-glucocerebrosidase (NLGase); β-hexosaminidase A (Hex A); UDP-N-UDP-N-acetylgalactosaminyltransferase (GalNAc-T); β-galactosidase, β-galactocerebrosidases (β-Gal); sphingomyelinase (SMase); sphyngomyelin sinthase 2 (SMS2); sialyl acyltrasferas (SAT); Neuraminidase 3 (Neu3). Image from [137].

Biochemical role of lipids

Several evidence in literature suggest that lipids serve not only as structural components of cell membranes, but also as bioactive molecules, playing fundamental roles in cell signaling and regulatory pathways [181, 182].

Ceramide, ceramide-1-phosphate, sphingosine, and sphingosine-1-phosphate have been shown to be involved in the regulation of many considerable cellular events, such as proliferation, differentiation, motility, growth, senescence, and apoptosis [183]. Cer and S1P appear to have opposing roles in these processes, and thus the metabolically linked balance between them determines the entry into one or more of these pathways. Referring to complex GSLs, they play a crucial role in cell physiology by serving as antigens, mediators of cell adhesion, binding agents for microbial toxins, and modulators of signal transduction [184]. Moreover, as many reports indicate that most of the PM-associated glycohydrolases are are identical to the enzymes found in lysosomes [175, 176], at the cell surface these enzymes may directly impact the metabolism of SLs. This influence extends to cellular effects and the regulation of the levels of bioactive sphingoid molecules, such as Cer and S1P [41].

As written before, SLs together with cholesterol, saturated phospholipids and a specific pool of proteins organize protein-lipid macromolecular complexes at the PM, called lipids rafts. Lipid rafts were initially defined as membrane domains, specifically organized structures that exhibit distinct molecular compositions and properties differing from the surrounding membrane, created as a result

of the lateral segregation of sphingolipids. However, this definition was later modified, introducing the idea that lipid rafts are dynamic nanoscale membrane regions enriched in sphingolipids, gangliosides, and proteins, that are stabilized by the presence of cholesterol within a liquid-ordered phase [142, 185, 186]. Lipids rafts are also known as detergent resistant membrane domains (DRMs) as they are resistant to solubilization by non-ionic detergents, such as Triton X-100 and Brij-96. The complex processes governing the formation and dynamics of lipid rafts are not yet completely understood, nonetheless, changes in the lipid composition of the membrane upon stimuli impact the lateral organization of molecules within these rafts [187]. Most probably, SLs modulate the functional characteristics of many membrane proteins either by making lateral interactions with them or by short-range alterations of the physico-chemical properties of the protein membrane microenvironment [41]. Indeed, one of the most important properties of lipid rafts is that they can include or exclude proteins to variable extents [151]. In general, binding to rafts recruits proteins to a new environment, where the local activity of kinases and phosphatases can modify the phosphorylation state, subsequently leading to downstream signaling events.

Proteins, that are noticed to be residing in lipids rafts involve glycosylphosphatidylinositol (GPI)-anchored proteins, dually acylated proteins, such as Src-family kinases or the α-subunits of heterotrimeric G proteins, cholesterol-linked and palmitoylated protein, and transmembrane proteins. It is unclear why these proteins can be found in lipid rafts, however, some evidence suggests that amino acids in the transmembrane domains near the exoplasmic leaflet are significant, as well as specific post-translational modifications, like palmitoylation or myristoylation. Moreover, a monomeric transmembrane protein may exhibit a brief residence time in lipid rafts, but when the same protein is crosslinked or oligomerized, its confinement within rafts increases [188].

The distribution of lipid rafts over the cell surface depends on the cell type. Generally, they are more abundant at the PM level, but they are also present in intracellular membranes and extracellular vesicles, as Golgi, ER and endosomes [189]. For example, in polarized bronchial epithelial cells lipid rafts accumulate at the apical PM, where also CFTR is located.

Cholesterol

Cholesterol is the principal sterol synthesized by animal cells. It serves as biosynthetic precursor for synthesizing several hormones, vitamin D and bile acids [190], but is also an essential component of eukaryotic cellular membranes, contributing to the control of their physiological properties. Besides

its structural role, cholesterol also plays a crucial role in regulating cell function and vesicles formation [191]. Cholesterol is incorporated into the phospholipid bilayer of cell plasma membranes with its polar hydroxyl group situated near that of the phospholipid, to maintain membrane integrity [192]. As already mentioned, the lipid composition of the PM, including cholesterol and SLs, is a major determinant of membrane function, governing permeability and curvature as well as influencing the recruitment and activity of associated membrane proteins. Additionally, cholesterol restricts the permeability of the phospholipid bilayer, acting as a barrier that separates intracellular contents from the extracellular milieu [192].

Cellular cholesterol levels are tightly regulated within a narrow range through sophisticated homeostatic pathways, primarily taking place in the ER, the site for sterol synthesis. Cholesterol can be synthetized either as de novo, mainly in the liver and intestines, or it can also obtain from the diet. Triglycerides and cholesterol are combined with Apo proteins in the liver, forming a package that is subsequently released into the circulation as very low-density lipoproteins (VLDL). This packaging is necessary because the hydrophobic nature of cholesterol makes it unlikely for it to be transported through the blood. VLDL contains triglycerides, cholesterol, and phospholipids, and its degradation results in the formation of low-density lipoproteins (LDL) that are the main transporters of cholesterol in the circulation [193]. They are transported to peripheral tissues, where LDL is recognized by LDL receptors situated on cell membranes, and subsequently internalized via clathrin mediated endocytosis. Besides LDL, high-density lipoproteins (HDL) facilitate the transport of cholesterol from peripheral tissues back to the liver through a reverse transport mechanism [194].

The heterogeneous distribution of cholesterol among intracellular membranes is facilitated by both vesicular and non-vesicular transport between organelles. Nevertheless, its uneven distribution is predominantly reliant on non-vesicular transfer routes, mediated by soluble carriers known as lipid-transfer proteins. The content of membrane cholesterol can increase either through the secretory pathway or by endocytosis of LDL, which is then undergoes hydrolysis by acid lipases in the endocytic pathway releasing free cholesterol [195]. Recycling endosomes, rich in LDL-derived cholesterol as well as endocytosed PM cholesterol, can also deliver cholesterol to the cell surface.

Sphingolipids in Cystic Fibrosis

Lung sphingolipids

Similar to other tissues and organs, sphingolipids play a critical role in the lung, serving both as signaling molecules and as integral components of membranes and extracellular fluids.

Human airway epithelial cells contain a wide variety of SLs with a complex pattern, including Cer, PSLs, globosides, like globotetraosylCer and globotriaosylCer, the major class of neutral glycolipids, as well as LacCer, GlcCer and tetrahexosylCer (asialoGM1). In addition, among sialylated GSLs, in the lung tissue fourteen different types of gangliosides are present. The most abundant is GM3, followed by GM1, disialo GD3, and trisialosyllactosylCer GT3 [196, 197].

The role of SLs and SL metabolism in lung development has been widely investigated. Different studies reported the involvement of Cer in both apoptotic endothelial cell death and decreased pulmonary barrier function [41]. In fact, many bacteria employ the sphingomyelinase enzyme as common virulence factor that directly convert SM into Cer at the cell surface [198]. Ceramide in the plasma membrane promotes the development of an inflammatory phenotype leading to pulmonary infections caused by a several pathogens, such as *Neisseria gonorrhoeae*, *Neisseria meningitidis, Staphylococcus aureus, Pseudomonas aeruginosa,* or measles virus, rhinovirus [180]. Cer is suitable to manage bacterial and viral infections owing to its advantageous biophysiological properties. It is characterized by high hydrophobicity, low amphiphilicity and is able to create small, Cer-enriched membrane domains thanks to hydrophobic interactions. As a result of many different stimuli, such as bacterial infections, there is a continuous binding of these membrane domains, leading to the formation of large, Cer-rich platforms throughout the PM [45, 198]. They have diverse biophysical properties, and can amplify initial signals by trapping and activating receptors and signaling molecules [199].

Sphingolipids involvement in Cystic Fibrosis lung disease and infection

An increasing number of studies indicate that SLs play an important regulatory role in CF in relation to pulmonary infections and inflammation [83, 175, 198, 200].

Bacteria can bind to different receptors expressed on epithelial cell surface, such as Toll like receptors 2, 4 and 5. This binding activates a series of kinases leading to the nuclear translocation of transcription factors and expression of pro-inflammatory genes [201]. Indeed, in CF patients, there is a basal pro-inflammatory state, with large amount of pro-inflammatory mediators, such as interleukin (IL)-8, IL-6, and tumor necrosis factor (TNF)-α produced in the airways. This condition causes a massive recruitment of neutrophils and macrophages. However, these immune cells are unable to effectively eliminate bacteria, leading to the intensification of inflammation and persistent infection, responsible for the pathological manifestations of CF lung disease [61, 62].

Regarding complex GSLs, some studies reported that gangliosides belonging to the cell surface of epithelial cells could operate as receptors for microorganisms. In particular, some strains of *P.*

aeruginosa are able to bind to asialo-GM1 and asialo-GM2, moreover, the B subunit of cholera toxin can bind to GM1 ganglioside [202].

On the other hand, discrepant findings are outlined about the role of Cer in CF inflammation and infection, reported by the Gulbins group [63, 201] and by Guilbault and co-workers [203, 204]. Respectively, the Gulbins group showed accumulation of ceramide in the airway epithelium of a CF mouse model, along with qualitative evidence of increased staining for ceramide in the airway epithelium of people with CF. In contrast, Guilbault and colleagues demonstrated decreased ceramide levels in a different mouse model, and in the serum of CF patients. For the latter findings, Vilela and co-workers tried to explain the possible molecular mechanism involved. They stated that CF tracheal epithelial cells exhibit elevated glutathione levels, which might reduce intracellular Cer content by inhibiting neutral sphingomyelinase. Additionally, the heightened activation of the pro-inflammatory transcription factor NF-kB appears to be associated with Cer deficiency [205]. A conclusive explanation for these contradictory results remains elusive. However, potential factors such as differences in the methods employed for ceramide measurement, distinctions in the characteristics of various strains of cystic fibrosis mice, and variations in diets have all been suggested as contributing factors. Despite all this, major part of the latest studies stands next to the evidence pointing out the increased ceramide levels in CF pathology, responsible for pulmonary inflammation. In fact, it was noted that deficient concentrations of acid ceramidase contribute to elevated levels of ceramide in airway epithelial cells and alveolar macrophages of both CF mice and humans, especially for Cer species with carbon chains C16:0, C18:0, and C20:0 [206]. This increase in ceramide results in chronic inflammation, accelerated cell death, release of DNA into the bronchial lumen and thereby an impairment of mucociliary clearance. In addition, the inefficient processing of ceramide contributed to reduced levels of sphingosine, which correlates with the ineffective management of infection and inflammation. This disproportionate relationship between Cer and sphingosine enhances susceptibility to microbial colonization [207]. Moreover, the acidic pH in airway epithelial cells of CF individuals also could contribute to the increased production of Cer, as most of the glycohydrolases, which are responsible for GSL degradation, work at low pH values [72].

Lipid rafts have been demonstrated to play a role in various signaling pathways and are also implicated in the internalization of diverse microorganisms [139, 140, 208]. As previously explained, lipid rafts are dependent on the presence of cholesterol [44, 45] and sphingolipids, such as ganglioside GM1 in the cell membrane [41, 42]. Reorganization of lipid rafts into larger membrane platforms is triggered by various stimuli, in particular by bacteria and viruses, at the interaction site of the pathogen with the cells. After infection, aSMase translocates from intracellular compartments to the extracellular leaflet of the membrane in epithelial cells, where it is clustered and colocalized with

these microorganisms. Activation and translocation of aSMase correlates with the hydrolysis of sphingomyelin and the consequent release of ceramide, leading to the aggregation of lipid rafts into large membrane platforms promoting the internalization of the pathogen [199]. Their formation actives the start of signaling, either by concentrating a small number of suitable proteins into a large local concentration, or by exclusion of certain proteins from this microenvironment [209]. Therefore, the localization of a protein to lipid rafts often indicates that the protein is essential for some signaling process. It is hypothesized that CFTR is recruited to ceramide-enriched membrane platforms upon infection with *P. aeruginosa* [76], and that CFTR and GM1 colocalize at the site of *P. aeruginosa* internalization in epithelial cells [210]. Interestingly, pharmacological inhibition of aSMase can decrease Cer levels at the PM level, leading to an improvement in the inflammatory response to *P. aeruginosa* infections in lungs of CF mice [63]. In addition, pharmacological inhibition also of NLGase has been found to diminish the immune response to *P. aeruginosa* infection, by down-regulation of pro-inflammatory cytokines, and reducement of Cer formation [211].

CFTR deficiency and its correlation with sphingolipids

As explained before, literature describes CFTR as a transmembrane protein associated with lipid rafts [41-45, 210]. Given this characteristic, it is reasonable to hypothesize that the stabilization of the protein or the modulation of its function is influenced by interactions within the microenvironment where the protein resides, particularly by sphingolipids and cholesterol.

Indeed, some studies reported a relationship between CFTR expression and SL synthesis [137, 208]. Mutated CFTR or its reduced expression leads to an increased SL synthesis by enhancing the expression of serine-palmitoyl CoA. As a consequence, content of SM, ceramide and sphinganine at the PM level is increased [208]. Furthermore, it has been observed that the absence of CFTR leads to a modification in plasma membrane ceramide composition, characterized by a higher content of long-chain ceramide species, specifically C22, C24, and C26 [212]. The increased SL synthesis can be interpreted as a compensatory mechanism to PM destabilization due to lack of CFTR protein.

Also, a direct correlation between PM levels of ganglioside GM1 and CFTR expression was described. First of all, it was proved in bronchial epithelial cells of CF patients with F508del-CFTR that reduced levels of CFTR in the PM is consistent with a reduced level of this ganglioside. Moreover, CFTR was reported to reside in the same PM microenvironment as the GM1 in case of WT-CFTR cells, which consistency is missing upon the F508del mutation, suggesting that GM1 is an interactor of CFTR [43]. On the other hand, CFTR-silenced human airway cells showed a decreased content of GM1 at the PM and, as GM1 was reported to cluster β1-integrin in the cell membrane, a lower β1-integrin signaling [42]. As a consequence, cell motility is reduced contributing

to diminished wound repair in human airway of CF patients [213]. Interestingly, administration of GM1 to cells partially restores cell migration and CFTR recovery. In addition, the recuperation of CFTR in CFTR-silenced cells by CFTR modulator therapies, significantly increases GM1 levels [42, 43]. Nevertheless, the pharmacological inhibition of CFTR in normal, non-CF cells decreases GM1 content.

Data was also published about the involvement of the PM microenvironment in the regulation of CFTR function. Indeed, it was described that the decreased CFTR current can be caused by the formation of Cer from SM hydrolysis, as the confinement of CFTR in ceramide-enriched membrane platforms complicates channel activation by regulatory domain phosphorylation [214]. An aggravating circumstance is the presence of *P. aeruginosa*, which has a SMase activity as a virulence factor that hydrolyses SM *in-situ*, leading to the production of Cer. The reduced CFTR expression and chloride secretion caused by *P. aeruginosa* is accompanied also by an impaired mucociliary clearance and, as consequence, a decreased ability to clear bacteria [198, 210]. Furthermore, Cer produced by bacterial SMase has an effect on CFTR stabilization, even influencing the regulation of scaffolding protein, such as NHERF1 [215], and ERM (ezrin/radixin/moesin). The ERM complex regulates cytoskeletal PM interaction, and by recruiting PKA to the proximity of CFTR, leads to its activation [38]. Some data reported that Cer promotes ERM dephosphorylation and, as consequence, its inactivation through protein phosphatases, resulting in a decreased activation of also the CFTR [180].

In addition, the detection of CFTR in a detergent resistant membrane fraction isolated from airway epithelial cells suggests that it is recruited to a plasma membrane microenvironment that is also enriched in cholesterol [45]. Indeed, it has been revealed that human primary bronchial epithelial cells harbor two dynamically distinct populations of CFTR in the plasma membrane. One that is in clusters and displays confinement in lipid rafts, shows slow dynamics and sensitivity to cholesterol concentration, and another that is diffusely distributed along the PM, more abundant, relatively unconfined, showing higher dynamics. Therefore, these findings indicate that stability, cell surface density, and size of CFTR clusters are cholesterol dependent, consistent with their association with membrane microdomains [44, 45, 216].

Even though various studies have provided clear evidence that cystic fibrosis lung disease involves altered sphingolipid metabolism, the direct contribution of SLs to the pathogenesis of CF remains unclear. Advancements in comprehending the pivotal role of SLs in the pathophysiology of CF could potentially pave the way for the development of innovative SL-based therapeutic strategies aiming at enhancing the stability and function of the CFTR protein at the cell PM.

AIM

The recent pharmacological therapies for the treatment of Cystic Fibrosis are based on the development of small molecules able to correct the folding defects of the CFTR protein (correctors) and ameliorate its functionality as a channel, once reached the plasma membrane (potentiators).

For CF patients carrying the most frequent CFTR mutation, F508del-CFTR, the first therapeutic approach was based on the use of Orkambi, a combination therapy that includes a corrector, Lumacaftor or VX-809, and a potentiator, Ivacaftor or VX-770. Unfortunately, this treatment showed a time limited effect on the improvement of the disease phenotype having slight and very variable impacts on lung function of CF patients [121, 122]. In fact, several studies indicated a possible side effect of the potentiator Ivacaftor on the stability of rescued CFTR by correctors [43, 121-123]. Besides Orkambi, there are currently three other available CFTR modulators to treat CF patients. The recently approved one, Kaftrio, seems to be the most effective. It is a triple combination of two correctors, Elexacaftor or VX-445, and Tezacaftor or VX-661, and the potentiator Ivacaftor. This formulation has been shown to improve therapeutic efficacy in CF patients who carry at least one CFTR allele with the F508del mutation. Despite the fact that the potentiator Ivacaftor is also present in the new formulation, in cellular models Kaftrio shows a less significant instability effect of the corrected protein at the PM than is observed in case of Orkambi. [133-135]. Indeed, many factors contribute to PM CFTR stability and function, like its compartmentalization in lipid rafts, which are restricted areas of the PM composed by phospholipids, cholesterol, sphingolipids, with particular regards to monosialoganglioside 1 (GM1), and an important pool of proteins, including the scaffolding proteins of CFTR, ezrin and NHERF-1 [41-45]. Interestingly, it has been proved that in bronchial epithelial cells the lack of CFTR in the PM, such as in case of patients carrying the mutation F508del, is associated with a decreased content of GM1. Restoration of its level, instead, could stabilize CFTR, further supporting a possible role of the ganglioside in the CFTR interactome. Moreover, recent works indicated that cholesterol depletion reduces CFTR clustering in membranes domains and the fraction of CFTR in the confined populations, whereas these are both increased upon cholesterol augmentation indicating a dependence of CFTR dynamics and distribution on cholesterol.

Based on these considerations, there is a clear need to develop new approaches to further stabilize F508del-CFTR at the cell surface rescued by CFTR modulators. Therefore, with the aim of contributing to the advancement of new therapeutic strategies that would make pharmacological treatments more effective for CF patients, the main objective of my PhD project was to investigate whether modifying the cellular content of ganglioside GM1 and/or cholesterol is adjuvant to stabilize F508del-CFTR rescued by Kaftrio treatment. Furthermore, I also analyzed the effect of Kaftrio on the protein, lipid, and enzyme composition involved in sphingolipid metabolism, in immortalized human bronchial epithelial cells expressing either the WT or the F508del-CFTR.

METHODS

Cell models

To carry out the experiments, three main cell lines were used; CFBE41o-, WT CFBE, and F508del CFBE, that are a generous gift from Giannina Gaslini medical Hospital of Genova belonging to "Cell line and DNA Biobank from patient affected by Genetic Disease". The WT and F508del CFBE cell lines were obtained from CFBE41o- cells that are human bronchial epithelial cells derived from CF patients with homozygous F508del mutation that lost CFTR expression. They were immortalized with the origin of replication defective SV40 plasmid (pSVori-). Starting from this parental cell line, the lines overexpressing the wild-type CFTR (WT-CFTR, WT CFBE cell line) and the mutated CFTR (F508del/F508del-CFTR, F508del CFBE cell line) were obtained through stable overexpression. The cDNAs of the two protein variants were cloned into a lentiviral vector under the control of the human cytomegalovirus (hCMV) promoter. The expression of CFTR has also been coupled to a resistance to the antibiotic puromycin, which makes it possible to select only recombinant cells.

The cell lines are grown in disposable flasks of 75 cm^2 using Eagle's Minimum Essential Medium (E-MEM, Sigma M2279), supplemented with 10% of foetal bovine serum (FBS), 2mM L-glutamine, 100 U/ml Penicillin, 100 µg/ml /Streptomycin, and puromycin 0.5 µg/mL (for WT CFBE) or 2 µg/mL (for F508del CFBE) cells. Cells were cultured as monolayer in a humidified atmosphere at 37°C and 5% CO_2. After reaching 90 % of confluence, cells were detached from the flasks using 0,5 g/L Trypsin with 0,2 g/L EDTA in PBS (10 min, 37 °C) and plated at a density of 1,6 $x10^4$ cells/ cm^2 for Ø 60 mm petri dishes and 2 $x10^4$ cells/ cm^2 for 6-well plates, according to the experiment to be performed.

Polarization of F508del CFBE cells

F508del CFBE cells were seeded onto Transwell Clear permeable filter inserts (12 mm in diameter, pore size 0.4 µm; Corning, Wiesbaden, Germany) at a density of 2×10^5 cells per cm^2 and grown in Eagle's minimum essential medium (EMEM) supplemented with 10% foetal calf serum (FCS), 0.1 mM non-essential amino acids (NEAA), 2 mM L-glutamine, 100 µg/ml Streptomycin and 100 U/ml Penicillin, at 37°C in a 5% CO_2 incubator. Starting on day 1 (i.e. 24 h after seeding), the volumes of the apical and basolateral chambers were set as follows. For liquid-covered culture (LCC) of cells, apical/basolateral fluid volumes were 500 µl/1,500 µl; for cells to be cultured under air-interfaced culture (AIC) conditions, the apical medium was removed and the volume on the basolateral side was replenished to 650 µl. The culture medium was changed every other day thereafter for 30 days.

Cell treatment with CFTR modulators

Cells were subjected to treatment with the correctors VX-445 (Elexacaftor) and VX-661 (Tezacaftor) and the potentiator VX-770 (Ivacaftor). The combination of the two correctors with the potentiator constitutes the formulation of the drug Kaftrio, supplied by MedChemExpress. VX-445, VX-661, and VX-770 were solubilized in dimethylsulfoxide (DMSO) and administered directly into the cell culture medium at the following concentrations: 3 μM for VX-661, 2 μM for VX-445 and 5 μM for VX-770. As control, cells were treated with the same volume of DMSO at the concentration of 0,1 % (v:v). Each of the modulators was administered to the cells for 24 hours.

Cell feeding with ganglioside GM1, Liga20 and LDL

GM1 or the molecular species of GM1 were solubilized in the complete cell culture medium at the final concentration of 50 μM. In particular, appropriate amount of GM1 powder was solubilized in methanol in a glass tube and dried under gentle nitrogen flux. After the total evaporation of the solvent, complete cell medium was added and 5 cycles of shaking and sonication were performed allowing the complete solubilisation of the ganglioside. Liga20 was solubilized as GM1 but at the concentration of 10 μM. Both GM1 ganglioside, or its molecular species, and Liga20 were administered to cells for a 24-hour incubation time at 37°C. After, cells were washed, harvested with detergents containing protease inhibitor cocktail and processed for immunoblotting experiments as described below in the "sample preparation" paragraph.

The commercially available h-LDL, human low-density lipoprotein, (Medix Biochemica) is a 0.2 micron filtered solution with 15% sucrose obtained from human plasma and is directly administered to the cell culture medium of cells at a final concentration of 400 μg/ml. Cell were incubated with LDL for 48 hours at 37°C and cells were collected for immunoblotting analyses as described below in the "sample preparation" paragraph.

Pseudomonas Aeruginosa infection

Live, PAO1 wild-type, non-mucoid, piliated and motile laboratory strains of *Pseudomonas aeruginosa* were used for infecting F508del CFBE cells. Prior to the experiment, bacteria from overnight cultures in Trypticase soy agar (TSA) plates were grown in 20 ml of TSB broth at 37°C in

agitation until a OD at 660 nm of about $1x10^9$ colony-forming units/ml (CFU/ml) was obtained, as determined by dilution plates. Bacteria were washed twice with PBS at 4°C to eliminate products secreted into the extracellular environment, then bacteria were resuspended to a final dilution in cell culture medium. The doses of bacteria were determined by plating aliquots of dilutions on TSA plates. Cells were infected with PAO1 (50-100 CFU/cell) at 37°C, 5% CO_2 for 4 hours in the absence of antibiotics.

Treatment with cycloheximide

The day after seeding F508del CFBE cells on Ø 60 mm petri dishes, cells were subjected to the different treatments with correctors (VX-445 and VX-661) and potentiator (VX-770) and/or exogenous GM1, in the presence or not of PAO1 infection for 4 hours. Cells were collected at different time points, such as 8, 9, 11 and 13 hours after the addition of cycloheximide at a concentration of 100 µg/ml to the cell cultures. CFTR content was evaluated by Western Blot analysis.

Cell viability assays

Calcein assay

Calcein assay is a cell viability assay based on the use of the calcein-acetoxymethyl ester (Calcein-AM), a highly lipophilic cell-permeant dye which rapidly crosses the PM of viable cells. Once internalized, cellular esterases remove the acetoxymethyl ester group from calcein which thus can emit fluorescence and can no longer cross the PM of cells. F508del CFBE cells were seeded in a 96-well microplate at a density of 1,8 $x10^4$ cells/cm^2. The day after seeding, cells were treated with 400 µg/ml LDL for 24 hours or for 48 hours with the presence of Kaftrio (3µM VX-661, 2µM VX-445, 5µM VX-770) in the last 24 hours. After the removal of culture medium, cells were washed once with PBS solution (137 mM NaCl, 2,7 mM KCl, 10 mM Na_2HPO_4, 1,76 mM KH_2PO_4, pH 7,4) and then incubated with Calcein- AM solution at the final concentration of 0.005 µg/µl solubilized in cell culture medium (15 minutes, 37 °C). At the end of incubation, Calcein-contained solution was discarded, and cells were lysed by the addition of 1 % Triton X-100 in TNEV buffer. The microplate was incubated in mild agitation for 10 minutes in dark conditions and then the reaction volume was transferred to a black microplate (Black, 96- well, OptiPlate- 96 F, Perkin Elmer) for the fluorescence detection by a Victor microplate reader (Perkin Elmer) (ex/ em 495/ 515 nm).

Samples preparation

Cell lysates were prepared from cells cultured and processed either in Ø 60 mm petri dishes or 6-well plates. For lipid and enzymatic activity analysis, the medium was removed by aspiration and then two washes were carried out with cold PBS. To obtain cells lysates, cells were harvested in Milli-Q water supplemented with protease cocktail inhibitor (Sigma P8340) using disposable scrapers and transferred to 2 ml Eppendorf tubes. They were then subjected to 3 cycles of sonication using an ultrasonic pulse homogenizer at 25 db for 10 seconds. After determining the protein content of the samples, cell lysates were subjected to lyophilisation to proceed with the lipid analysis.

Instead, for immunoblotting analysis, the medium was removed by aspiration and then two washes were carried out with cold PBS followed by harvesting cells in RIPA buffer (150 mM NaCl, 50 mM Tris-HCl pH 7.4, 1% Triton 100, 0.5% Na deoxycholate, 0.1% SDS) supplemented with Protease Inhibitor Cocktail (Sigma P8340) using disposable scrapers and transferring them to 1,5 ml Eppendorf tubes. These aliquots were subjected to lysis on ice for 20 minutes to obtain complete disruption of the cell membranes. Subsequently, cell lysates were centrifuged at 15000g for 10 minutes at 4°C to sediment any insoluble material. At the end, supernatants were transferred into new Eppendorf tubes before proceeding with the protein assay. Denatured cell lysates were stored at −80°C and thawed immediately before performing electrophoretic separation.

Identification of the protein content

Determination of the protein content through DC-protein assay

Protein content of lysates dedicated either for lipid analyses or enzymatic activity analysis was determined using DC Protein Assay (Bio-Rad), which is based on Lowry's method. The assay was performed in a 96-well microplate using 5 µl of H_20 for the background, 5 µl of bovine serum albumin (BSA) with increasing concentrations for the standards (0,375 µg/µL, 0,75 µg/µL and 1,5 µg/µL respectively), and 5 µl of each cell lysate. After sequential addition of 25 µl of reagent A (alkaline solution of copper tartrate) and 200 µl of reagent B (dilution of Folin reagent), the microplate was incubated in mild agitation for 15 minutes at RT, followed by spectrophotometric reading at 750 nm wavelength by a microplate reader (Victor, Perkin-Elmer). Protein content was calculated by interpolation of the average absorbance value of the sample within the calibration curve built using BSA standards. The assay was considered linear in a 0.2-2 mg/ml range.

Determination of the protein content through BCA-protein assay

In order to quantify the protein content of the lysates dedicated for immunoblotting, the BCA (bicinchoninic acid) protein assay was used (µQPRO–BCA kit Micro Cyanagen). This protein assay is based on the biuret reaction, which is the reduction of Cu^{2+} to Cu^{+} by proteins in an alkaline solution with concentration-dependent detection of the monovalent copper ions. The assay was performed in a 96-well microplate using 150 µl of RIPA buffer 0.1X for the background, 150 µl of BSA resuspended in 0.1X RIPA buffer at different concentrations (4 µg/mL, 8 µg/mL, 16 µg/mL, 32 µg/mL) as standards, and 150 µl of the samples diluted 1:100 with RIPA buffer 0.1X. Subsequently, 150 µl of the solution used for the colorimetric reaction was added to each well, containing reagents A (alkaline solution of sodium potassium tartrate), B (4% BCA in H_2O) and C (4% CuSO4 in H_2O) mixed in a 25:24:1 ratio. The microplate was incubated in mild agitation for 2 hours at 37°C, followed by spectrophotometric reading at 570 nm wavelength by a microplate reader (Victor, Perkin-Elmer). Protein content was calculated by interpolation of the average absorbance value of the sample within the calibration curve built using BSA standards. The assay was considered linear in a 2-40 µg/ml range.

Immunoblotting

Aliquots of lysates dedicated to the analyses of CFTR by immunoblotting experiments were denatured in Laemmli buffer 5X (10% SDS, 0,5M DTT, 0,25 M Tris-HCl pH 6,8, 0,05% Bromophenol blue, 50% glycerol) and heated at 37°C for 10 minutes. Proteins were separated by SDS- PAGE using a 4- 20 % polyacrylamide gradient gel (Mini- PROTEAN® TGX™ Precast Gels, Bio-Rad) in a Mini- Protean- IV Cell electrophoretic cell. Also, Precision Plus Protein Standard (Bio-Rad) was loaded consisting of a mixture of polypeptides of known molecular weights between 10 and 250 kDa, used for the purpose of following the electrophoretic run and being able to visualize the migration of proteins at different molecular weights. The electrophoretic run was performed at constant voltage (60 V in stacking gel and 160 V in running gel) in running buffer (Tris-HCl 25 mM, glycine 192 mM and 0.1 % SDS, pH 8,3).

Separated proteins were transferred on Turbo Polyvinylidene-difluoride (PVDF) Mini-membrane (Bio-Rad) using a Trans-Blot® Turbo™ Blotting System (Bio-Rad) for 7 minutes at a constant voltage of 25 V and current intensity of 1.3 A. To verify the protein transfer, PVDF membranes were stained using Red Ponceau dye (Ponceau Red dye 0.1 %, Acetic Acid 5% in H_2O) for 5 minutes under

mild agitation. Membranes were then rinsed in Milli- Q H_2O and then in Tris-buffered Solution (Tris-HCl 10 mM, NaCl 150 Mm) with 0.1 % Tween-20 pH 8 (TBS-T 0.1 %) three times and blocked with blocking solution (5 % skim milk in TBS-T 0.1 %) for 2 hours at RT, in order to block unspecific binding sites. Afterwards, the PVDF membranes were incubated with different primary antibodies diluted in the blocking solution at the following dilutions: monoclonal mouse anti-CFTR (Cystic Fibrosis North American Foundation, Antibody 596), 1:2000; monoclonal mouse anti-zonula-occludens 1 (ThermoFisher , ZO-1-1A12) 1:500; monoclonal mouse anti-N-cadherin (BD, #610920), 1:1000; monoclonal mouse anti-E-cadherin (BD, #610181), 1:1000; monoclonal mouse anti-integrin β1 (BD, #610468), 1:1000; monoclonal mouse anti-EBP50 (NHERF1, BD, #611161), 1:500; monoclonal mouse anti-Ezrin (BD, #610603), 1:500; monoclonal mouse anti-Calnexin (BD, #610524), 1:1000; polyclonal mouse anti-GAPDH (Immunological Sciences, MAB-10578), 1:10000; monoclonal mouse anti- β-Actin (Cell Signaling, #3700), 1:2000; polyclonal mouse anti-caveolin-1 (BD, #610060), 1:5000. After overnight incubation at 4 °C in light agitation, the excess of the antibodies was removed washing the PVDFs three times in TBS-T 0.1 %. Then membranes were incubated for 1 hour at RT with the appropriate secondary antibody, such as; goat- anti-mouse horseradish peroxidase (HRP) conjugated (Thermo Fisher: dilution: 1: 2000 or 1: 10000 for highly diluted primary antibodies i.e. anti- GAPDH), or goat- anti-rabbit HRP-conjugated (Immunological Sciences, dilution: 1: 10000). Both secondary antibodies were conjugated to HRP and were diluted in blocking solution.

After removal of the secondary antibody solutions, membranes were washed three times in TBS-T 0.1 % and incubated with a commercial solution containing luminol (WESTAR ηC, Cyanagen) for 2 minutes in dark conditions to assess the peroxidase activity. The chemiluminescent signal was revealed through Alliance Mini HD9 (UV TECH Cambridge) digital system and quantified by ImageJ software. The chemiluminescent signal revealed was normalized on the signal of the housekeeping protein glyceraldehyde- 3-phosphate dehydrogenase (GAPDH).

Isolation and analysis of the proteins associated with the PM

Cell surface protein biotinylation and isolation of PM proteins by streptavidin pulldown assay

In order to evaluate the protein content at the plasma membrane level, CFBE epithelial bronchial cells were precipitated exploiting a biotin/streptavidin pulldown assay. F508del CFBE cells were treated or not with Kaftrio for 24 hours, also in the presence or not of GM1, its molecular species, Liga20 and/or LDL. At the end of incubation, medium was removed by aspiration and two washes were

carried out with cold PBS followed by incubation with 1 mg/ml of EZ-Link™ Sulfo-NHS-Biotin (Thermo Fisher Scientific, Waltham, MA, USA) in PBS, pH 7.4 (1 ml/MW6, 3 ml/ Ø 60 mm) for 30 minutes at 4°C. Under these experimental conditions the internalization of the biotin derivative does not occur and biotinylation is restricted to the cell apical surface proteins by the formation of an amide linkage between the biotin and a lysine residue. After biotin labeling, cells were rinsed three times with 100 mM Glycine in PBS to remove the excess of unbounded biotin and then washed twice with ice-cold PBS. Subsequently, cells were mechanically harvested directly in the lysis buffer consisting in 1% Triton X-100 in 10 mM TNEV buffer (10 mM Tris-HCl, 150 mM NaCl, 5 mM EDTA, pH 7.5) supplemented with Protease Inhibitor Cocktail (Sigma-Aldrich, St. Louis, MO, USA). Cells were transferred in Eppendorf tubes and lysed for 20 minutes in ice. Cell lysates were centrifuged at 4°C for 10 min at 15000g to remove nuclei and cellular debris. The resulting post nuclear supernatants (PNS) were assayed for protein content and aliquots were taken for immunoblotting, as described before.

Other aliquots, corresponding to 150-250 μg of proteins, were precipitated using 300 μL Dynabeads™ M-280 Streptavidin (Thermo Fisher Scientific). The mixtures were stirred overnight at 4°C and then the day after centrifuged to obtain the SAP (supernatant after precipitation) containing the intracellular proteins, and the pellet, namely the precipitate, containing the biotinylated, cell surface proteins, with the help of a multimagnet. To disrupt the link between the biotin and the streptavidin and to recover the biotinylated proteins the precipitate was first subjected to lipid extraction following the protocol described below in the "total lipid extraction" paragraph. Afterwards, the precipitate was incubated at 60°C for 15 minutes, and then at 100°C for 5 minutes in Laemmli buffer 1X to obtain the fraction corresponding to the cell surface proteins (P60 and P100), Aliquots of PNS, SAP, P60 and P100 were analysed by immunoblotting for CFTR and other proteins, loading a ratio 1:1 for PNS and SAP, and 1:6 for PNS/SAP and P60/P100.

Detection of biotinylated proteins

For the detection of specific antigens associated with the fractions PNS, SAP, P60 and P100, the same protocol was followed described for immunoblotting. For the observation of the pattern of biotinylated proteins, after incubation with the blocking solution, PVDF membranes were directly incubated with streptavidin conjugated to HRP (Vector, SA 5004), diluted in blocking solution 1: 2000, for 2 hours at RT. Afterwards, they were washed three times in TBS- T 0.1 % and incubated with a commercial solution containing luminol, as previously described.

Evaluation of the lipid content

Sphingolipid labelling with [1- ^{3}H]-sphingosine

Cells plated in Petri dishes (Ø 60 mm) were fed with radioactive [1-^{3}H]-sphingosine to metabolically label at the steady state all cell's sphingolipids, and the phosphatidylethanolamine, a glycerophospholipid derived from the catabolism of [1-^{3}H]-sphingosine. Briefly, radioactive sphingosine solubilized in methanol was dried under nitrogen flow and the residue was solubilised in complete culture medium through 5 cycles of shaking and sonication, at the concentration of $3x10^{-8}$ M (specific radioactivity 1.36 Ci/mmol), which is largely below to the cytotoxic one. An aliquot of the culturing medium was counted by liquid scintillation with an instrument that counts the beta-particles, namely the Beta-counter (PerkinElmer), to evaluate the percentage of solubilisation of the tritiated sphingosine. After a 2-hour long incubation (period called pulse), the radioactive medium was replaced with fresh culture medium, and cells were maintained in culture for another 48 hours (period called chase) and then they were treated with CFTR-modulators (3 μM VX-661, 2 μM VX-445, 5 μM VX-770) for 24 hours. To quantify the radioactivity internalized by the cells, the radioactivity of both cell culture mediums (after-pulse and after-chase periods) was counted. Afterwards, cells were harvested as described in the "sample preparation" paragraph to perform lipid analyses.

Total lipid extraction

To perform lipid extraction, cell lysates were subjected to lyophilisation to remove water. Lyophilised pellets were resuspended in $CHCl_3$: CH_3OH: H_2O (2: 1: 0.1, v: v: v). After the addition of each solvent, the samples were vortexed, sonicated in a H_2O bath for 5 minutes and then mixed at 1,400 rpm for 10 minutes at RT using ThermoMixer® (Eppendorf). Consequently, samples were centrifuged at 13,000 g for 10 minutes at RT. The supernatants, containing the total lipid extracts (TLE), were collected in Eppendorf of 2 ml, while the pellet was subjected to a second extraction with $CHCl_3$: CH_3OH (2: 1, v: v), repeating all the steps described before. Each supernatant of the second extraction was added to the corresponding first one and all the total lipid extracts were dried under nitrogen flow and resuspended in a known amount of $CHCl_3$: CH_3OH (2: 1, v: v) before proceeding with the lipids analyses by High- Performance Thin Layer Chromatography. The radioactivity of the TLEs' was counted with the Beta Counter.

Two- phase partitioning

Aliquots of the TLE were then subjected to a two- phase partitioning, resulting in the separation of an aqueous phase containing the more hydrophilic lipids, mostly the gangliosides, and an organic phase containing the more hydrophobic lipids. Aliquots of TLE, corresponding to equal amounts of radioactivity per sample, were dried under nitrogen flow and then resuspended in 1 ml of $CHCl_3$: CH_3OH (2: 1, v: v) and 20 % of Milli- Q H_2O. Samples were vortexed, sonicated in a H_2O bath for 5 minutes and mixed at 1,400 rpm for 10 minutes at RT using ThermoMixer® (Eppendorf). Afterwards, samples were centrifuged at 500 g for 10 minutes at RT obtaining the separation of the two phases. The upper aqueous phase (AP) was collected in Eppendorf of 1.5 ml while the lower organic phase (OP) was subjected to a second extraction with 400 µl of $CHCl_3$: CH_3OH: H_2O (3: 48: 47, v: v: v), vortexed, sonicated in a H_2O bath for 5 minutes and then mixed at 1,400 rpm for 10 minutes at RT using ThermoMixer® (Eppendorf). After centrifugation at 500 g for 10 minutes at RT, again, the two phases were obtained and the upper, aqueous phase of each sample was transferred to the tube containing the previously taken aqueous solutions.

All the AP were subjected to H_2O dialysis to remove the salts, then they were lyophilised, and resuspended in the appropriate volume of $CHCl_3$: CH_3OH (2: 1, v: v). Instead, the OP were dried under nitrogen flow and resuspended in a known volume of $CHCl_3$: CH_3OH (2: 1, v: v) before proceeding with the lipid analyses by High- Performance Thin Layer Chromatography (HPTLC). The radioactivity of the aliquots of the AP and OP was counted with the Beta Counter, as described before.

Lipid analysis by High- Performance Thin Layer Chromatography

For the analyses of the radioactive lipids, the radioactivity associated with the TLE, AP, and OP was evaluated by liquid scintillator and equal amounts of radioactivity (1000 disintegrations per minute/dpm) were loaded on mono-dimensional HPTLC (Silica gel 60; Merck Millipore™ - stationary phase) for lipid separation. In the case of endogenous lipid pattern, equal amounts of cell proteins of OP were loaded on HPTLC. The following solvent systems were used as mobile phases: to separate lipids of the TLE and the OP to analyse neutral glycolipids: $CHCl_3$: CH_3OH: H_2O (110: 40: 6, v: v: v); to separate lipids of the AP in order to evaluate the ganglioside pattern: $CHCl_3$: CH_3OH: 0.2 % $CaCl_2$ (50: 42: 11, v: v: v); to separate the cholesterol content of cells: C_6H_{14}: $CH_3CO_2CH_2CH_3$ (3:2, v: v).

The identification of lipids after separation was assessed by co- migration with authentic lipid standards. Radioactive lipids were detected and quantified by radioactivity imaging performed with

a BetaIMAGER^{TM} Tracer instrument (BioSpace) where counting each detected radioactive emission provides a real-time two-dimensional image of the spatial distribution of radioactivity on the HPTLC. The radioactivity associated with individual lipids was determined with M3 Vision software and normalized on the radioactivity of each sample, expressed as percentage. On the other hand, endogenous lipids of the OP were detected by spraying the HPTLC with anisaldehyde reagent, quantifying the intensity of the bands with ImageJ software and normalizing them on the samples' protein content. Data are expressed as fold change (in percentage) with respect to untreated cells.

Evaluation of enzymatic activities

Evaluation of enzymatic activities in total cell lysates

Enzyme activities of glycohydrolases were determined in lysates of CFBE41o-, WT CFBE, and F508del CFBE cells treated or not with Kaftrio. Evaluated enzymes were the following: β-glucosidase (β- Glc TOT), β- glucocerebrosidase (GCase), non- lysosomal β- glucocerebrosidase (NLGase), β-galactosidase (β- Gal), total β-Hexosaminidase (β- Hex TOT), β-Hexosaminidase A+S (β- Hex A+S), sphingomyelinase (SMase), α- mannosidase (α- Man) and β- mannosidase (β- Man). The enzymatic assays involve the use of fluorogenic substrates composed of the specific saccharide recognized by the enzyme conjugated to the fluorophore methylumbelliferone (MUB). The different enzymes catalyse the covalent bond cleavage and release MUB. In this condition MUB at alkaline pH emits a fluorescent signal, which can be detected by a fluorimeter (Victor, Perkin- Elmer) at excitation/ emission 360/ 450 nm.

Cell lysates obtained from the three different cell lines, treated or not with Kaftrio, were prepared in H_2O as described in the "sample preparation" paragraph, and then assayed for protein content by DC protein assay (Biorad). The assay was set up in triplicate in 96-well transparent plate, with a final reaction volume of 100 µl. As background for each enzymatic assay, wells have been set up with the same experimental conditions replacing the volume of the cell lysate with equal volume of H_2O, to evaluate substrates auto-hydrolysis. Each reaction mixture has been put at 37 °C on gently agitation for at least 1 hour, then 10 µl of the reaction mixture were transferred to a black 96- well plate (Black, 96- well, OptiPlate 96 F, Perkin Elmer) and 190 µl of 0.25 M glycine pH 10.7 was added to stop the reaction and to reach the maximum fluorescence emission peak of the free MUB. Plates were analysed through a microplate reader (Victor, Perkin Elmer). Picomoles of the converted substrates were calculated with a free MUB standard at known concentration and the specific activity of the enzymes was expressed as picomoles of converted substrate/ hours/ mg of proteins.

As for the substrates used, MUB-β-Glc, MUG-β-Gal, MUG, MUGS, MUB-α-Man, and MUB-β-Man were all purchased from Glycosynth, and HMUB-PC from Moscerdam.

β- Glc TOT, GCase and NLGase

Aliquots of the lysates corresponding to 20 μg of proteins were pre-incubated for 30 minutes at RT in a 96- well plate with a reaction mixture composed of: 25 μl of McIlvaine buffer 4X (0.4 M citric acid, 0.8 M Na_2HPO_4) pH 5.2 to assay GCase or pH 6 to assay NLGase, the specific inhibitor of the other counter- enzyme to discriminate either GCase or NLGase activity, if needed, and H_2O to reach to the final volume of 75 μl. Lysates were pre-incubated for 30 minutes at RT with the inhibitors; conduritol B epoxide (CBE) used at the final concentration of 0.5 mM to inhibit GCase; while AMP-DNM (Adamantane- pentyl- dNM;N- (5-adamantane-1-yl-methoxy-pentyl)-Deoxynojirimycin) has been used at the final concentration of 5 nM to inhibit NLGase. The enzymatic reaction was then started adding 25 μl of the specific fluorogenic substrate, 4-Methylumbelliferyl-β-D-glucopyranoside (MUB-β-Glc) at a final concentration of 6 mM.

β- galactosidase, β- hexosaminidase, α- and β- mannosidase

Aliquots of the lysates corresponding to 8 μg (for β-Gal and β- Hex tot) or 16 μg (for β-Hex A+S, α- and β- Man) of proteins were incubated with a reaction mixture composed of: 25 μl of McIlvaine buffer 4X pH 5.2, 50 μl of the specific florigenic substrate 4-Methylumbelliferyl-β-D-galactopyranoside (MUB-β-Gal) for β- Gal, 4-Methylumbelliferyl N-acetil β-D-glucosaminide (MUG) for β- Hex tot, 4-Methylumbelliferyl-β N-acetil β-D-glucosaminide-6-sulfate (MUGS) for β-Hex A+S, 4-Methylumbelliferyl α-D-mannopyranoside (MUB-α-Man) for α-Man and 4-Methylumbelliferyl β-D-mannopyranoside (MUB-β-Man) for β- man at a final concentration of 500 μM, and H_2O to a final volume of 100 μl.

SMase

Aliquots of the lysates corresponding to 20 μg of proteins were incubated with a reaction mixture composed of: 25 μl of McIlvaine buffer 4X pH 5.2, 50 μl of the specific florigenic substrate 6-hexadecanoyl amino-4-Methylumbelliferyl-phosphorylcholine (HMU-PC) at a final concentration of 250 μM, and H_2O to a final volume of 100 μl. In addition, for the detection of fluorescence due to hydrolysis of HMU-PC a concentration of 0.2 % Triton X-100 had to be added to the glycine solution.

GM3 Synthase and Sialidase Neu3

GM3 synthase activity was measured using the radioactive derivative of its natural substrate, [^{3}H(sphingosine)]-LacCer. The assay is performed in 150 mM sodium cacodylate-HCl buffer pH 6.6, using an aliquot of cell lysate at the final concentration of 20 mg of cell protein/ml, in presence of protease inhibitors. The day before the scraping of cells, the buffer mixture, containing LacCer micelles, is prepared as the following: in each reaction tube, 10 µl of Triton CF-54 1.5% (v:v) in $CHCl_3$: CH_3OH (2:1, v:v) were mixed with 0.5–50 nmol of [^{3}H(sphingosine)]-LacCer (corresponding to 45 nCi) from a stock solution in $CHCl_3$: CH_3OH (2:1, v:v), and dried under nitrogen flow. To this mixture, 8 µl of 750 mM sodium cacodylate-HCl buffer pH 6.6, 4 µl of 125 mM $MgCl_2$, and 4 µl of 125 mM 2-mercaptoethanol were added. Tubes were vortexed and sonicated and maintained overnight at 4°C. The day after, cells were harvested, collected, and homogenized with a Dounce homogenizer (10 strokes, tight) in 150 mM sodium cacodylate-HCl buffer, pH 6.6, in the presence of protease cocktail inhibitor (Sigma P8340). Then, 10 µl of 5 mM CMP-NeuAc, and 10 µl of cell homogenate (containing 200 µg of proteins) were added to the buffer mixture in a total reaction volume of 50 µl. Negative controls were performed using heat-inactivated cell homogenates (samples boiled at 100 °C for 3 minutes). The incubation was performed at 37 °C for 3 hours with continuous shaking.

Instead, activity of sialidase Neu3 was determined in the total cell homogenate using 6 µM [3-^{3}H(sphingosine)]-GM3 as natural substrate in the presence of detergent Triton X-100. The substrate is prepared as the following: in each reaction tube 5 nmoles of GM3 were mixed with 45 nCi of [^{3}H]GM3 and dried under nitrogen flow. Afterwards, 10 µl of Triton X-100 (0.5% v:v) were added and tubes were sonicated and vortexed 5 times followed by a gentle shaking at 37°C for 30 minutes with ThermoMixer® (Eppendorf). Subsequently, cells were harvested, collected, and homogenized in water in the presence of protease cocktail inhibitor (Sigma P8340). 35 µl of cell lysate (corresponding to 50 µg of proteins), and 5 µl of 0.1 M sodium acetate/acetic acid buffer pH 4.5 were added to each reaction tube already containing the GM3 micelles in a total reaction volume of 50 µl. The incubation was carried out for 1 h at 37 °C with gentle shaking.

Both reactions were stopped by the addition of 1.5 ml of $CHCl_3$: CH_3OH (2:1, v:v). Aliquots of the lipid extracts, obtained from each enzymatic reaction mixtures, were analysed by HPTLC using the solvent system $CHCl_3$: CH_3OH: 0.2 % $CaCl_2$ (50: 42: 11, v: v: v). After the chromatographic run, the separated radioactive lipids were detected and quantified by radioactivity imaging performed with BetaIMAGER^{TM} Tracer instrument (BioSpace) and the radioactivity associated with the individual lipids was determined with the specific M3 Vision software. By digital autoradiography

quantification the intensity of the bands was identified, one corresponding to the radioactive substrate, the other to the radioactive product.

Evaluation of enzymatic activities at the cell surface of living cells

For the same enzymes whose activity was assessed in cell lysates of CFBE41o-, WT CFBE and F508del CFBE cells treated or not with Kaftrio, as described in the previous paragraph, cell surface-associated enzymatic activity was also evaluated.

In this case, a protocol developed for measuring surface enzymatic activities in living cells was used, which involves plating cells directly into the wells of a 96-well plate and using the same MUB/HMUB-conjugated florigenic substrates used previously, dissolved directly in DMEM-F12 medium at pH 6. For each cell line, 3 $x10^4$/ cm^2 cells were plated in each well in triplicate of all the enzymes previously considered. The following day, cells were treated with the components of Kaftrio or DMSO for the control condition for 24hours, after which the assay was performed. To assess the possible auto-fluorescence of the substrates, 100 µl of them were added to wells in which cells were not plated. The enzymatic reaction was conducted for 2 hours at 37°C under mild agitation. At the end of incubation, 10 µl of the reaction mixture was transferred to 96-well black plate (Black, 96-well, OptiPlate 96 F, Perkin Elmer) and 190 µl of 0.25 M glycine pH 10.7 was added to stop the reaction and to reach the maximum fluorescence emission peak of the free MUB. Fluorescence was assessed by a spectrophotometer (Victor, Perkin Elmer, λex/λem=360nm/450nm) and compared to a standard of known concentration of free MUB or free HMUB.

Cells from the three cell lines were plated in triplicate to wells that were not subjected to evaluate the enzymatic activity but to determine the protein content with DC protein assay (Bio-Rad) after lysis in H_2O carried out directly in the well. In this way, enzyme activity could be expressed as picomole of product formed/hour/mg of protein.

β- Glc TOT, GCase and NLGase

The medium was removed by aspiration from each well and then one wash was carried out with 100 µl of DMEM-F12. The wells used to assess GCase and NLGase activity were preincubated for 30 minutes at room temperature with the inhibitors; 50 µl of DMEM-F12 in the presence of either AMP-DNM at a concentration of 400 nM to assess GCase activity or CBE at a concentration of 40 mM to assess NLGase activity.

Then, the preincubation solution was removed and 100 µl of MUB-β-Glc in DMEM-F12 was added at a final concentration of 6 mM to the cell monolayers, to which the two different inhibitors were appropriately administered. Similarly, the same substrate in DMEM-F12 was added, but without the presence of any inhibitors, to the wells used for the evaluation of β-Glc tot activity.

β- galactosidase, β- hexosaminidase, SMase, α- and β- mannosidase

To evaluate the activity of the other enzymes, medium was aspirated from the wells, and they were washed with DMEM-F12. Afterwards, 100 µl of the appropriate substrate dissolved in DMEM-F12 was added to each well. The following substrates and concentrations were used: MUB-β-Gal at the concentration of 500 µM for β-Gal activity; MUG at the concentration of 1 mM for β-Hex tot activity; MUGS at the concentration of 1 mM for β-Hex A+S activity; MUB-α-Man at the concentration of 1 mM for α-Man activity, MUB-β-Man at the concentration of 1 mM for β-Man activity.

SMase

To evaluate the activity of the SMase, medium was removed from the wells, and they were washed with DMEM-F12. Afterwards, 100 µl of the substrate HMU-PC at the concentration of 10 µM dissolved in DMEM-F12 was added to each well. In addition, for the detection of fluorescence due to hydrolysis of HMU-PC a concentration of 0.2 % Triton X-100 had to be added to the glycine solution.

Statistics

All the experiments were performed in triplicate and repeated three times. Data are represented as the mean values ± standard deviation and were tested for statistical significance exploiting Student's t-test analysis (GraphPad Prism software), with $p < 0.05$ as significant.

RESULTS

In-depth characterization of the effect of CFTR variant expression on membrane organization in bronchial epithelial cells.

As it is well known, in airway epithelial cells CFTR is associated with other proteins forming a macromolecular complex that, along with cholesterol and sphingolipids, is essential for its stability and function at the PM level. Based on this premise, I assessed whether the expression of different forms of CFTR has a specific effect on the protein, lipid, and/or enzyme composition involved in sphingolipid metabolism in immortalized human bronchial epithelial cells, and how the treatment with CFTR modulators could have an impact on these patterns. Three cell lines were used to conduct the experiments; CFBE41o- (parental cells) which have lost CFTR expression, as well as two other cell lines generated from CFBE41o- cells by stable transfection to overexpress either the WT form of CFTR (WT CFBE cells) or the most common CFTR mutation, F508del (F508del CFBE cells).

First, I carried out immunoblotting experiments to evaluate the CFTR expression in the presence or absence of Kaftrio. As can be seen in Figure 15, which shows the analysis of CFTR expression in CFBE41o-, WT CFBE, and F508del CFBE cell lysates, an extremely different protein pattern is observed in the three cell lines. In particular, the electrophoretic mobility of the protein indicates the degree of CFTR maturation: the mutated form, corresponding to the immature, incompletely glycosylated protein, has a molecular weight of approximately 140 kDa and is referred to as "band-b", while the protein that undergoes proper trafficking to the Golgi apparatus and complete glycosylation reaching therefore a through maturation has a higher molecular weight, approximately 160 kDa, and is referred to as "band-c". In case of WT CFBE cells, mainly the mature form of the protein (band-c) is expressed, as expected. Instead, in cells overexpressing the mutated protein, F508del-CFTR, the only form of the protein visible by immunoblotting is the immature form, band-b. Nevertheless, in case of the CFBE41o- cell line, characterized by the loss of CFTR expression, neither the immature nor the mature form of the protein is observed.

To date, the mutated protein, F508del-CFTR, can be rescued treating cells with Kaftrio, a CFTR-modulator consisting of two correctors, VX-661 (Tezacaftor) and VX-445 (Elexacaftor), and a potentiator, VX-770 (Ivacaftor). These three drugs were administered to the F508del CFBE cells at final concentrations of 3 μM for VX-661, 2 μM for VX-445, and 5 μM for VX-770, respectively. Cells were incubated for 24 hours, and then harvested, lysed and cell lysates were analysed by immunoblotting. As observed in Figure 15, Kaftrio has an important effect in the maturation of the mutated protein, leading to the appearance of the band-c in F508del CFBE cells. However, when

Kaftrio is administered to cells overexpressing the WT form of the protein, it enhances the expression of WT-CFTR. Clearly, no effect was observed on CFBE41o- cells.

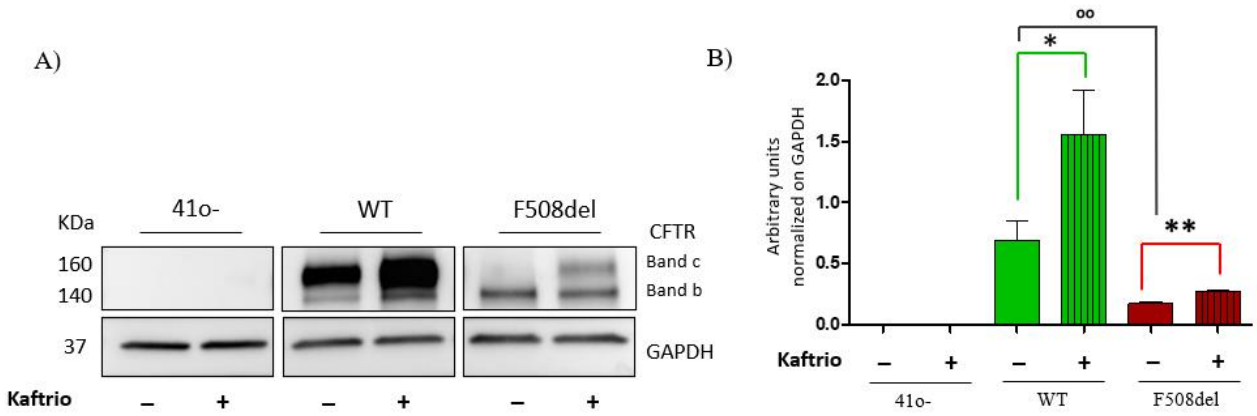

Figure 15. Expression of CFTR in CFBE41o-, WT CFBE, and F508del CFBE cells, treated or not with Kaftrio.

CFBE41o-, WT CFBE, and F508del CFBE cells were incubated for 24 hours with 3 μM VX-661, 2 μM VX-445, and 5 μM VX-770, and subsequently subjected to lysis. Equal amounts of proteins from lysates of cells were separated by SDS-PAGE, followed by electroblotting and chemiluminescent immunodetection after membrane incubation with primary antibodies and HRP-conjugated secondary antibodies. The figure shows a representative image of immunoblotting against CFTR and GAPDH (A), and a graphical representation of the data obtained after semi-quantitative densitometric analysis with ImageJ software (B). Changes in CFTR expression levels are expressed in arbitrary units as a ratio of the expression of band-c and-b, normalized on GAPDH. *p<0,05, **p<0,01 vs untreated cells, °°p<0,01 vs WT CFBE control cells.

Subsequently, with immunoblotting experiments I assessed the expression of different proteins that are significant in the stabilization of CFTR at the PM level. In the past, it has been observed that the expression of aberrant forms of CFTR influences the protein pattern. To better characterize this aspect, I analysed the expression of NHERF-1 and Ezrin, the main scaffolding proteins belonging to the macromolecular complex of CFTR, that are responsible for its stability and functionality at the PM level, also after treatment with Kaftrio.

As shown in Figure 16, a higher expression of NHERF-1 can be observed in CFBE41o- cells compared to cell lines overexpressing the wild type, as well as the mutated form of CFTR. However, Kaftrio treatment appears to increase the expression of the protein in WT CFBE and F508del CFBE cells. Conversely, no significant variation in Ezrin expression was observed in neither of the cell lines nor following Kaftrio treatment.

In addition, I evaluated the expression of caveolin-1 (CAV-1), a typical protein in lipid rafts which organizes membrane invaginations that can also facilitate the internalization of external elements. Immunoblotting was used to investigate whether CFTR expression, or the lack of it, on the cell surface influences the expression of CAV-1. Increased levels of CAV-1 can be observed in cells overexpressing WT-CFTR compared to CFBE41o- parental cells, which do not express CFTR. Interestingly, the expression of the mutated form of CFTR in F508del CFBE cells, where there is a decreased level also of the CFTR due to the mutation, further decreased the expression of CAV-1. The drug treatment appears to have no effect on the expression levels of this protein.

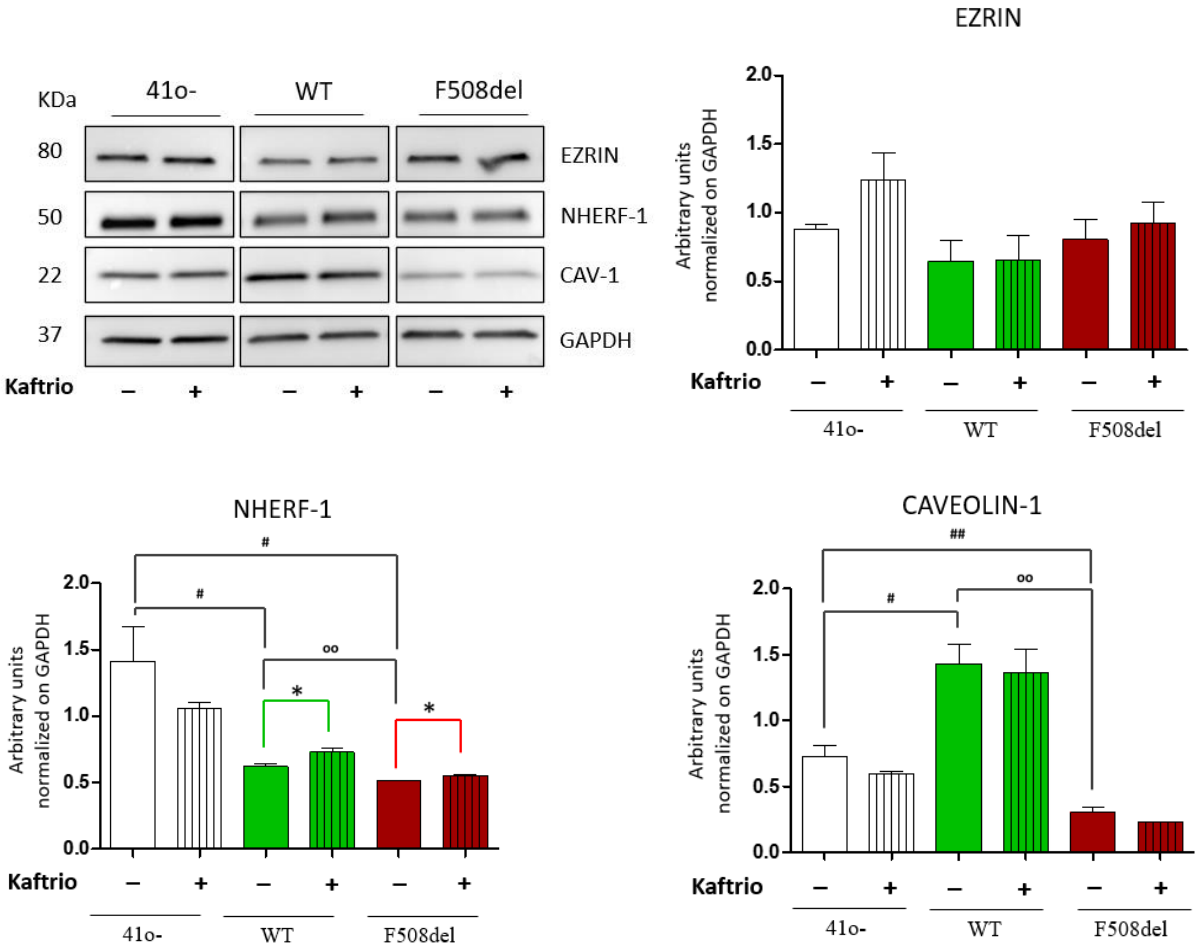

Figure 16. Expression of EZRIN, NHERF-1, and Caveolin-1 in CFBE41o-, WT CFBE, and F508del CFBE cells, treated or not with Kaftrio.

Representative images of immunoblotting showing the expression of EZRIN, NHERF-1, GAPDH. and CAV-1 (caveolin-1), and their relative quantifications. CFBE41o-, WT CFBE, and F508del CFBE cells were incubated for 24 hours with 3 µM VX-661, 2 µM VX-445, and 5 µM VX-770 and subsequently subjected to lysis. Equal amounts of proteins from lysates of cells were separated by SDS-PAGE, followed by electroblotting and chemiluminescent immunodetection after membrane incubation with primary antibodies and HRP-conjugated secondary antibodies. Changes in protein expression levels are expressed in arbitrary units as a ratio of their expression normalized on GAPDH. *p<0,05 vs untreated cells, #p<0,05, ##p<0,01 vs CFBE41o- control cells, °p<0,05, °° p<0,01 vs WT CFBE control cells.

After evaluating the expression of both CFTR and other important proteins in the macromolecular complex by immunoblotting experiments, I moved on to analyse alterations regarding the lipid counterpart in the three different cell lines.

Among the lipids that are enriched within membrane lipid rafts, a particularly relevant class consists of the sphingolipids. Therefore, the aim of the following experiments was to evaluate the possible effect of the variants of CFTR on the sphingolipid pattern. To achieve this, sphingolipids were labelled at the steady state with radioactive sphingosine ([1-^{3}H]-sphingosine), of all three cell lines. This type of assay allows, on the one hand, the labeling of all sphingolipids present in the cell, and on the other hand, the labeling of phosphatidylethanolamine obtained through the catabolic recycling of radioactive sphingosine that carries tritium in position 1. Following isotopic labeling, cells were incubated for 24 hours with the combination of VX-661, VX-445 and VX-770 or with DMSO as a control condition, as described in the "methods" section. Total lipid extracts were obtained from cell lysates, which were subsequently subjected to partitioning, separating therefore the sphingolipids into two phases: an organic phase (OP) containing the more hydrophobic lipids, and an aqueous phase (AP) containing the more hydrophilic lipids, mainly consisting in gangliosides.

As can be observed in Figure 17, most of the radioactivity measured is found in the organic phase considering all the cell lines, indicating that more than 90% of the radioactivity is associated with the hydrophobic lipids. Regarding the aqueous phases, it is observed that among the cell lines, F508del CFBE cells have the highest percentage of radioactivity. Treatment with Kaftrio does not have any effect on the distribution of radioactivity.

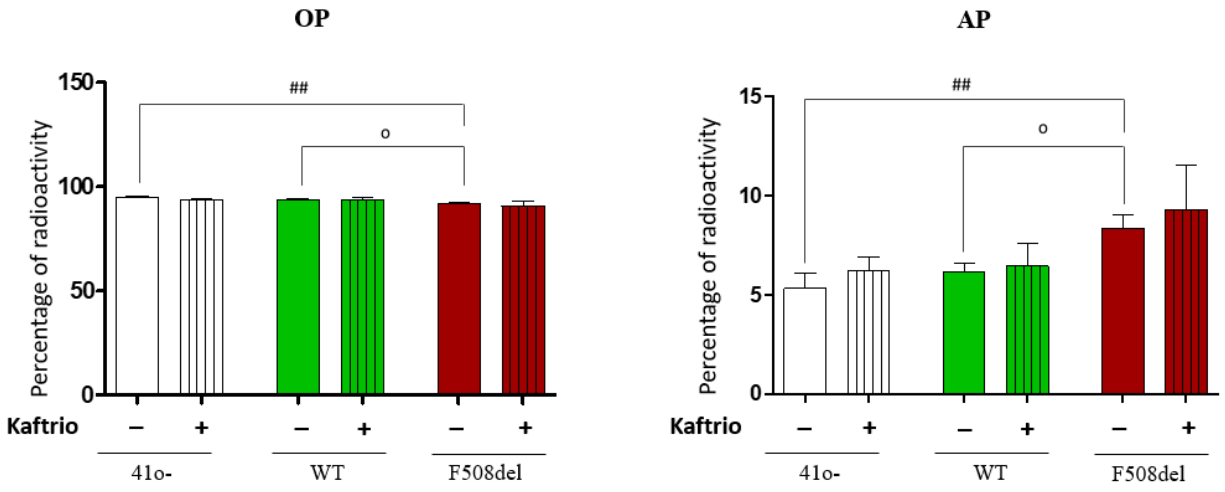

Figure 17. Percentage of radioactivity associated with the Organic Phase (OP) and Aqueous Phase (AP).

The figure represents the distribution of the radioactivity, expressed as percentage, associated to OP and AP. CFBE41o-, WT CFBE, and F508del CFBE cells were subjected to metabolic labeling at the steady state of sphingolipids with radioactive sphingosine. The radioactive sphingosine was solubilized in cell culture medium in which cells were incubated for a 2-hour pulse period. The radioactive medium was then replaced with complete medium for a 48-hour chase period. Cells were subsequently treated with the combination of modulators (3 μM VX-661, 2 μM VX-445, 5 μM VX-770) for 24 hours. Total lipid extracts were obtained from cell lysates and then partitioned into aqueous phase (AP) and organic phase (OP). Radioactivity was measured using a Beta Counter instrument. ##p<0,01 vs CFBE41o- control cells, °p<0,05 vs WT CFBE control cells.

In the following step, the different lipid components present in the organic phase and the aqueous phase were analysed.

Wherefore, after partitioning of the radioactively labelled lipid extracts, both the OP and the AP were analysed separately through separation by HPTLC (High-Performance Thin-Layer Chromatography) followed by the detection of radioactive lipids using digital autoradiography with the BetaIMAGER^{TM} Tracer System. For the separation of the lipids of the OP, the $CHCl_3$: CH_3OH: H_2O solvent system was used in a ratio of 110:40:6 by volume, whereas for the lipids of the AP I used the $CHCl_3$: CH_3OH: $CaCl_2$ (0.2%) solvent system in a ratio of 50:42:11 by volume.

In Figure 18, the lipid composition of the OP is reported. Most of the radioactivity in the organic phase is associated with two lipids: phosphatidylethanolamine (PE) and sphingomyelin (SM). When comparing different cell lines, differences in the distribution of radioactivity associated with each lipid were observed. Primarily in case of lactosylceramide (LacCer), which levels are considerably higher in cells overexpressing WT-CFTR compared to both the parental and mutated CFTR-expressing cell lines. Conversely, WT CFBE cells have a lower PE content compared to F508del CFBE cells.

Treatment with Kaftrio does not result in changes in the distribution of radioactivity among the various lipid species present in OP considering CFBE41o- cells. However, it leads to a significant reduction in the levels of LacCer both in WT CFBE cells and in cells overexpressing the mutated CFTR. In addition, in case of F508del CFBE cells Kaftrio decreases also the globotriaosylceramide (Gb3Cer) content.

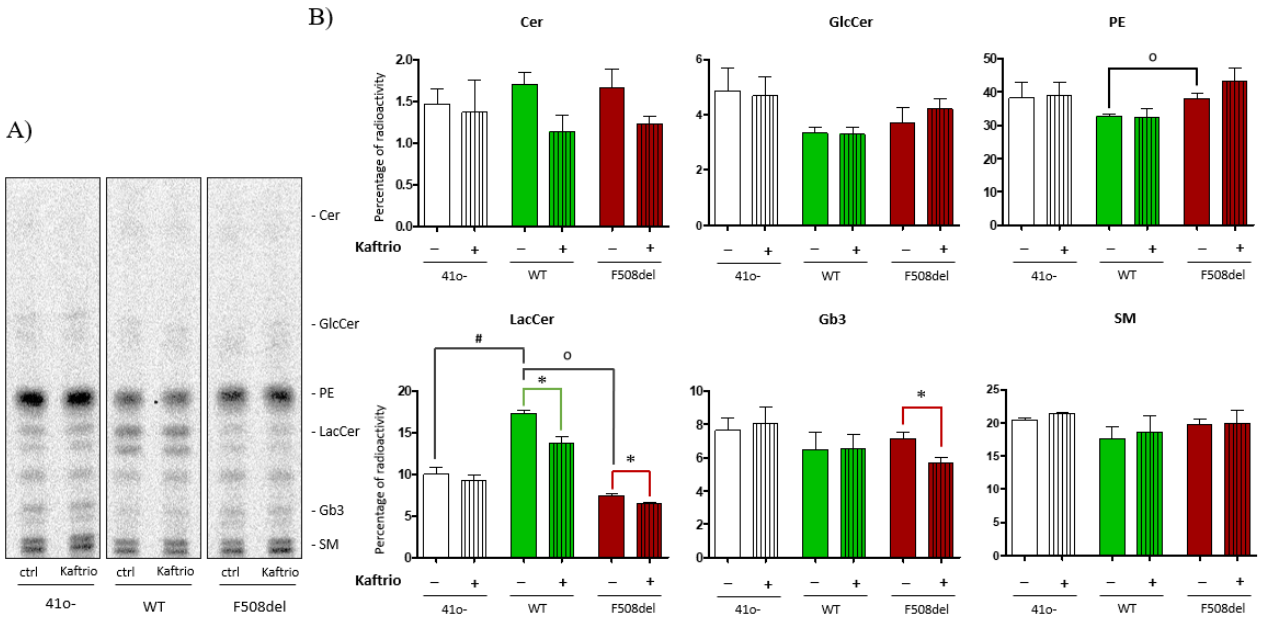

Figure 18. Lipid composition of the organic phase.

The organic phase obtained from partitioning was analysed by HPTLC (High-Performance Thin-Layer Chromatography). A total of 1000 dpm (disintegrations per minute) were spotted for each sample. Silica gel plates were used as the stationary phase, and the solvent system used was a mixture of $CHCl_3$: CH_3OH: H_2O in a ratio of 110:40:6 by volume. Radioactive lipids were visualized by BetaIMAGER™ Tracer System, and their identification was based on co-migration with known chromatographic standards. The figure includes a representative image of the TLC (A) and the corresponding graphical representations of the data obtained after analysis using the M3 Vision software (B). The values shown in the graphs represent the mean ± standard deviation and are expressed as percentage of radioactivity associated with each sample. *p<0,05 vs untreated cells, #p<0,05 vs CFBE41o- control cells, °p<0,05 vs WT CFBE control cells.

Subsequently, the aqueous phase, containing the main gangliosides, was analysed in all cell lines. As can be seen in Figure 19, diverse percentage distribution of radioactivity among the various ganglioside species can be observed in all cell lines. It can be appreciated that GM3 is the most abundant ganglioside considering all the cell lines, and its content is significantly higher in CFBE cells overexpressing F508del-CFTR compared to CFBE41o- cells. In contrast, for GM2 and GM1, cells overexpressing the mutated form of CFTR have significantly lower content compared to both the parental and WT-CFTR expressing cells. For what concerns GT1b, it is observed that its content in the F508del CFBE cell line is lower than in the WT CFBE line, which even shows a higher content of this ganglioside compared to the parental cells.

Treatment with Kaftrio has no effect on the distribution of radioactivity among the various ganglioside species present in AP regarding CFBE41o- cells. Nevertheless, in case of F508del-CFTR Kaftrio alters the ganglioside composition. For instance, the levels of GM1 and GD1a both increase upon treatment, as well as the content of GT1b, which increases considerably also in cells overexpressing WT-CFTR.

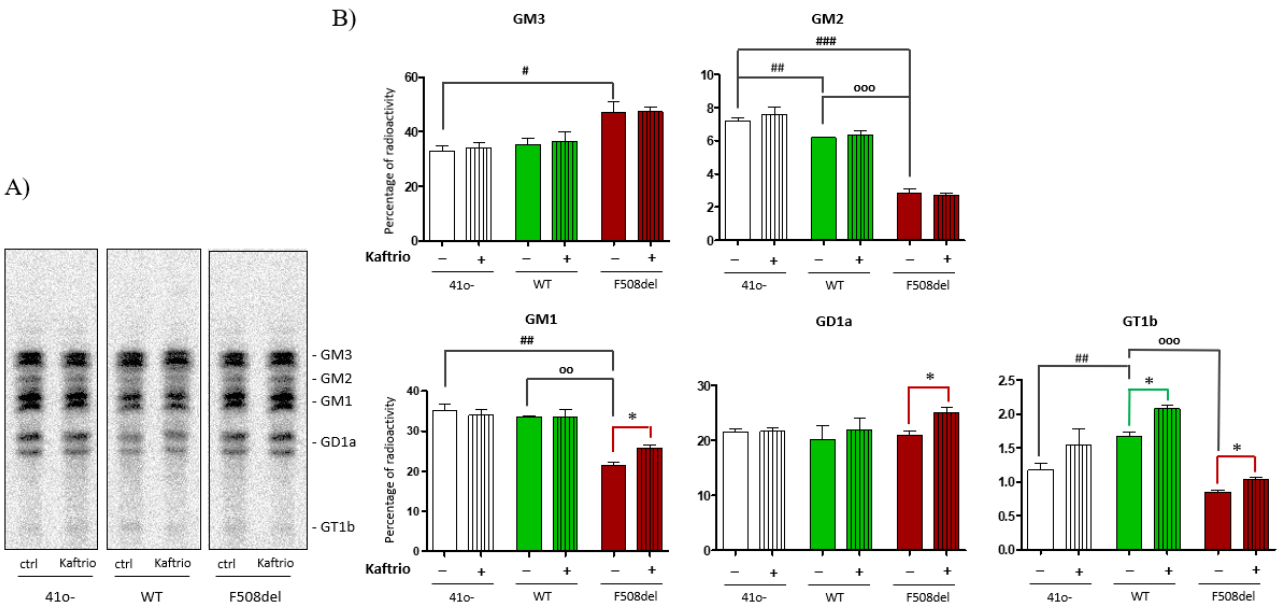

Figure 19. Lipid composition of the aqueous phase.

The aqueous phase obtained from partitioning was analysed by HPTLC. A total of 1000 dpm were spotted for each sample. Silica gel plates were used as the stationary phase, and the solvent system used was a mixture of $CHCl_3$: CH_3OH: $CaCl_2$ (0.2%) in a ratio of 50:42:11 by volume. Radioactive lipids were visualized by BetaIMAGER™ Tracer System. The figure includes a representative image of the TLC (A) and the corresponding graphical representations of the data obtained after analysis using the M3 Vision software (B). The values shown in the graphs represent the mean ± standard deviation and are expressed as percentage of radioactivity associated with each sample. *p<0,05 vs untreated cells, #p<0,05, ##p<0,01, ###p<0,001 vs CFBE41o- control cells, °p<0,05, °°p<0,01, °°°p<0,001 vs WT CFBE control cells.

Since I observed significant differences in the lipid pattern between WT CFBE and F508del CFBE cells, even after Kaftrio treatment, whereas not in case of CFBE41o- cell line, I decided to evaluate the effect of the single components of Kaftrio on the lipid composition in the two CFBE cell lines overexpressing either the WT protein or the mutated one.

Therefore, following isotopic labeling of WT CFBE and F508del CFBE cells, they were treated with the single modulators, such as 3 μM VX-661, 2 μM VX-445, and 5 μM VX-770, or their combination, as Kaftrio. After a 24-hour incubation with the CFTR modulators, total lipid extracts were obtained from cell lysates, which were subsequently subjected to partitioning separating the aqueous phase and the organic phase.

The lipid patter of the OP is shown in Figure 20. As observed in the previous experiment, most of the radioactivity in the organic phase is associated with the PE and SM. The Cer, GlcCer, PE and SM contents are mainly similar in the two cell lines and their levels are not influenced significantly by the modulators. Only for LacCer, I observed significantly higher levels in WT CFBE cells with respect to CFBE cells expressing the mutated protein, however, in both cell lines its level is notably decreased upon treatment with either the potentiator, VX-770, or Kaftrio. Considering instead the levels of the Gb3, its content is higher in F508del CFBE cells, and the treatment with the VX-770 or Kaftrio induces its decrease.

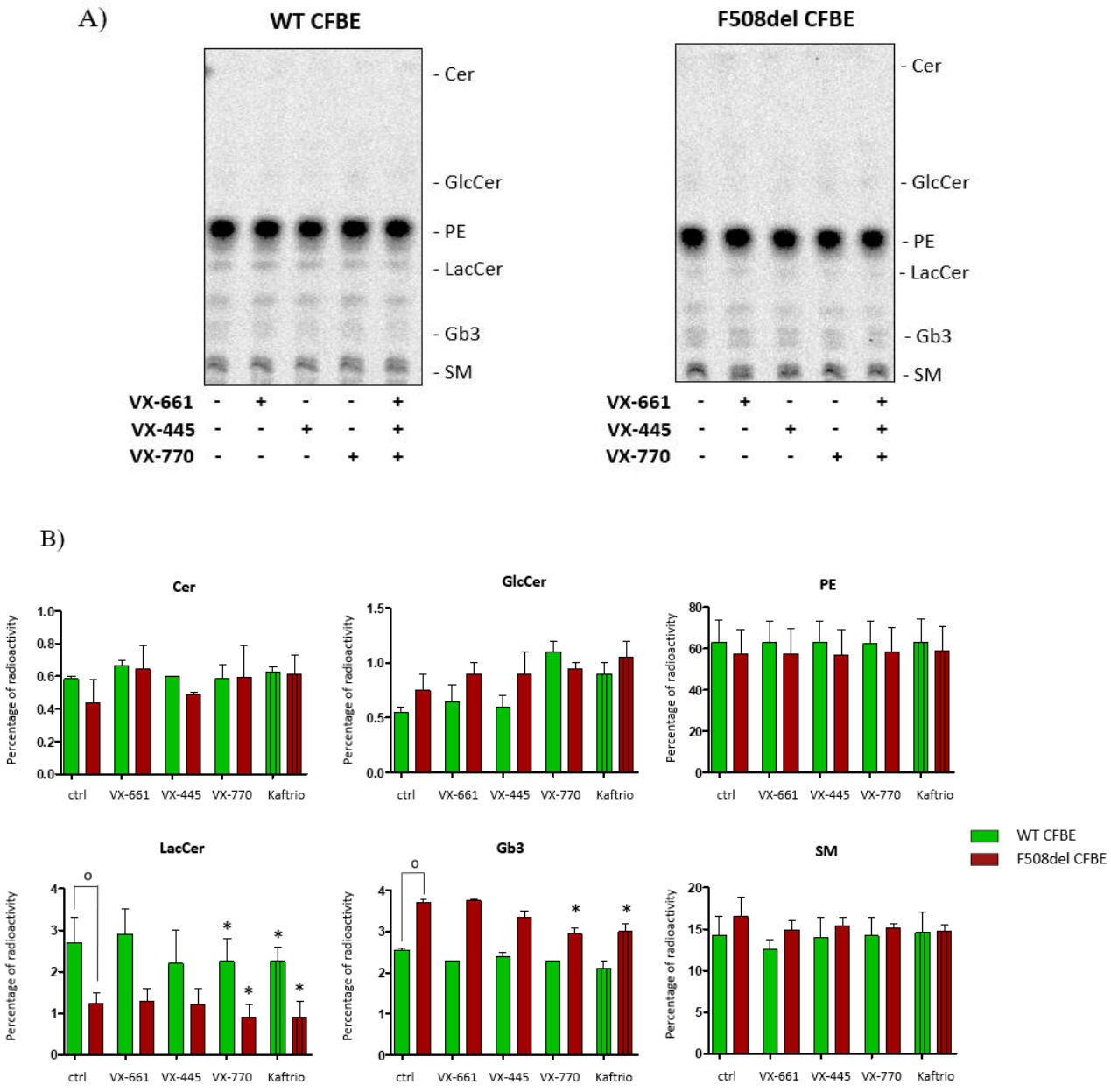

Figure 20. Effect of CFTR-modulators on the lipid composition of the OP.

The figure reports a representative digital autoradiography of two HPTLC loaded with aliquots of the organic phases (OP) obtained from either WT CFBE or F508del CFBE cells (A), and the corresponding graphical representations of the data obtained after analysis using the M3 Vision software (B). Cells were treated or not with correctors (3 μM VX-661, 2 μM VX-445) or potentiator (5 μM VX-770) singularly or in combination for a 24-hour incubation time after feeding cells with radioactive sphingosine. Then cells were subjected to lipid extraction, followed by partitioning to obtain the OP. Lipids were separated by HPTLC using the solvent system $CHCl_3$: CH_3OH: H_2O in a ratio of 110:40:6 by volume. The values shown in the graphs represent the mean ± standard deviation and are expressed as percentage of radioactivity associated with each sample. *p<0,05 vs untreated cells, °p<0,05 vs WT CFBE control cells.

In Figure 21 are reported the analyses of the AP. The most profuse ganglioside is the GM3, and its content tends to be higher in F508del CFBE cells compared to WT CFBE cells, as observed before. Controversially, GM2 and GM1 levels are significantly lower in CFBE cells overexpressing the F508del-CFTR, as is the case for GT1b. The treatment with the single drugs of Kaftrio formulation does not exert any effect on the distribution of radioactivity in the different ganglioside species. However, in case of F508del-CFTR Kaftrio induces an increase in the levels of both GM1 and GD1a, as well as in the levels of GT1b, which increases significantly also in cells overexpressing WT-CFTR.

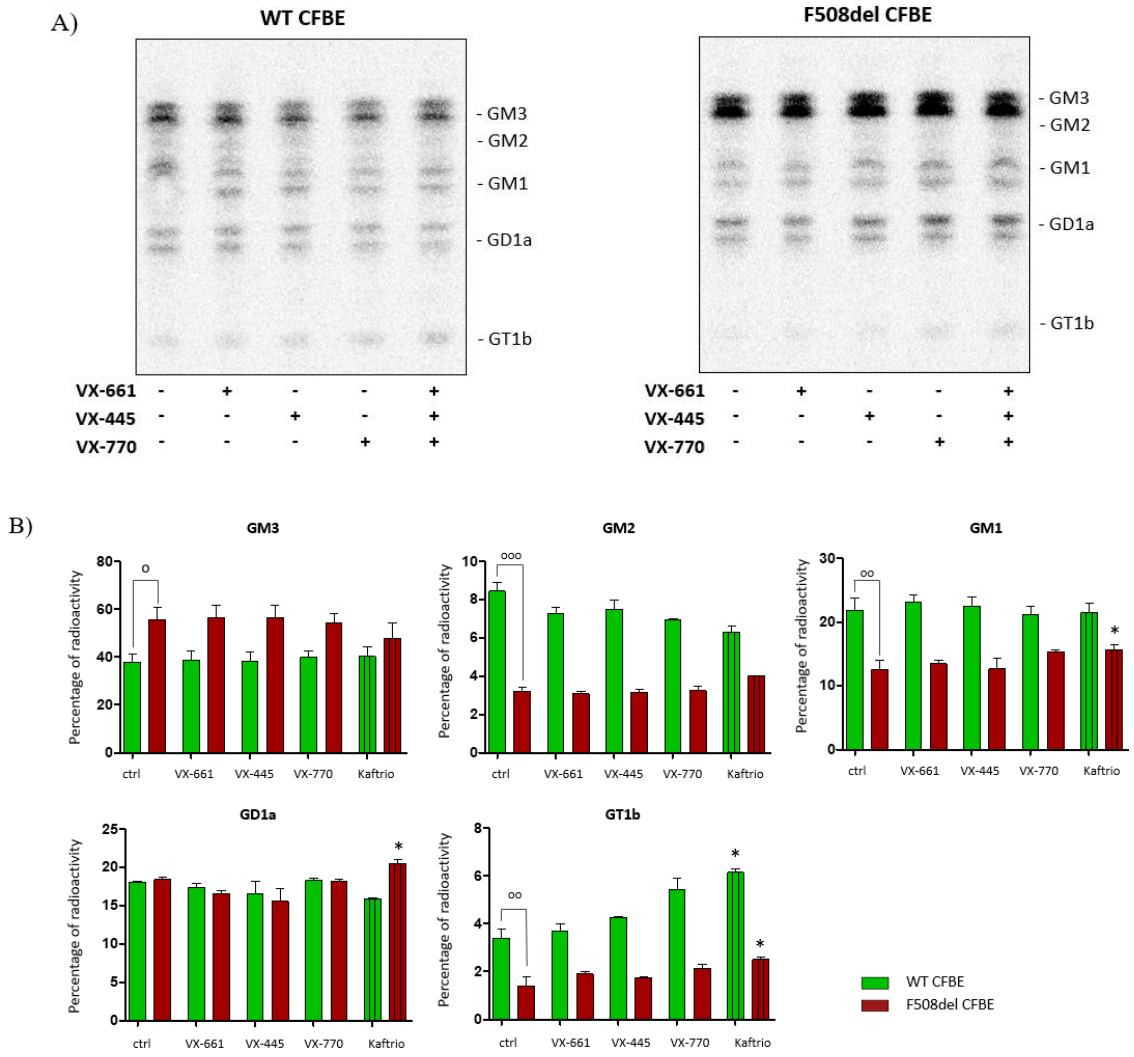

Figure 21. Effect of CFTR-modulators on the lipid composition of the AP.

The figure reports a representative digital autoradiography of two HPTLC loaded with aliquots of the aqueous phases (AP) obtained from either WT CFBE or F508del CFBE cells (A), and the corresponding graphical representations of the data obtained after analysis using the M3 Vision software (B). Cells were treated or not with correctors (3 μM VX-661, 2 μM VX-445) or potentiator (5 μM VX-770) singularly or in combination for a 24-hour incubation time after feeding cells with radioactive sphingosine. Then cells were subjected to lipid extraction, followed by partitioning to obtain the AP. Lipids were separated by HPTLC using the solvent system $CHCl_3$: CH_3OH: $CaCl_2$ (0.2%) in a ratio of 50:42:11 by volume. The values shown in the graphs represent the mean ± standard deviation and are expressed as percentage of radioactivity associated with each sample. *p<0,05 vs untreated cells, °p<0,05, °°p<0,01, °°°p<0,001 vs WT CFBE control cells.

Since besides the SLs also cholesterol is involved in the organisation of the lipid environment of CFTR, I examined the differences in the cholesterol content of both WT CFBE and F508del CFBE cells treated or not with the correctors and potentiator.

CFBE cells overexpressing either the WT or the mutated form of the CFTR were treated with the single modulators (3 μM VX-661, 2 μM VX-445, and 5 μM VX-770) or their combination, as Kaftrio. After a 24-hour incubation, total lipid extracts were obtained from cell lysates, as described in the "methods" section, and analysed by HPTLC using the solvent system C_6H_{14}: $CH_3CO_2CH_2CH_3$ (3:2, v: v). As it can be seen from Figure 22, the cholesterol content of F508del CFBE cells is remarkably diminished with respect to WT CFBE cells. Moreover, considering the effect of the single modulators, apart from the corrector, VX-661, all of them cause a lower or higher but significative decrease in the cholesterol content, as well as Kaftrio, reducing even more the level of this lipid.

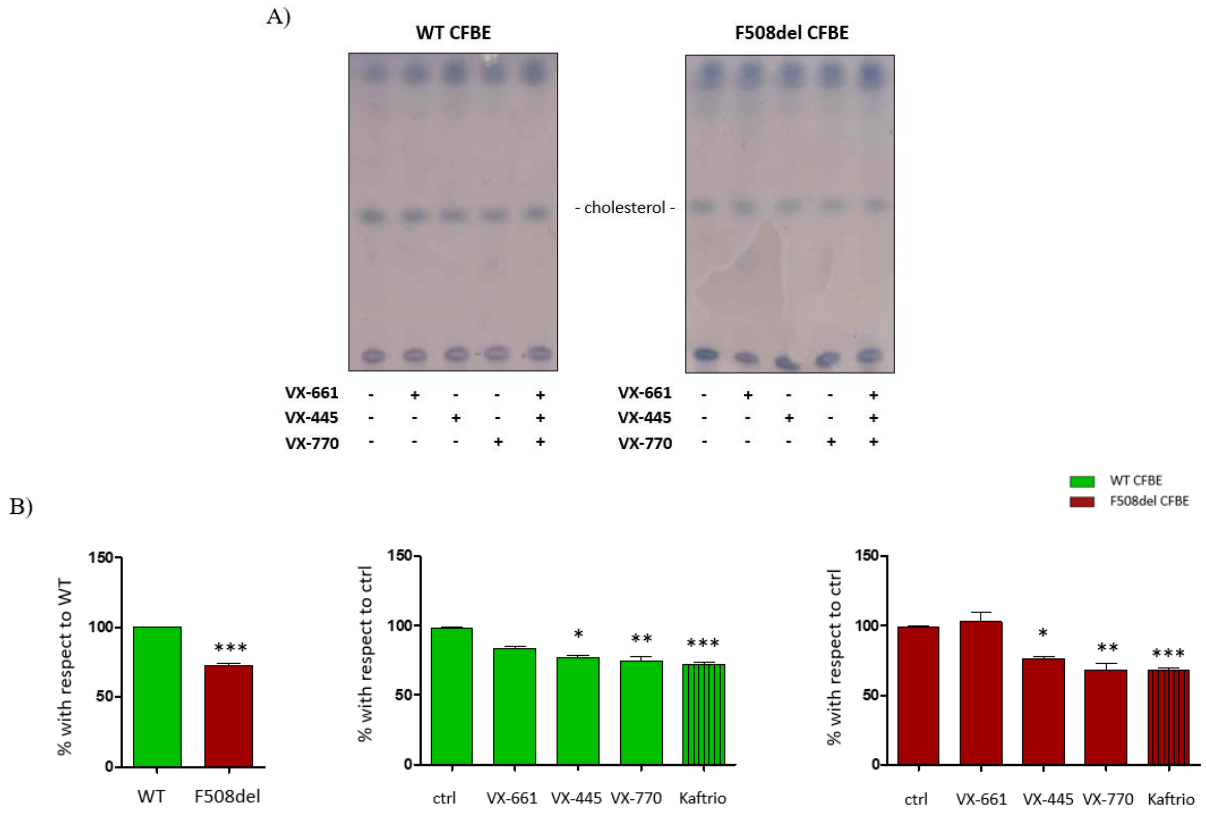

Figure 22. Evaluation of cholesterol content in WT and F508del CFBE cells, also after Kaftrio treatment.

The figure reports a representative endogenous cholesterol pattern of two HPTLC loaded with the total lipid extracts obtained from WT CFBE and F508del CFBE cells (A), and the corresponding graphical representations of the data obtained (B). Cells were treated or not with the CFTR-modulators (3μM VX-661, 2μM VX-445, 5μM VX-770, or their combination as Kaftrio), for a 24-hour incubation time, then cells were harvested, lysed, and subjected to lipid extraction. Lipids were separated by HPTLC using the solvent system C_6H_{14}: $CH_3CO_2CH_2CH_3$ in a ratio of 3:2 by volume. Data was obtained by spraying the prepared TLC with anisaldehyde, and by quantifying the intensity of the bands with ImageJ. Data are expressed in the graphs as fold change (%) with respect to untreated/WT cells. *p<0.05, **p<0.005, ***p<0.0005 vs untreated/WT cells.

As I have already observed, the presence of different forms of CFTR has a specific effect on the expression of important proteins of the CFTR macromolecular complex, as well as on the lipid composition. As follows, I evaluated possible alterations in the activity of enzymes involved in the sphingolipid pathway, considering all three cell lines. The data from literature suggest that the expression of the mutated forms of CFTR influences the endo-lysosomal compartment. Accordingly, I assessed the enzymatic activity of key lysosomal glycohydrolases, particularly those involved in the sphingolipid catabolism, primarily in total cell lysates. These cell lysates were obtained from the three cell lines, CFBE41o-, WT and F508del CFBE cells, treated or not with the combination of modulators for 24 hours. A protein assay was performed to ensure that the enzymatic analysis was conducted using the same amounts of cellular proteins, as described in the "methods" section. Total enzymatic activities were measured as picomoles of product formed per hour per milligram of protein, and they were normalized to the activity measured in CFBE41o- control cells. The graphs are presented in Figure 23.

Total β-glucosidase (β- Glc TOT) activity seems to be augmented in F508del CFBE cells with respect to WT CFBE and CFBE41o- cells, moreover, considering all cell lines, Kaftrio increases its level. The activity of the lysosomal β-glucocerebrosidase (GCase) appears to be higher in cells overexpressing either the WT- or the mutated CFTR, compared to the parental cell line. Specifically, in F508del CFBE cells, this activity is nearly double that of CFBE41o- cells. In all three cell lines, there is a tendency for an increase in GCase activity following treatment with Kaftrio, although this is significant only in the case of CFBE41o- cells.

Regarding β-galactosidase (β-Gal) activity, an increase is observed in both WT and F508del CFBE cells, approximately 1.3-fold and 1.5-fold of that observed in CFBE41o- cells. However, unlike in case of GCase, treatment with modulators results in a statistically significant decrease in β-Gal enzymatic activity in cells overexpressing CFTR, both in the WT and mutated forms.

For what concerns total β-hexosaminidase activity (β-Hex TOT), it is significantly higher in WT CFBE cells compared to the other cell lines considered. β-Hex is a dimeric enzyme composed of two subunits and exists in three isoforms in human cells: Hex A (consisting of one α subunit and one β subunit), Hex B (consisting of two β subunits), and Hex S (consisting of two α subunits). Total β-Hex activity is evaluated using the florigenic substrate 4-MUB-N-acetyl β-D-glucosaminide (MUG), which is a substrate for both subunits. However, it is possible to discriminate its activity using the florigenic substrate 4-MUB-N-acetyl β-D-glucosaminide-6-sulfate (MUGS), which allows assessment of Hex S activity in addition to the fraction of Hex A activity, attributable to the α subunit. The enzymatic activity expressed on the MUGS substrate, indicated in the graph as β-Hex A+S, is

considerably lower (about 1/20) with respect to the total activity, in all three cell lines. On the other hand, it is interesting to note that this activity increases in F508del cells, constituting approximately 1/12 of the total hexosaminidase activity. Treatment with modulators induces a significant decrease in both total activity and α subunit-specific activity in CFTR-expressing cells, WT or F508del, while it has no effect on the parental cell line.

The evaluation of total sphingomyelinase (SMase) enzymatic activity presented some issues, as it was highly variable within the triplicate and did not allow for significant deviations to be observed either between different cell lines or between control cells and those treated with Kaftrio.

Finally, the enzymatic activity of two other enzymes were analysed, that unlike the previous ones, do not act directly on the sphingolipid component but can provide indications about the effect of CFTR expression and modulator treatment on the endo-lysosomal compartment. These enzymes are two mannosidases, α-mannosidase (α-Man) and β-mannosidase (β-Man), capable of removing terminal mannose residues linked by α 1-3, α 1-6, and β 1-4 bonds. For both enzymes, the expression of the mutated form of CFTR appears to have an effect in increasing their activity (1.4 times and 2 times with respect to CFBE41o- for α-Man and β-Man, respectively). Instead, the expression of the WT protein has the opposite effect on the activity of these two enzymes; α-Man decreases slightly compared to parental CFBE cells, while β-Man increases (1.5 times that of CFBE41o-). Once again, as observed for the other enzymes, with the sole exception of GCase which behaves oppositely, treatment with Kaftrio leads to a reduction in the enzymatic activities of both α-Man and β-Man in CFTR-expressing cell lines.

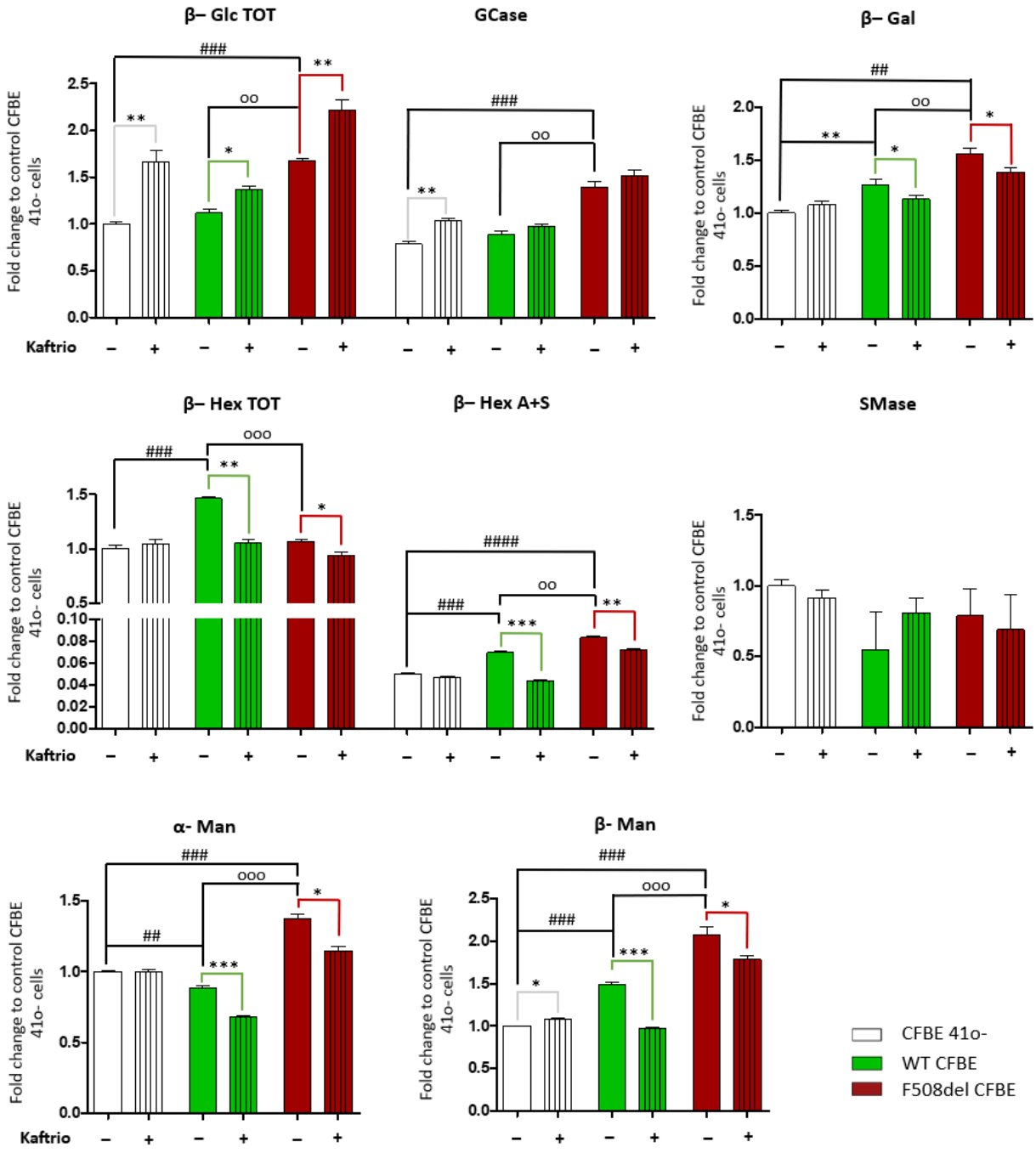

Figure 23. Effect of Kaftrio on the activity of lysosomal hydrolases in total cell lysates.

CFBE41o-, WT CFBE, and F508del CFBE cells were treated or not with the combination of modulators (3 μM VX-661, 2 μM VX-445, 5 μM VX-770) for 24 hours, and cellular lysates were obtained as described in the "methods" section. Protein concentration was determined using the DC protein assay, and enzymatic assays were performed at an equal protein concentration. The enzymatic activities of β- Glc TOT, GCase, β-Gal, β-Hex TOT, β-Hex A+S, SMase and α-Man, β-Man were determined using florigenic substrates. The values represented in the graphs are the mean ± standard deviation of enzymatic activities calculated as picomoles of product formed per hour per mg of protein, normalized to the activity measured in CFBE41o- control cells. *p<0.05, **p<0.01, ***p<0.001 vs untreated cells, ##p<0.01, ###p<0.001, ####p<0.0001 vs CFBE41o- control cells, °°p<0.01, °°°p<0.001 vs WT CFBE control cells.

Cells respond to alterations in the endo-lysosomal compartment through the activation of lysosomal exocytosis. This process involves the fusion of the lysosomal membrane with the cell plasma membrane, resulting in the release of the lysosomal content into the extracellular environment, and the association of lysosomal enzymes, present on the inner side of the lysosomal membrane, with the outer surface of the plasma membrane. Based on this evidence, I evaluated the enzymatic activities of the same enzymes considered previously, along with the addition of NLGase described as a non-lysosomal β-glucocerebrosidase predominantly associated with the cell surface, at the PM level.

Enzymatic activities associated with the cell surface were assessed directly on live cells plated in a 96-well plate and treated or not with modulators for 24 hours. After surface enzymatic assays, protein quantification was performed to assess the cellular protein content in each well. This allowed the calculation of enzymatic activities, expressed as picomoles of product formed per hour per milligram of cellular proteins. The graphs representing surface enzymatic activities, normalized to the activity measured in CFBE41o- control cells, are shown in Figure 24. As observed previously, both β-Glc TOT and GCase activity is increased in cells expressing the CFTR protein, particularly in F508del CFBE cells, compared to parental cells that lack CFTR expression. Surface β-Glc TOT activity results from the contributions of NLGase, a typical membrane enzyme, and of the lysosomal enzyme GCase, which is present on the surface due to lysosomal exocytosis. Both enzymes contribute roughly equally to β-Glc TOT activity but are influenced differently by treatment with Kaftrio. While Kaftrio treatment increases NLGase activity in all three cell lines, an opposite trend is observed for GCase. Surface enzymatic activity of β-Gal, as observed before for its total activity, is significantly higher in CFTR-expressing cells compared to CFBE41o- cell line, however, no effect on surface enzyme activity was observed following treatment with the CFTR modulator. Regarding the surface β-Hex TOT activity, the cell lines expressing different forms of CFTR exhibit higher enzymatic activity compared to the parental line. An effect of Kaftrio treatment is detected only in F508del cells, which show a reduction in β-Hex TOT activity. When evaluating β-Hex A+S activity, increased values are observed only in cells expressing the mutated form of CFTR, with a notable decrease in its activity following Kaftrio treatment. The measurement of the surface activity of plasma membrane associated SMase shows that its activity is higher in WT cells compared to parental cells, and it is further elevated in F508del cells. In CFTR-expressing lines, Kaftrio has the effect of reducing SMase enzymatic activity. Finally, the levels of activity of both surface associated mannosidases are higher in cells expressing the mutated form of CFTR regarding the other cell lines. Treatment with the drug leads to a tendency of reducing both α-Man and β-Man activities associated with the plasma membrane in all three cell lines, although the reduction is statistically significant only for α-Man activity in WT cells and β-Man activity in F508del cells.

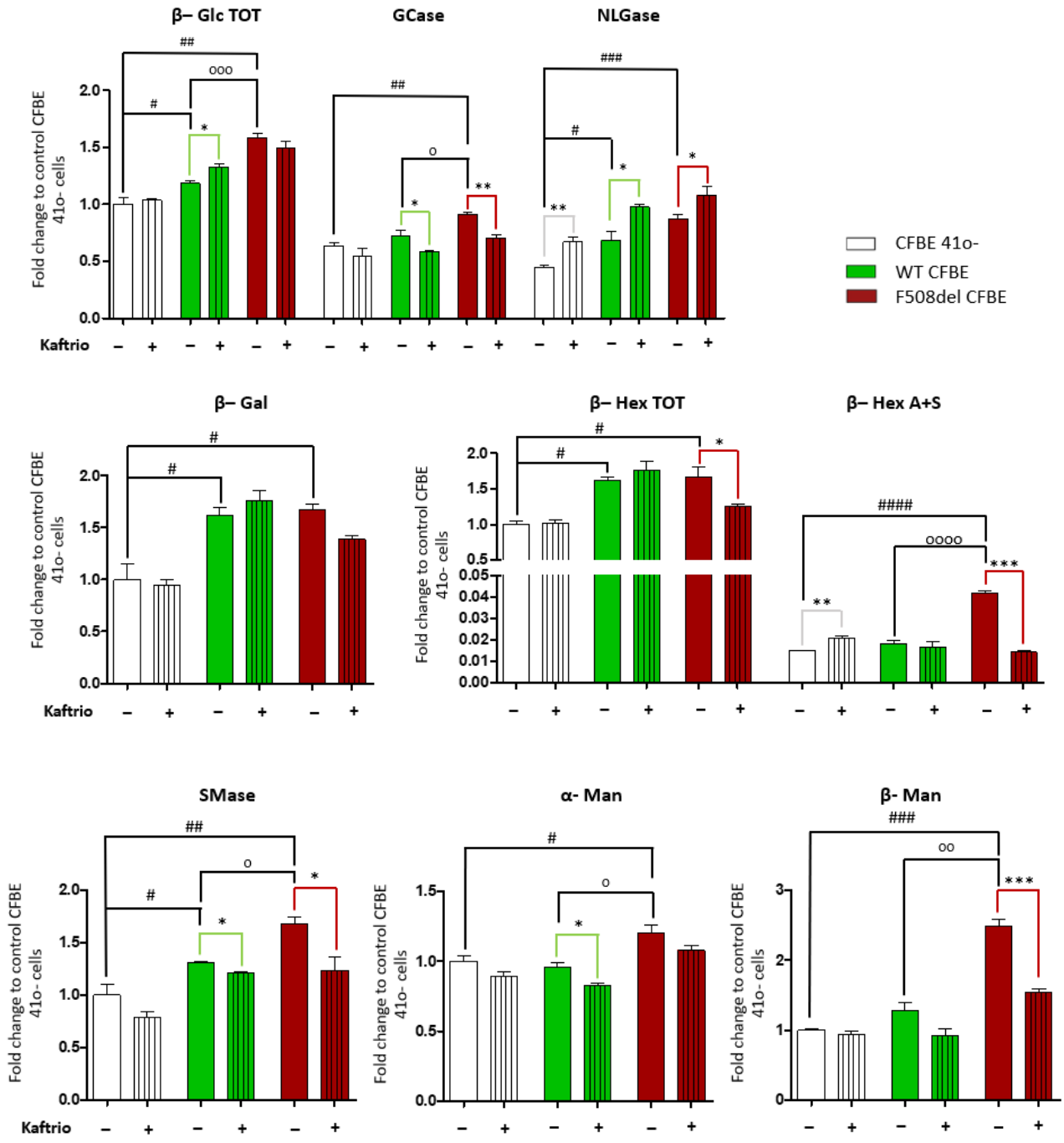

Figure 24. Effect of Kaftrio on the activity of lysosomal hydrolases on the cell surface.

CFBE41o-, WT CFBE, and F508del CFBE cells were plated in 96-well plates and treated or not with the combination of modulators (3 μM VX-661, 2 μM VX-445, 5 μM VX-770) for 24 hours. PM associated activities of β-Glc TOT, GCase, NLGase, β-Hex TOT, β-Hex A+S, β-Gal, SMase, α-Man, and β-Man were determined on living cells by a high throughput assay using artificial florigenic substrates. The values represented in the graphs are the mean ± standard deviation of enzymatic activities calculated as picomoles of product formed per hour per mg of protein, normalized to the activity measured in CFBE41o- control cells. *p<0.05, **p<0.01, ***p<0.001 vs untreated cells, #p<0.05, ##p<0.01, ###p<0.001, ####p<0.0001 vs CFBE41o- control cells, °p<0.05, °°p<0.01, °°°p<0.001, °°°°p<0.0001 vs. WT CFBE control cells.

I have distinguished some variations in the activity of glycohydrolases involved in the sphingolipid pathway regarding CFBE41o-, WT CFBE and F508del CFBE cells, especially after treatment with Kaftrio. Nevertheless, the most striking differences were noted in case of the two CFBE cell lines overexpressing either WT-CFTR or F508del-CFTR.

Thereafter, I assessed the effect of the single components of Kaftrio on the total enzymatic activity of the main hydrolases, in particularly those involved directly in the sphingolipid catabolism. Hence, cell lysates were obtained from WT and F508del CFBE cells treated or not with the single modulators, such as 3 μM VX-661, 2 μM VX-445, and 5 μM VX-770, or their combination, as Kaftrio. A protein assay was conducted to perform the analysis using the same amounts of proteins. Total enzymatic activities were measured as picomoles of product formed per hour per milligram of proteins and the corresponding graphs are presented in Figure 25.

As it can be observed, the enzymatic activity of almost all enzymes analysed, with the only exception of β-Hex TOT, is notably higher in F508del CFBE cells with respect to WT cells, confirming also the results obtained previously. Treatment with the correctors, both VX-661 and VX-445, does not induce any modifications in the enzymatic activity of all hydrolases considered, however, the potentiator, VX-770, does. In case of β- Glc TOT, GCase and NLGase, the VX-770 increased their enzymatic activity considering both cell lines. The activity of β- Glc TOT and NLGase was elevated also after administration of all the modulators, as Kaftrio, in both cell lines, whilst is case of GCase, it seems to lead only to a tendency for increase. This evidence suggests that the increasing enzymatic activity of these lysosomal enzymes is due to the effect of the potentiator, and that the increase in β-Glc TOT activity after treatment is attributable to an augmented activity of the non-lysosomal β-glucocerebrosidase. On the other hand, as seen before, Kaftrio, but not the single modulators, cause a significative decrease in the enzymatic activities of both β-Hex TOT and β-Hex A+S in WT and F508del CFBE cells, whereas β-Gal activity is decreased only in cells expressing the mutated protein.

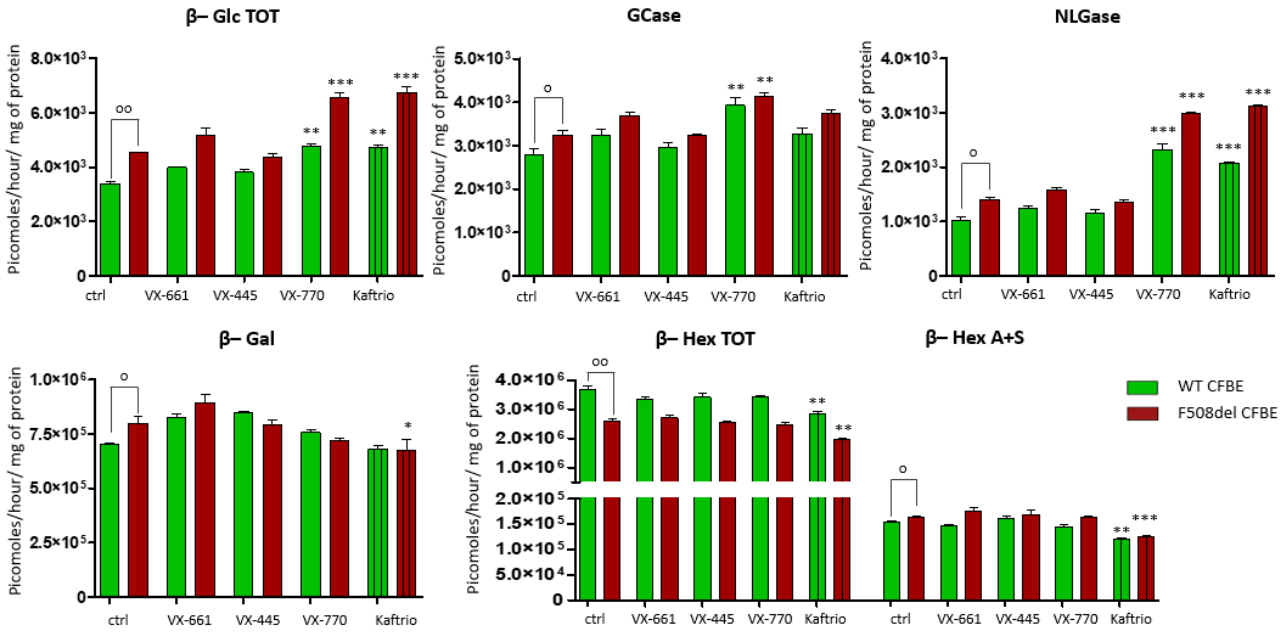

Figure 25. Effect of CFTR-modulators on the activity of lysosomal hydrolases in total cell lysates.

WT CFBE and F508del CFBE cells were treated or not with correctors (3 μM VX-661, 2 μM VX-445) or potentiator (5 μM VX-770) singularly or in combination for a 24-hour incubation time, and cellular lysates were obtained as described in the "methods" section. Protein concentration was determined using the DC protein assay, and enzymatic assays were performed at an equal protein concentration. The enzymatic activities of β-Glc TOT, GCase, NLGase, β-Gal, β-Hex TOT and β-Hex A+S were determined using florigenic substrates. The values represented in the graphs are the mean ± standard deviation of enzymatic activities calculated as picomoles of product formed per hour per mg of protein. *p<0.05, **p<0.005, ***p<0.0005 vs untreated cells, °p<0.05, °°p<0.005 vs WT CFBE control cells.

Finally, considering the effect of Kaftrio on the sphingolipid pattern and on the enzymatic activity of lysosomal glycohydrolases, both in total cell lysates and at the cell surface, I investigated its impact on two key enzymes involved in the metabolism of sphingolipids in CFBE cells overexpressing the WT or the F508del-CFTR. Particularly, I evaluated the activity of the GM3 synthase, known also as sialyl-transferase 1 (SAT1), and of the sialidase Neu3. GM3 synthase is an important enzyme in the biosynthesis of the ganglioside GM3. It transfers a sialic acid onto the LacCer hence forming the GM3, which is the precursor of all complex gangliosides, including GM1 and GD1a. On the other hand, sialidase Neu3 is an essential enzyme in the catabolism of gangliosides, as it cleaves the terminal sialic acid residues from gangliosides to form less complex one. In particular, it is responsiben for the formation of LacCer by removing the sialic acid from GM3.

For this reason, WT and F508del CFBE cells were treated with the two correctors, 3 μM VX-661, 2 μM VX-445, and the potentiator, 5 μM VX-770, for a 24-hour incubation time. The day after, cells were harvested, collected, and homogenized to obtain the cell homogenates. Appropriate volumes of

cell homogenates were used together with the relevant radioactive derivative of the natural substrate of each enzyme. Then, aliquots of the lipid extracts, obtained from each enzymatic reaction mixtures, were analysed by HPTLC. Results of the activity measured for GM3 synthase and sialidase Neu3 are showed in Figures 26 and 27, respectively.

The activity of GM3 synthase is higher in F508del CFBE cells respecting WT CFBE cells, and this result corrisponds with the higher GM3 levels in cells expressing the mutated protein, found previously in the lipis analyis experiements. Interestingly, treatment with Kaftrio elevates its activity only in the mutated cell line. These results are in line with the previous findings about the increased content of the GM1 and GD1a of treated F508del CFBE cells and a parallel reduction of the lactosylceramide (Figure 26).

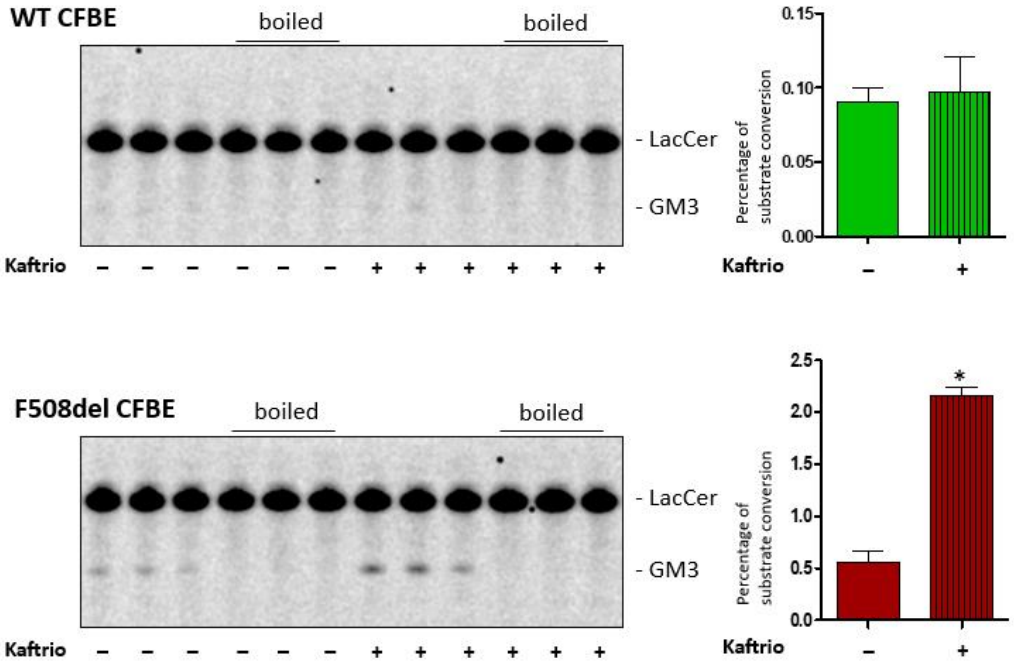

Figure 26. Evaluation of the effect of Kaftrio on the enzymatic activity of GM3 synthase.

CFBE cells overexpressing WT or F508del CFTR were treated or not with Kaftrio (3 μM VX-661, 2 μM VX-445 and 5 μM VX-770) for 24 hours. Aliquots of cell lysates were used for the enzymatic assay, together with the radioactive natural substrate of the GM3 synthase enzyme (^{3}H-Lactosylceramide). Boiled aliquots of cell lysates were used as control. An aliquot of the lipid extract obtained from the enzymatic reaction mixture was separated by HPTLC using the solvent system $CHCl_3$: CH_3OH: 0.2 % $CaCl_2$ (50: 42: 11, v: v: v), and the radioactivity associated with the sphingolipids was measured by digital autoradiography and quantified by M3 Vision software. In the graph, data are reported as percentage of the substrate conversion in ^{3}H-GM3 by the GM3 synthase enzyme. *p< 0.05 vs untreated cells.

Regarding the sialidase Neu3 activity, as shown in Figure 27, WT CFBE cells are charaterized by a significantly higher activity with respect to F508del CFBE cells, nearly double, explaining the elevated levels of the LacCer or GM1 in WT CFBE cells. Treatment with Kaftrio reduces the sialidase activity in both cell lines further supporting preceding findings about the increased levels of GD1a in treated cells.

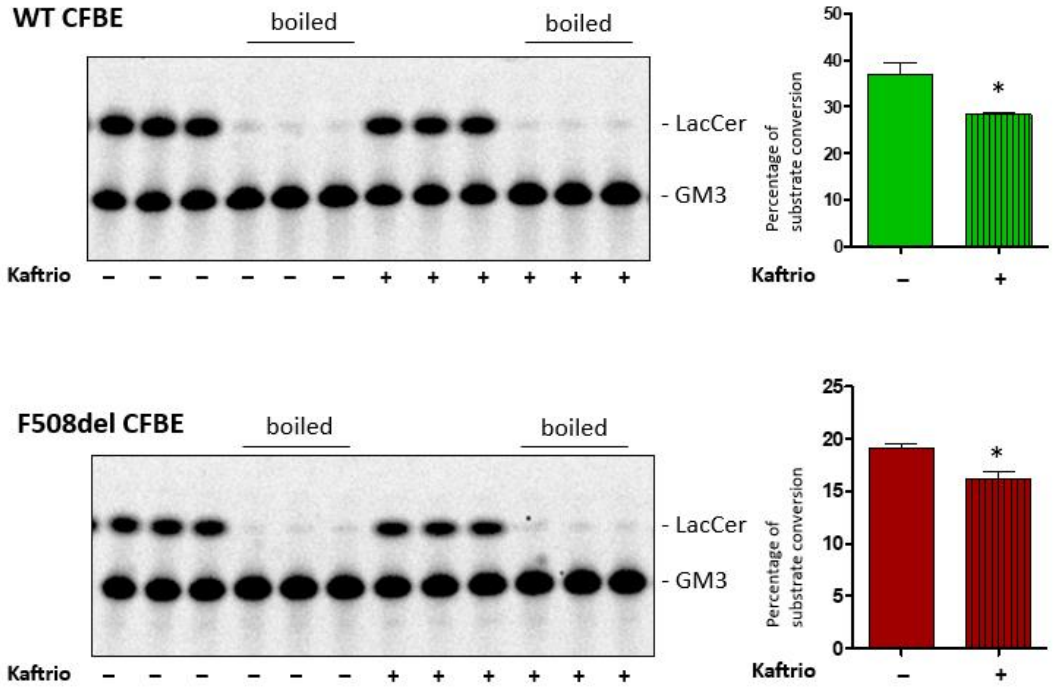

Figure 27. Evaluation of the effect of Kaftrio on the enzymatic activity of the sialidase Neu3.

CFBE cells overexpressing the WT or F508del CFTR were treated or not with Kaftrio (3 μM VX-661, 2 μM VX-445 and 5 μM VX-770) for 24 hours. Aliquots of cell lysate were used for the enzymatic assay, together with the radioactive natural substrate (^{3}H-GM3). Boiled aliquots of cell lysates were used as control. An aliquot of the lipid extract obtained from the enzymatic reaction mixture was separated by HPTLC using the solvent system $CHCl_3$: CH_3OH: 0.2 % $CaCl_2$ (50: 42: 11, v: v: v), and radioactivity associated with the sphingolipids was measured by digital autoradiography and quantified by M3 Vision software. In the graph data are reported as percentage of substrate hydrolysis to ^{3}H-Lactosylceramide by the sialidase enzyme. *$p < 0.05$ vs untreated cells.

Effect of the ganglioside GM1, its derivative Liga20, and its molecular species on the maturation of F508del-CFTR rescued by Kaftrio.

Despite Kaftrio displays an important beneficial role in the maturation of the F508del-CFTR, several indications point out the necessity to further improve the rescue of the mutated protein. It was seen that exogenous administration of the ganglioside GM1 to F508del CFBE cells treated with Orkambi counteracted the destabilizing effects of the potentiator VX-770 on the stability of the rescued CFTR, increasing both the cellular content of the mature form of the protein and its channel activity [43]. To this purpose, part of my PhD project was aimed to investigate the possible beneficial effects of GM1 administration on the maturation and stabilisation of F508del-CFTR rescued by Kaftrio treatment.

Therefore, F508del CFBE cells were fed with the correctors VX-661 and VX-445, alone or in combination with the potentiator VX-770, and in presence or not of exogenously administered GM1. I have used the same concentration for GM1 as described in *Mancini et al, 2020* [43]. As shown in Figure 28, treatment with the correctors improves the formation of the band-c of F508del-CFTR supporting an increase in the active form of the protein. With the addition of the VX-770 the band-c undergoes to only a slight decrease, a side-effect of the potentiator described in diverse articles. Upon the exogenous administration of GM1, the effect of the two correctors is more evident not only for the increase of the band-c but also of the band-b. Nevertheless, in presence of the GM1 the negative effect of the VX-770 is still present, even if the total amount of CFTR, consisting in the band-c and -b, is higher when compared to the condition without GM1. Furthermore, I tested the effect of the GM1 analogue, Liga20, on the maturation of F508del-CFTR. First, I evaluated whether this molecule is toxic for bronchial epithelial cells testing the same concentration used for the ganglioside GM1. The treatment showed a possible toxic effect at 50 μM or above (data not shown), for this reason in my experiments I decided to use the concentration of 10 μM where no toxic effect was observed. As shown in Figure 28, the data obtained with the co-treatment of F508del CFBE cells with Liga20, either in presence of the two correctors, VX-661 and VX-445, or the Kaftrio formulation, are similar to those obtained after administering GM1 simultaneously to the CFTR modulators.

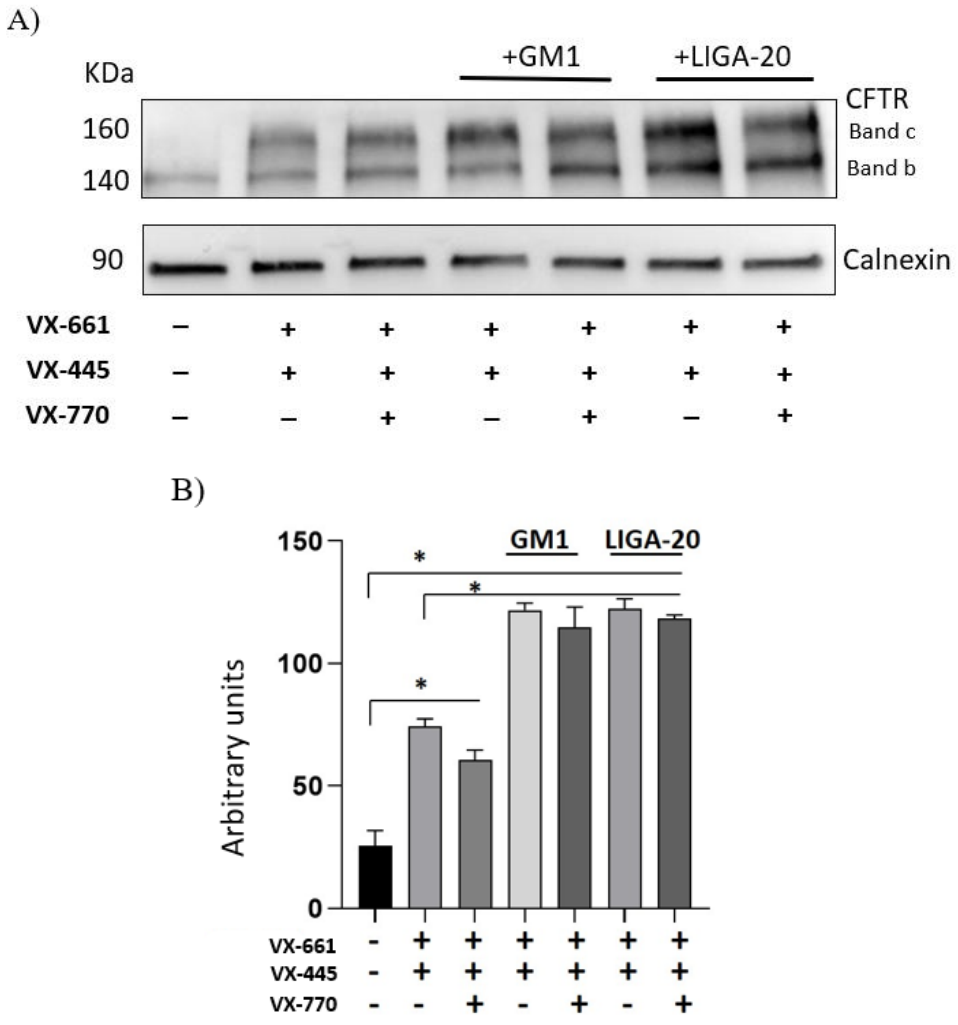

Figure 28. Effect of GM1 and Liga20 on the rescue of F508del-CFTR in cells treated with Kaftrio.

The figure shows a representative Western Blot against CFTR (A) and its relative quantification (B). Calnexin was used as loading control. CFBE cells overexpressing F508del-CFTR were treated with the correctors VX-661 (3 μM) and VX-445 (2 μM) alone or in combination with the potentiator VX-770 (5 μM) for 24 hours in the presence or not of 50 μM GM1 or 10 μM Liga20. Data are presented in the graph as ratio of the expression of band-c and -b, normalized on Calnexin, *$p<0.01$ vs untreated cells.

These data are promising as they indicate a possible additive effect of these lipids to Kaftrio treatment on the rescue of F508del-CFTR. However, these results are obtained evaluating the CFTR in a total cell lysate and not at the cell PM where the protein is located and exerts its function. For this reason, I proceeded to isolate the cell surface proteins, including CFTR, with respect to the intracellular counterpart by a pull-down assay based on the biotinylation of the proteins associated with the external leaflet of the PM and their recovery with magnetic beads conjugated with streptavidin.

First, F508del CFBE cells were treated or not for 24 hours with the components of Kaftrio, and the day after they were incubated with EZ-Link™ Sulfo-NHS-Biotin for 30 minutes at 4°C. Under these experimental conditions the internalization of the biotin does not occur and biotinylation is restricted to the apical surface proteins. Then, cells were harvested, lysed and PM proteins were precipitated using streptavidin conjugated magnetic beads. The conventional method for the recovery of precipitated proteins from the magnetic beads indicates to boil the beads in order to disrupt the linkage between the biotin and streptavidin. Unfortunately, this condition resulted incompatible with the detection of the CFTR because the protein undergoes to a degradation, as observed in the lane P100 in Figures 29 and 30. I tried to reduce the temperature to 60°C in order to preserve CFTR, but in this condition the recovery of biotinylated proteins was rather low (data not shown). To promote the dissociation, based on previous experience, I decided to remove the lipids remained associated with the precipitated proteins to induce a partial denaturation of the proteins and thus favour the subsequent dissociation. Accordingly, I first subjected the precipitate to a lipid extraction (see in the methods), and afterwards I added Laemmli buffer 1X and warmed up the precipitate at 60°C to recover biotinylated proteins.

This condition allowed to isolate 90-95% of the biotinylated proteins without the contamination of intracellular components. It is indicated by an enrichment of β1-integrin, a PM protein, and by the absence of intracellular markers, GAPDH and Calnexin, in the P60 fraction, a portion corresponding to cell surface proteins (Figure 29). As expected, I found that the F508del-CFTR corrected with Kaftrio is associated with the PM and, interestingly, I found in the P60 fraction both band-c and -b of CFTR suggesting that also the immature form of CFTR is able, at least in part, to reach the PM. In addition, the presence of NHERF-1 in the precipitate indicates that under these experimental conditions I was able to isolate the CFTR interactome.

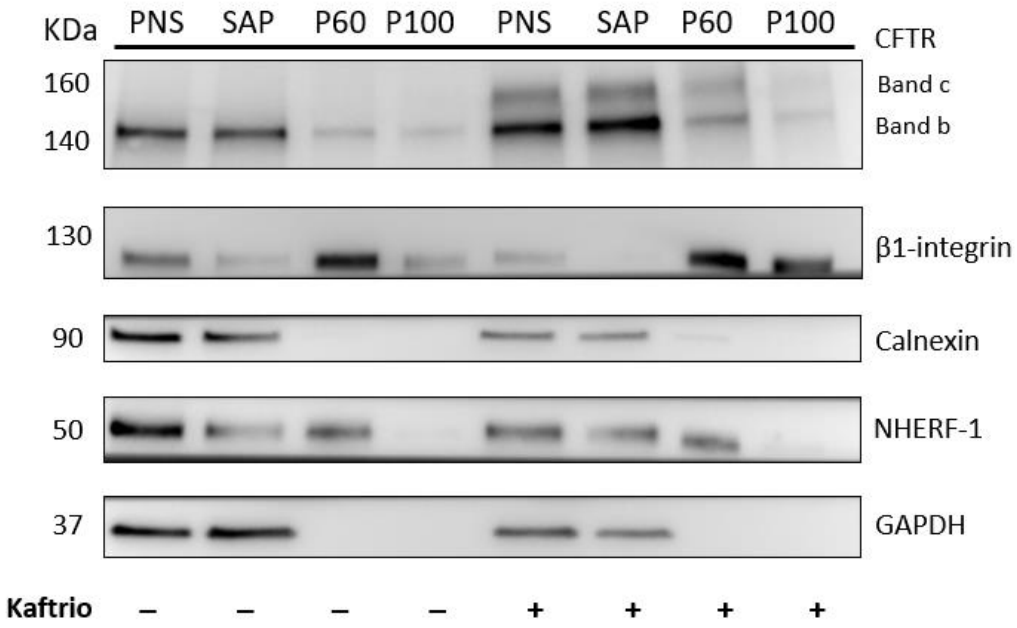

Figure 29. Plasma membrane association of mutated CFTR in F508del CFBE cells treated with Kaftrio.

The figure shows a representative Western Blot against CFTR, β1–integrin, Calnexin, NHERF-1, and GAPDH. CFBE cells overexpressing the F508del-CFTR were treated with 3 μM VX-661, 2 μM VX-445 and 5 μM VX-770 for 24 hours. After Kaftrio treatment, cell surface proteins were biotinylated. Cells were then lysed in microdomain preserving conditions and post nuclear supernatant (PNS) was subjected to precipitation with streptavidin-conjugated beads in order to isolate intracellular proteins (SAP, supernatant after precipitation), from cell surface proteins (P60, precipitate obtained at 60°C; P100, precipitate obtained at 100°C). Ratio 1:1 for PNS and SAP, and 1:6 for PNS/SAP and P60/P100.

Subsequently, I tried to isolate the F508del-CFTR rescued by Kaftrio in a more physiological cellular model represented by polarized F508del CFBE cells. Cells were plated in Transwell Clear permeable filter inserts and kept in culture for 30 days. Then they were treated with the CFTR modulators, VX-661, VX-445 and VX-770 for 24 hours. In this case, the biotinylation, applied only at the apical side of the polarized culture, allowed to isolate the cell surface proteins inserted into the apical plasma membrane, among these also the rescued F508del-CFTR.

As shown in Figure 30, the effect of Kaftrio on the maturation of the F508del-CFTR is more evident when compared to that observed in the conventional, non-polarized cell culture (Figure 29). Also in this experiment, F508del-CFTR rescued by Kaftrio is associated with the apical PM (P60 fraction) showing both isoforms corresponding to the band-c and band-b. Isolation of the PM proteins were successful as N-cadherin, a PM marker, can be observed in the P60 fraction, whilst Calnexin and GAPDH, as intracellular markers, in the SAP (Supernatant After Precipitation) fraction. Moreover, I believe that the presence of the marker Zonula Occludens (ZO)-1, both in the SAP and P60 fractions, can be considered an indication for the formation of the epithelium, as this protein is a tight junction

protein present at the cytoplasmic surface of intercellular junctions. It seems, that the treatment with Kaftrio, however, decreases the content of ZO-1 at the PM. Additionally, the identification of NHERF-1 in the precipitate suggests that, in these experimental conditions, I successfully segregated the CFTR interactome.

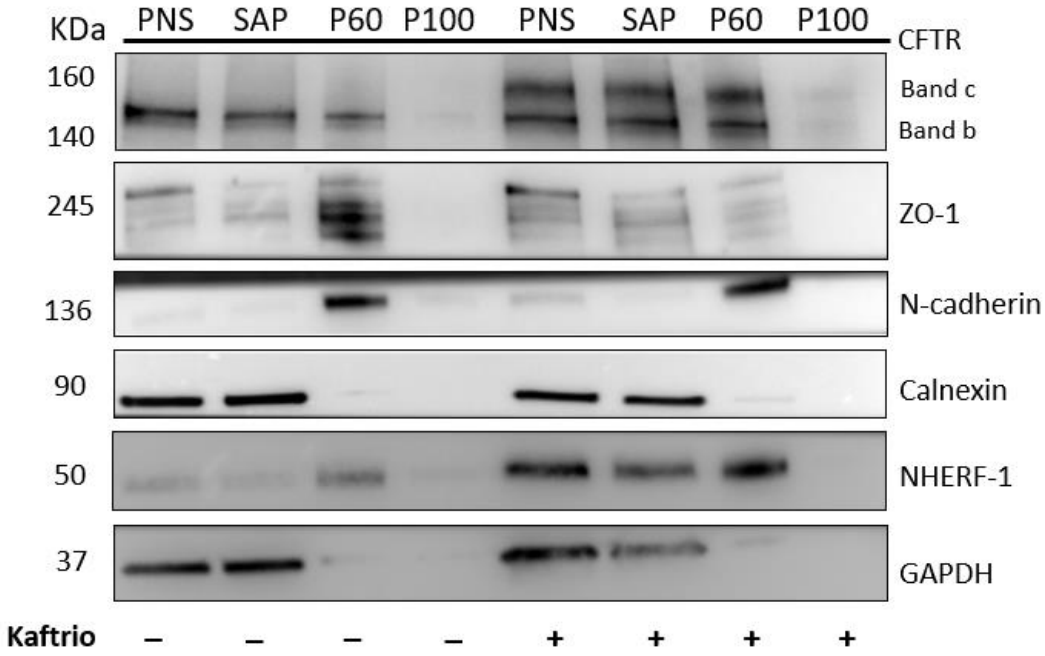

Figure 30. Apical plasma membrane association of mutated CFTR in polarized F508del CFBE cells treated with Kaftrio.

The figure shows a representative Western Blot against CFTR, ZO-1 (Zonula Occludens-1), N-cadherin, Calnexin, NHERF-1, and GAPDH. Polarized CFBE cells overexpressing the F508del-CFTR were treated with 3 μM VX-661, 2 μM VX-445 and 5 μM VX-770 for 24 hours. After Kaftrio treatment, apical cell surface proteins were biotinylated. Cells were then lysed in microdomain preserving conditions and post nuclear supernatant (PNS) was subjected to precipitation with streptavidin-conjugated beads. SAP (supernatant after precipitation), P60 (precipitate obtained at 60°C), P100 (precipitate obtained at 100°C). Ratio 1:1 for PNS and SAP, and 1:6 for PNS/SAP and P60/P100.

Once stabilizing the protocol of biotinylation and verifying that Kaftrio is able to recover the F508del-CFTR, especially the band-c, mature form the protein at the cell surface, I proceeded with the evaluation of the maturation and stabilization of F508del-CFTR at the PM level after treating cells with Kaftrio in the presence or absence of GM1 and its derivative, Liga20.

F508del CFBE cells were treated or not with the components of Kaftrio and GM1 or Liga20 for 24 hours, and the day after they were incubated with EZ-Link™ Sulfo-NHS-Biotin for 30 minutes at 4°C. Analysing the samples through immunoblotting, data reported in Figure 31, as already demonstrated, I observed that F508del-CFTR corrected with Kaftrio is associated with the PM,

finding in the P60 fraction both band-c and -b of CFTR. In addition, upon the administration of either the GM1 or the Liga20, I have noted a slight but significative increase in the content of the band-c, mature form of CFTR, associated with the cell surface with respect to cells treated only with Kaftrio. Furthermore, the presence of NHERF-1 in the precipitate indicates that I was able to isolate the interactome of CFTR.

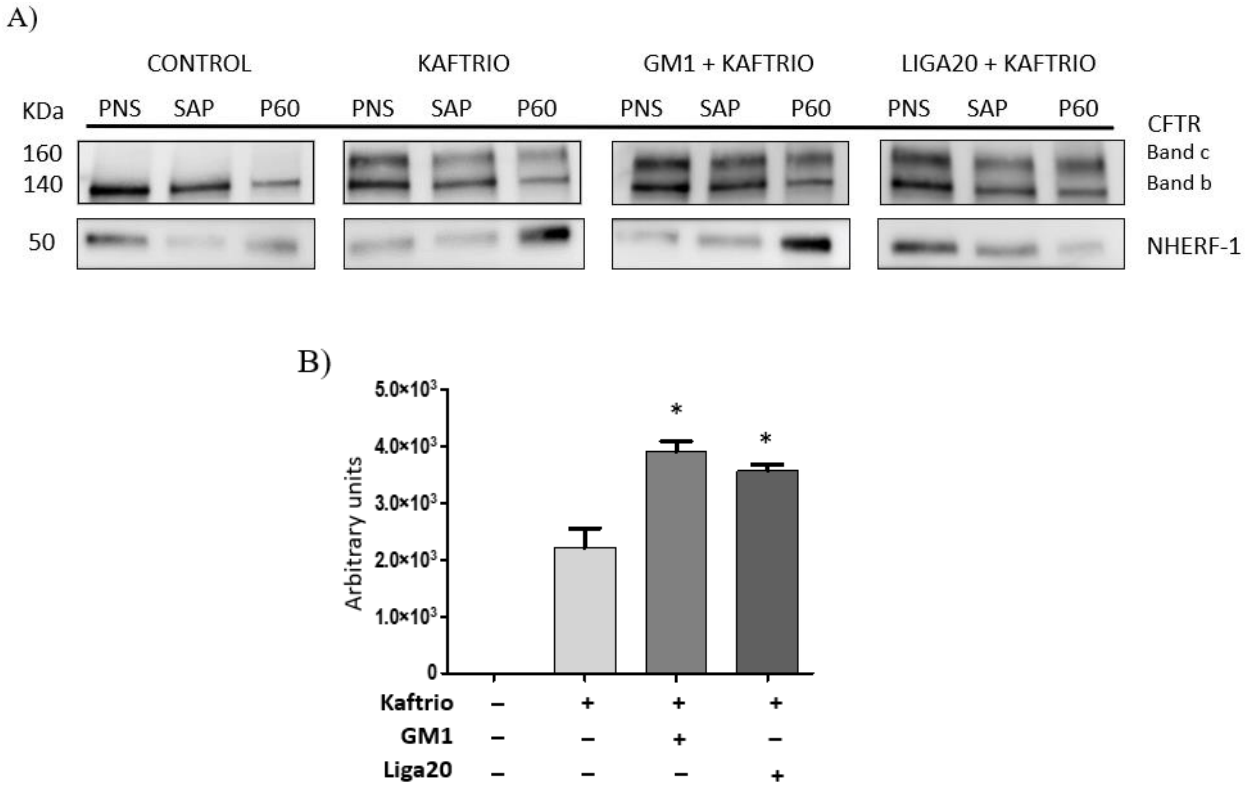

Figure 31. Effect of GM1 and Liga20 administration on the expression of CFTR at the PM level in F508del CFBE cells treated with Kaftrio.

Representative Western Blot against NHERF-1 and CFTR (A) and its quantification (B). CFBE cells overexpressing the F508del-CFTR were treated with 3 μM VX-661, 2 μM VX-445 and 5 μM VX-770 for 24 hours, in the presence or not of 50 μM GM1 or 10 μM Liga20. After treatment, cell surface proteins were biotinylated, then cells were lysed in microdomain preserving conditions. Consequently, post nuclear supernatant (PNS) was subjected to precipitation with streptavidin-conjugated beads in order to isolate PM proteins. Data are presented as arbitrary units of the precipitated band-c of CFTR considering all conditions. *p<0,05 vs Kaftrio. SAP (supernatant after precipitation), P60 (precipitate obtained at 60°C). Ratio 1:1 for PNS and SAP, and 1:6 for PNS/SAP and P60.

To verify the efficacy of the precipitation, I used N-cadherin as a PM marker and GAPDH and Calnexin as intracellular markers. As shown in Figure 32, N-cadherin is present only in the precipitate (P60), whereas GAPDH and Calnexin were detectable only in SAP, suggesting a high purification in term of proteins associated with the PM, for all the conditions tested.

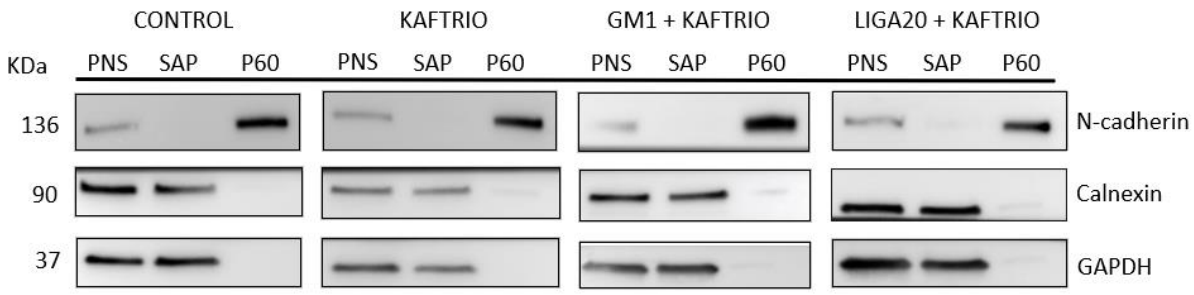

Figure 32. Quality control of the isolation of PM proteins of F508del CFBE cells treated with Kaftrio in the presence or absence of exogenous GM1 and/or Liga20.

The figure shows a representative Western Blot against N-cadherin, Calnexin and GAPDH. CFBE cells overexpressing the F508del-CFTR were treated with 3 μM VX-661, 2 μM VX-445 and 5 μM VX-770 for 24 hours, in the presence or not of 50 μM GM1 or 10 μM Liga20. After treatment, cell surface proteins were biotinylated, then cells were lysed in microdomain preserving conditions. Consequently, the post nuclear supernatant (PNS) was subjected to precipitation with streptavidin-conjugated beads in order to isolate the cell surface proteins. SAP (supernatant after precipitation), P60 (precipitate obtained at 60°C). Ratio 1:1 for PNS and SAP, and 1:6 for PNS/SAP and P60.

Furthermore, I evaluated the pattern of the biotinylated proteins after treatment with Kaftrio and GM1 or Liga20, in all the fractions by incubation of the membranes with HRP-conjugated streptavidin. As it can be appreciated from Figure 33, proteins associated with the external leaflet of the PM are observable in the fraction containing the cell surface proteins (P60) and in the fraction containing all the proteins (PNS). Biotinylated proteins, however, are not present in the SAP fraction verifying that SAP contains only intracellular proteins. Hence, I can confirm that the biotinylation procedure allowed to purify almost 100% of the PM proteins without the contamination of intracellular components.

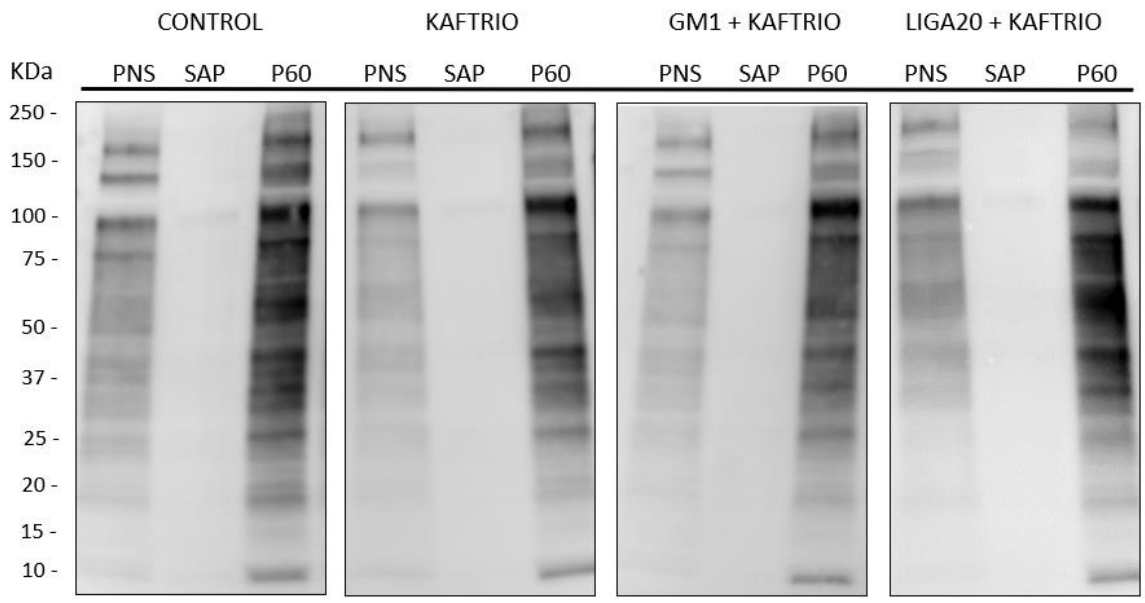

Figure 33. Pattern of the biotinylated proteins in F508del CFBE cells treated with Kaftrio in the presence of GM1 or Liga20.

The figure shows a Western Blot of biotinylated proteins in the different fractions. CFBE cells overexpressing the F508del-CFTR were treated with 3 μM VX-661, 2 μM VX-445 and 5 μM VX-770 for 24 hours, in the presence or not of 50 μM GM1 or 10 μM Liga20. After treatment, cell surface proteins were biotinylated, then cells were lysed in microdomain preserving conditions. Consequently, the post nuclear supernatant (PNS) was subjected to precipitation with streptavidin-conjugated beads. Aliquots of each condition were tested by immunoblotting incubating the membranes with HRP-conjugated streptavidin. SAP (supernatant after precipitation), P60 (precipitate obtained at 60°C). Ratio 1:1 for PNS and SAP, and 1:6 for PNS/SAP and P60.

The ganglioside GM1, that was administered to cells in all the previous experiments, consists of a mixture of GM1 with different acyl chain lengths (mainly 18 and 20 carbon atoms), like it is normally present as an endogenous compound in bronchial epithelial cells. Indeed, the acyl chain of the gangliosides, especially in case of the GM1, claims an important role in the segregation at the cell surface, in the organisation of the PM microenvironment in which the CFTR protein can also be found, and in the possibility of the ganglioside to become component of the external layer of the cell surface.

For this reason, I was wondering whether changing the length of the acyl chain of the GM1 could have a different effect on the recovery of the F508del-CFTR at the PM level in cells treated with Kaftrio. I tested the effect of different molecular species of GM1, which distinct in the acyl chain length, on the maturation and stability of F508del-CFTR at the cell surface. In particular, I fed F508del CFBE cells with three different GM1 molecular species at the same concentration used before, 50 μM; one with an acyl chain formed by 22 (C22), one formed by 10 (C10) and one formed by 4 (C4) carbon atoms. Cells were treated for 24 hours in the presence of the components of Kaftrio,

and the day after they were biotinylated, as described before. As it can be observed in Figure 34, administration of GM1 gangliosides with shorter acyl chains (C10 and C4) can have an important effect in increasing the level of the band-c of CFTR at the cell surface (fraction P60), with respect to GM1 ganglioside with longer acyl chains (GM1, and GM1 C22). Therefore, in cells treated with Kaftrio, these GM1 molecular species could enhance the stability of F508del-CFTR at the PM level.

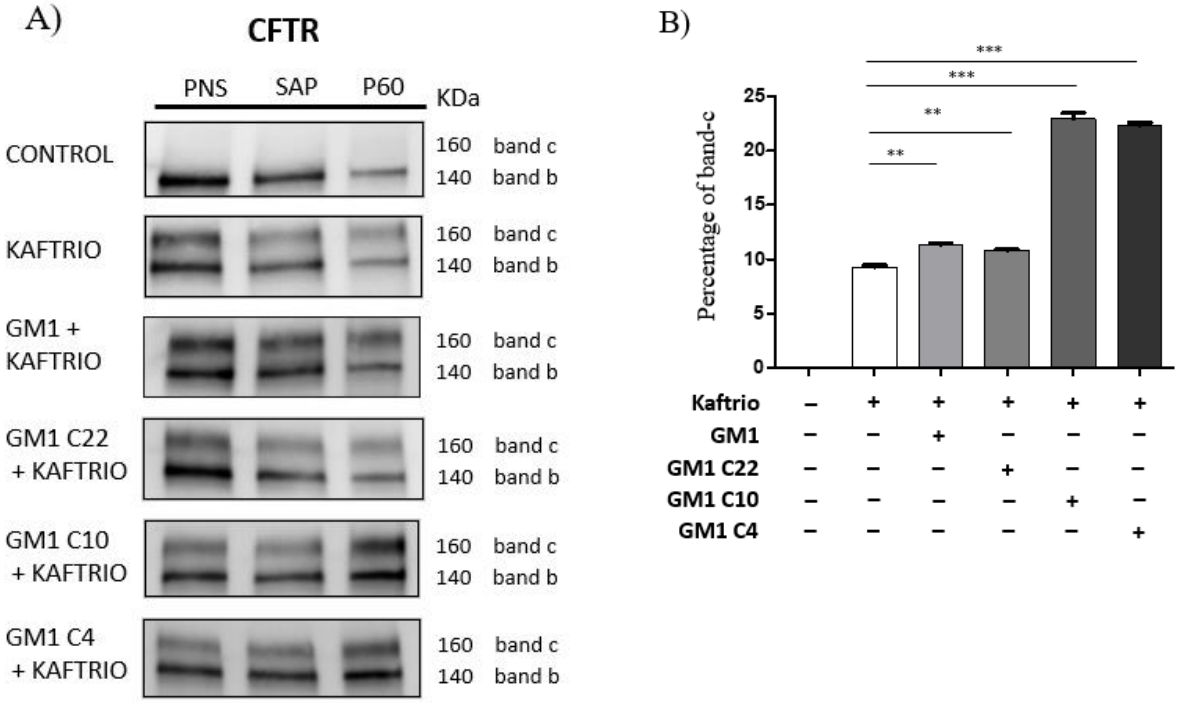

Figure 34. Effect of the molecular species of GM1 on the expression of CFTR at the PM level in F508del CFBE cells treated with Kaftrio.

Representative Western Blot against CFTR (A), and its quantification (B). CFBE cells overexpressing the F508del-CFTR were treated with 3 μM VX-661, 2 μM VX-445 and 5 μM VX-770 for 24 hours, in the presence or not of 50 μM GM1 or its molecular species. After treatment, cell surface proteins were biotinylated, then cells were lysed in microdomain preserving conditions. Consequently, post nuclear supernatant (PNS) was subjected to precipitation with streptavidin-conjugated beads in order to isolate PM proteins (P60). Data are presented as percentage of the precipitated band-c of CFTR with respect to the total band-c found in the PNS, for all the conditions tested, **p<0.005, ***p<0,0001 vs Kaftrio. SAP (supernatant after precipitation). Ratio 1:1 for PNS and SAP, and 1:6 for PNS/SAP and P60.

After assessing the effect of the different molecular species of GM1 on the expression of F508del-CFTR, I have also verified the presence of PM markers in the P60 fraction, such as N-cadherin, and intracellular markers in the SAP fraction, like Calnexin and GAPDH. What's more, the presence of NHERF-1 in the precipitate indicates the appropriate isolation of the CFTR interactome (Figure 35).

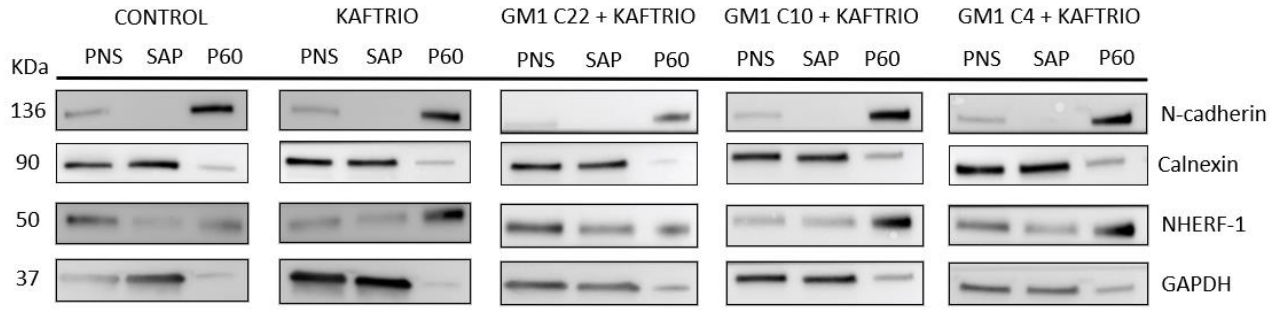

Figure 35. Quality control of the isolation of PM proteins of F508del CFBE cells treated with Kaftrio in the presence of the molecular species of GM1.

The figure shows a representative Western Blot against N-cadherin, Calnexin, NHERF-1 and GAPDH. CFBE cells overexpressing the F508del-CFTR were treated with 3 μM VX-661, 2 μM VX-445 and 5 μM VX-770 for 24 hours, in the presence of 50 μM of GM1 or its molecular species. After treatment, cell surface proteins were biotinylated, then cells were lysed in microdomain preserving conditions. Consequently, the post nuclear supernatant (PNS) was subjected to precipitation with streptavidin-conjugated beads. SAP (supernatant after precipitation), P60 (precipitate obtained at 60°C). Ratio 1:1 for PNS and SAP, and 1:6 for PNS/SAP and P60.

At last, the pattern of the biotinylated proteins was assessed in all the conditions by incubation of the membranes with HRP-conjugated streptavidin. In Figure 36, it can be seen that in the fraction containing the cell surface proteins (P60) the biotinylated proteins are perceptible, whereas, in the fraction containing the intracellular proteins (SAP), not. Therefore, I can confirm afresh that the biotinylation procedure allowed the isolation of more than 95% of the PM proteins without the contamination of intracellular components.

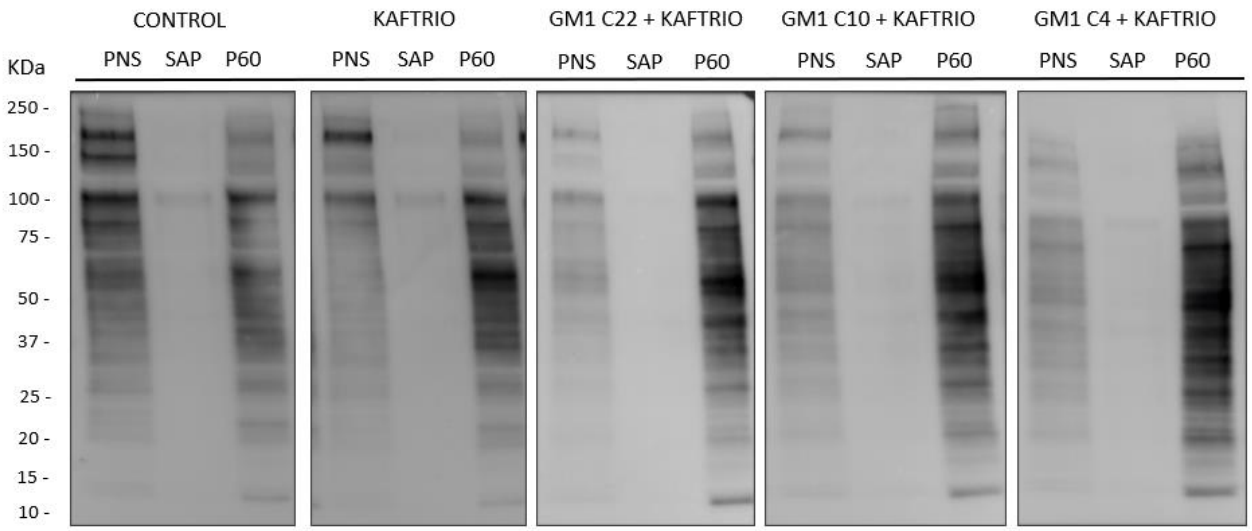

Figure 36. Pattern of the biotinylated proteins in F508del CFBE cells treated with Kaftrio in the presence of the molecular species of GM1.

The figure shows a Western Blot about the biotinylated, cell surface proteins. CFBE cells overexpressing the F508del-CFTR were treated with 3 μM VX-661, 2 μM VX-445 and 5 μM VX-770 for 24 hours, in the presence or not of 50 μM of GM1 or its molecular species. After treatment, cell surface proteins were biotinylated, then cells were lysed in microdomain preserving conditions. Consequently, the post nuclear supernatant (PNS) was subjected to precipitation with streptavidin-conjugated beads. Aliquots of each condition were tested by immunoblotting incubating the membranes with HRP-conjugated streptavidin. SAP (supernatant after precipitation), P60 (precipitate obtained at 60°C). Ratio 1:1 for PNS and SAP, and 1:6 for PNS/SAP and P60.

Effect of GM1 on CFTR expression in F508del CFBE cells corrected with VX-661, VX-445 or Kaftrio formulation, upon infection with PAO1.

The results obtained so far demonstrated the role of the ganglioside GM1 in the maturation and stabilization of F508del-CFTR at the PM of bronchial epithelial cells. As a next step, I therefore investigated the possible role of GM1 in counteracting the negative effect of *P. aeruginosa* (PAO1) infection on CFTR expression. F508del CFBE cells were treated with VX-661, VX-445 or Kaftrio formulation administering all three components, in the presence or not of 50 μM GM1 for 24 hours. Then cells were infected with PAO1 for 4 hours. At the end of incubation, cells were collected, lysed, and subjected to SDS-PAGE and Western Blot analysis.

The results shown in Figure 37, similar to those previously demonstrated by others, report that PAO1 reduced CFTR expression acting on both forms of the protein, the immature (band-b) and the fully glycosylated one (band-c). Nevertheless, GM1 administration, and new in this study, is able to mitigate the negative effect of the bacteria infection. Indeed, the presence of this ganglioside, regarding treatment either with the correctors alone (Figure 37A and B), or in case of Kaftrio formulation (Figure 37C) increased both the mature and immature form of CFTR with respect to infected cells in the absence of GM1. Noteworthy, in F508del CFBE cells treated with single correctors, either VX-661 or VX-445, the administration of GM1 resulted more effective in counteracting the action of PAO1, since the level of the mature form of CFTR protein was increased with respect to F508del-CFTR in absence of GM1. On the other hand, in CF cells treated with Kaftrio, GM1 only weakly reduced the negative effect of PAO1, most probably because Kaftrio itself appears to have a less significant destabilizing effect on the stability of the F508del-CFTR also upon infection.

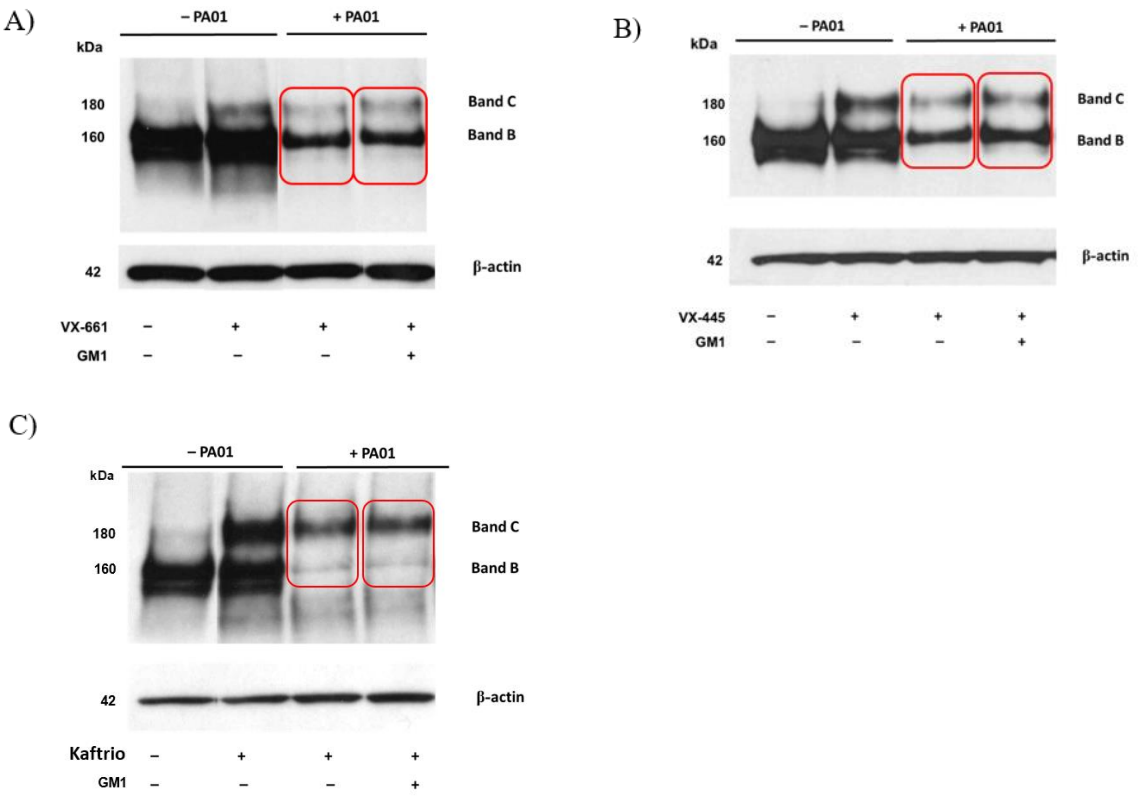

Figure 37. GM1 reduces the negative effect of PAO1 infection on CFTR expression in corrected CF cells.

The figure shows a representative Western Blot against CFTR in F508del CFBE cells treated with 3 µM VX-661 (A), 2 µM VX-445 (B), or Kaftrio formulation (3 µM VX-661, 2 µM VX-445 and 5 µM VX-770) (C) for 24 hours, in the presence or not of PAO1 infection (50 CFU/cell) for 4 hours, fed or not with 50 µM GM1. β-Actin was used as loading control.

It could be possible that the protective effect of GM1 on F508del-CFTR rescue in the presence of *P. aeruginosa* would be restricted to the stabilization of the protein on the PM, with limited effect on protein synthesis. To investigate this hypothesis, we performed experiments either to quantify the cell surface proteins by biotinylation of the PM or to inhibit the protein synthesis with cycloheximide, in presence of GM1 and PAO1.

First, as shown in Figure 38, we confirmed a reduction of the F508del-CFTR rescued by Kaftrio also at the plasma membrane level after infection of cells. Interestingly, we observed that in presence of the GM1 the reduction of the mutated channel due to the PAO1 infection is less marked suggesting a protective effect of the ganglioside.

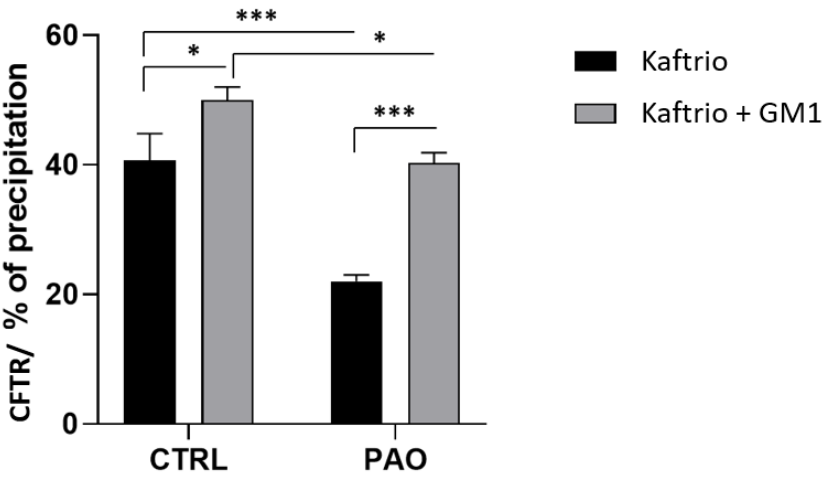

Figure 38. Effect of GM1 on the expression of CFTR at the PM level in F508del CFBE cells treated with Kaftrio, in presence or not of PAO1.

CFBE cells overexpressing the F508del-CFTR were treated with 3 μM VX-661, 2 μM VX-445 and 5 μM VX-770 for 24 hours, in the presence or not of 50 μM GM1, and were subjected to PAO1 infection for 4 hours (50 CFU/cell). After treatment, cell surface proteins were biotinylated, then cells were lysed in microdomain preserving conditions. Consequently, post nuclear supernatant was subjected to precipitation with streptavidin-conjugated beads in order to isolate PM proteins. Data are presented as percentage of the precipitated band-c and -b of CFTR, normalized on the efficiency of precipitation, *p<0.01, ***p<0,0001 vs untreated cells.

To further support the role of GM1 in the stabilization of the mature form of F508del-CFTR upon rescue with Kaftrio, in presence or not of PAO1 infection, experiments administering the protein synthesis inhibitor, cycloheximide (CHX) were performed. In particular, F508del CFBE cells were treated with Kaftrio ± GM1 for 24 hours, and then CHX was administered for either 8, 9, 11 or 13 hours, of which in the last 4 hours in the presence of PAO1 infection. Afterwards, at these different time points, cells were harvested, lysed and subjected to SDS-PAGE and Western Blot analysis in order to evaluate the mature form of CFTR. As reported in Figure 39, GM1 administration increases the PM stability of F508del-CFTR, rescued by Kaftrio, at all the analyzed time points. In addition, its stabilizing effect is maintained also in the presence of the infection with PAO1.

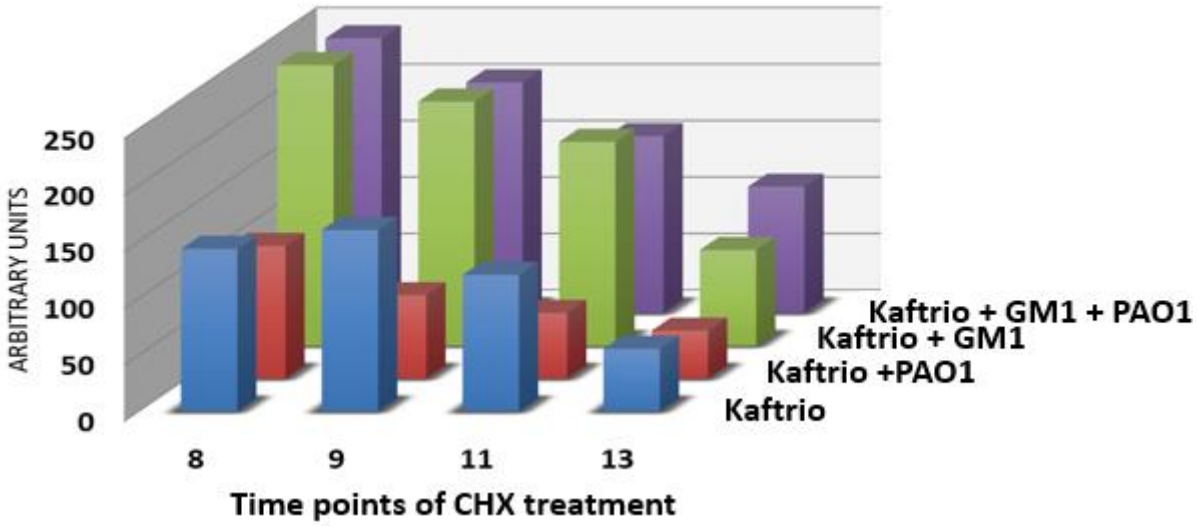

Figure 39. Effect of GM1 on rescued CFTR stabilization in F508del CFBE cells in presence of PAO1 infection, upon treatment with cycloheximide.

Graph reporting the quantification of the Western Blot analyses of CFTR evaluated in F508del CFBE cells treated with Kaftrio (3 μM VX-661, 2 μM VX-445 and 5 μM VX-770) ± GM1 (50 μM) ± PAO1 for 4 hours (50 CFU/cell) and with cycloheximide (CHX, 100 μg/mL). Cells were harvested and lysed at different time points: 8 h, 9 h, 11 h, and 13 h. The data are expressed as a ratio between the intensity of the band-c and that of the loading control, β-Actin, for each time point.

Evaluation of the effect of LDL-cholesterol administration on the maturation and stabilization of F508del-CFTR in bronchial epithelial cells treated with Kaftrio.

It is now known that in airway epithelial cells, CFTR is associated both with proteins and lipids in a macromolecular complex. Nevertheless, beyond the proteins, there are two key players in the organization of the CFTR interactome, the sphingolipids, especially the GM1, and the cholesterol. Previously, I have demonstrated how the exogenous GM1 administration can have an adjuvant effect to increase the efficacy of the CFTR-modulators on the rescued mutated-CFTR. Moreover, I have already observed that the level of cholesterol is decreased in CFBE cell line expressing the mutated form of CFTR with respect to WT CFBE cells, and that upon treatment with Kaftrio its level is further reduced. Therefore, I was wondering whether also cholesterol administration has a beneficial effect in the rescue of F508del-CFTR focusing on its maturation and stabilization in cells treated with Kaftrio.

For this purpose, I attempted to administer cholesterol exogenously to F508del CFBE cells. Because of its high insolubility in cell culture medium, and its toxicity to cells, I decided to try a rather physiological way of administration, the lipoproteins. Lipoproteins play a key role in the absorption and transport of dietary lipids by the small intestine, in the transport of lipids from the liver to peripheral tissues, and the transport of lipids from peripheral tissues to the liver and intestines. Among the various lipoproteins, the LDL (low density lipoprotein) are enriched in cholesterol, triglycerides, and phospholipids, carrying the majority of cholesterol that is in the circulation. For these reasons, I decided to choose LDL as administration vehicle of cholesterol to F508del CFBE cells.

In this aspect, first of all, I conducted a cell viability assay, namely the Calcein assay, in order to evaluate the eventual contingent cytotoxic effect of the LDL. As it can be appreciated from Figure 40, administering LDL to CFBE cells overexpressing the F508del-CFTR at 400 μg/ml concentration, either for 24 hours or for 48 hours of which in the last 24 hours in the presence of the components of Kaftrio, I did not observe any significant toxic effect.

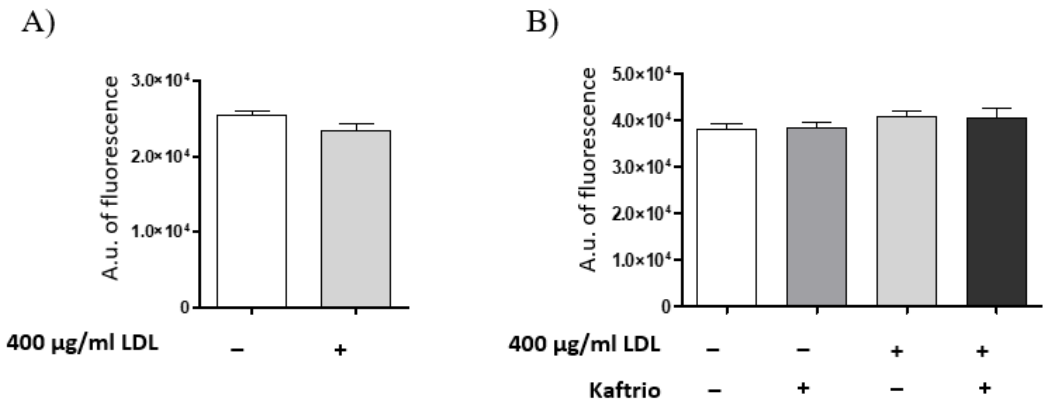

Figure 40. Evaluation of the effect of LDL on cell viability.

The figure represents the cell viability assessed by Calcein assay: CFBE cells overexpressing the F508del-CFTR were treated with 400 µg/ml LDL for 24 hours (A) or for 48 hours with the presence of Kaftrio (3µM VX-661, 2µM VX-445, 5µM VX-770) in the last 24 hours (B). After, cells were incubated with Calcein-AM diluted in cell culture medium (15 minutes, 37°C), then cells were lysed by the addition of 1% Triton X-100 in TNEV buffer. Fluorescence emission was measured by a fluorescence microplate reader. Data are expressed as arbitrary units of fluorescence (A.u).

Once verified the absence of toxicity of the LDL treatment conditions, I investigated the impact of LDL administration on the maturation and stabilization of F508del-CFTR rescued by Kaftrio. As shown in Figure 41, LDL treatment alone is able to significantly increase the CFTR expression, however, it does not have any effect in the CFTR rescue, resulting in a meaningful grow of only the immature form of the protein (band-b). Whereas, when used together with Kaftrio, LDL strongly emphasizes the CFTR correction regarding the expression of both bands, particularly band-c.

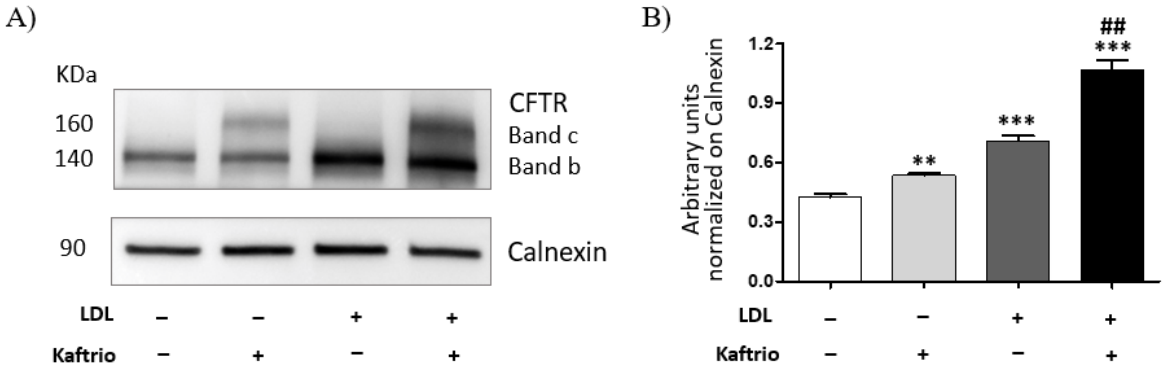

Figure 41. Effect of LDL on the rescue of F508del-CFTR in cells treated with Kaftrio.

The figure shows a representative Western Blot against CFTR, normalized on Calnexin (A), and its relative quantification (B). CFBE cells overexpressing F508del-CFTR were treated or not with 400 µg/ml LDL for 48 hours in the presence of Kaftrio (3µM VX-661, 2µM VX-445, 5µM VX-770) for the last 24 hours. Densitometric analyses were performed using ImageJ software. Data are presented in the graph as ratio of the expression of band-c and -b, normalized on Calnexin, **p<0,005, ***p<0.001 vs Ctrl, ##p<0.01 vs Kaftrio.

These data are well-seeming as they represent a possible cumulative effect of cholesterol to Kaftrio on the maturation of rescued F508del-CFTR. Nevertheless, these findings are obtained evaluating the CFTR in a total cell lysate and not at the cell surface where the protein should perform its function. In consequence, I proceeded to isolate the CFTR associated with the PM by a pull-down assay based on the biotinylation of cell surface proteins, and their recovery with magnetic beads conjugated with streptavidin. Thus, F508del CFBE cells were treated or not with LDL for 48 hours, of which in the last 24 hours also in the presence of the components of Kaftrio. After the treatments, cells were incubated with EZ-Link™ Sulfo-NHS-Biotin for 30 minutes at 4°C, and then harvested and lysed, using the same protocol as for the experiments conducted with GM1 administration. PM proteins were precipitated using streptavidin conjugated magnetic beads, as described before.

First, I evaluated the maturation and stabilization of F508del-CFTR at the PM level (Figure 42). As expected, I found that the F508del-CFTR corrected with Kaftrio is associated with the P60 fraction (fraction of the PM) where I found both band-c and -b of CFTR. Even if LDL alone does not contribute to CFTR rescue, it seems to have an important effect on the maturation and trafficking of the band -b, immature form of CFTR, since it is enriched in the P60. Moreover, upon combined treatment with Kaftrio, I observed a significative increase in the content of the band-c associated with the cell surface with respect to cells treated only with Kaftrio, suggesting a possible additive effect of LDL. In addition, the presence of NHERF-1 in the precipitate indicates that I was able to isolate the CFTR interactome.

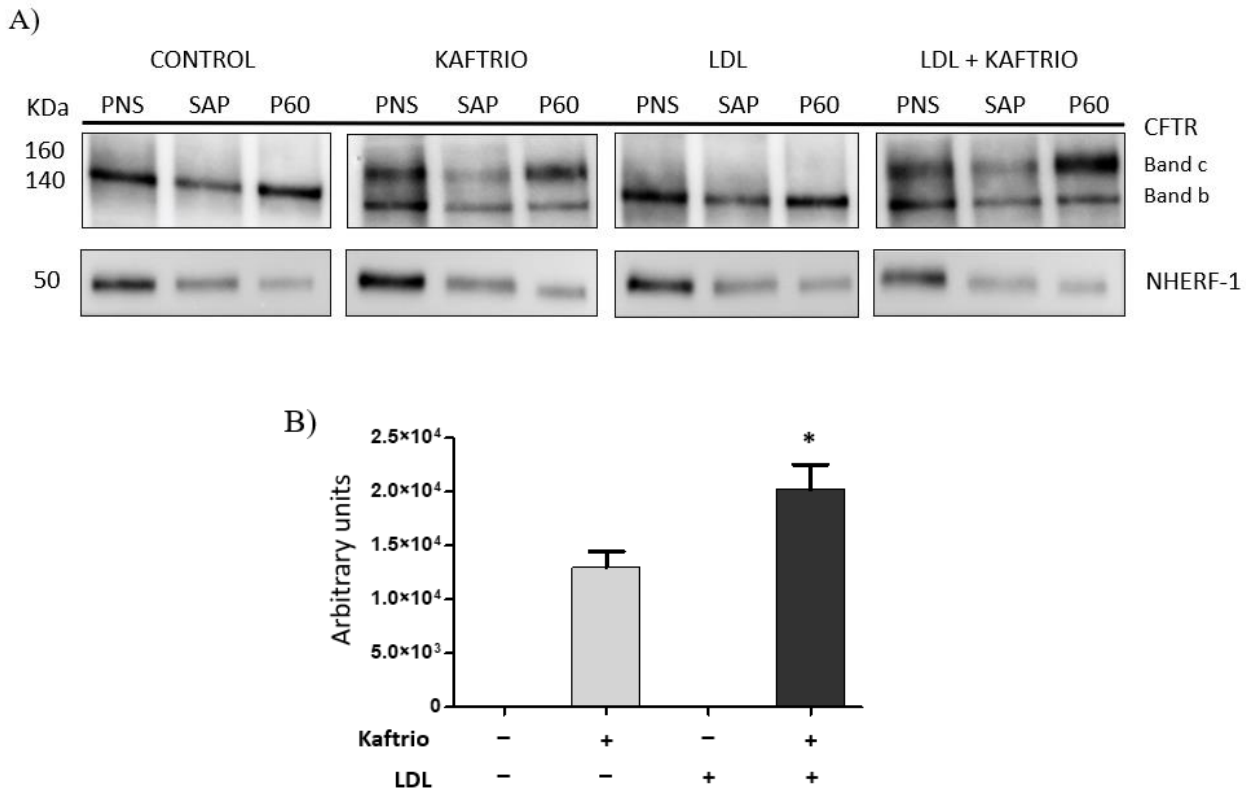

Figure 42. Effect of LDL administration on the expression of CFTR at the plasma membrane level in F508del CFBE cells treated with Kaftrio.

Representative Western Blot against NHERF-1 and CFTR (A) and its quantification (B). CFBE cells overexpressing F508del-CFTR were treated or not with 400 µg/ml LDL for 48 hours in the presence of Kaftrio (3µM VX-661, 2µM VX-445, 5µM VX-770) in the last 24 hours. After treatment, cell surface proteins were biotinylated, then cells were lysed in microdomain preserving conditions. Consequently, post nuclear supernatant (PNS) was subjected to precipitation with streptavidin-conjugated beads in order to isolate cell surface proteins (P60) from intracellular proteins (SAP-supernatant after precipitation). Data are presented as arbitrary units of the precipitated band-c of CFTR considering all conditions. *p<0,05 vs Kaftrio. Ratio 1:1 for PNS and SAP, and 1:6 for PNS/SAP and P60.

Subsequently, I investigated the quality of the precipitation using E-cadherin and Caveolin-1 as PM markers and GAPDH as an intracellular marker (Figure 43). E-cadherin is present mostly in the precipitate (P60), whereas GAPDH were detectable only in SAP suggesting a high purification in term of proteins engaged with the cell surface for all the conditions tested.

On the other hand, Caveolin-1, a typical protein of lipid rafts which organizes membrane invaginations, seems to be associated with the PM confirming the preservation of these lipid microdomains, in which also CFTR is located, throughout the biotinylation procedure. Interestingly, its level appears to be reduced upon the administration of LDL. This result could be explained by the caveolin's function, which promotes the internalization of external elements through clathrin recruitment. In fact, the cell uptake of LDL involves the LDL-receptors and is obtained by a clathrin mediated way. Consequently, the assimilation of exogenous LDL could potentially induce the internalization of Caveolin-1, leading to its diminished presence on the cell surface.

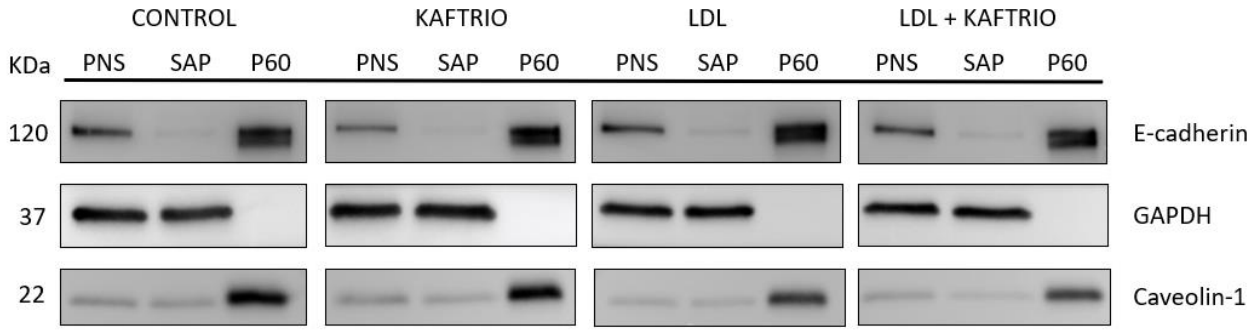

Figure 43. Quality control of the isolation of PM proteins of F508del CFBE cells treated with Kaftrio in the presence or absence of LDL.

Representative Western Blot against E-cadherin, GAPDH and Caveolin-1. CFBE cells overexpressing the F508del-CFTR were treated or not with 400 μg/ml LDL for 48 hours in the presence of Kaftrio (3μM VX-661, 2μM VX-445, 5μM VX-770) in the last 24 hours. After treatment, cell surface proteins were biotinylated, then cells were lysed in microdomain preserving conditions. Consequently, post nuclear supernatant (PNS) was subjected to precipitation with streptavidin-conjugated beads to isolate cell surface proteins within the precipitate (P60) from intracellular proteins (SAP-supernatant after precipitation). Ratio 1:1 for PNS and SAP, and 1:6 for PNS/SAP and P60.

Finally, the pattern of the biotinylated proteins was assessed in all the conditions by incubation of the membranes with HRP-conjugated streptavidin, as described before. As it can be observed from Figure 44, in the fraction containing the cell surface proteins (P60) the biotinylated proteins are present, whereas in the fraction containing the intracellular proteins (SAP) they are not observed. Therefore, I can state that I was able to isolate more than 95% of the PM proteins without the contamination of intracellular components.

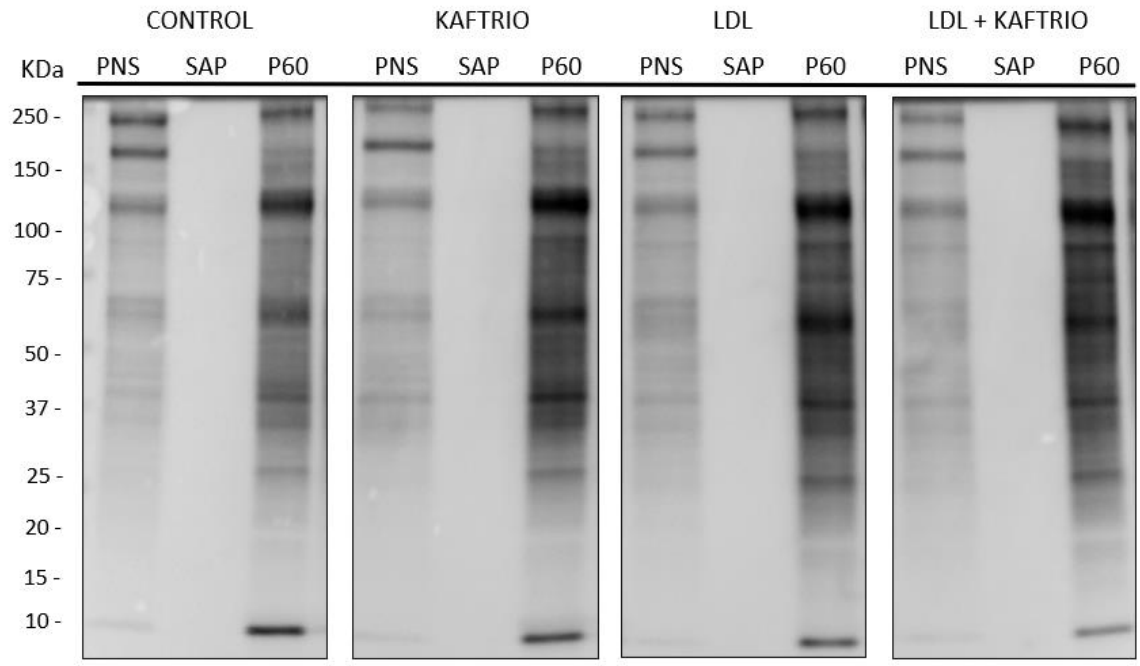

Figure 44. Pattern of the biotinylated proteins in F508del CFBE cells treated with Kaftrio in the presence of LDL.

The figure shows a Western Blot about the biotinylated, cell surface proteins. CFBE cells overexpressing the F508del-CFTR were treated or not with 400 μg/ml LDL for 48 hours in the presence of Kaftrio (3μM VX-661, 2μM VX-445, 5μM VX-770) in the last 24 hours. After treatment, cell surface proteins were biotinylated, then cells were lysed in microdomain preserving conditions. Consequently, the post nuclear supernatant (PNS) was subjected to precipitation with streptavidin-conjugated beads. Aliquots of each condition were tested by immunoblotting incubating the membranes with HRP-conjugated streptavidin. SAP (supernatant after precipitation), P60 (precipitate obtained at 60°C). Ratio 1:1 for PNS and SAP, and 1:6 for PNS/SAP and P60.

After obtaining these results administering LDL to CFBE cells, I was wondering whether the combination of the two lipids, GM1 ganglioside and cholesterol, both of which effect on the maturation and stabilization of F508del-CFTR is notable, could have an ulterior, additive effect in this matter. Therefore, CFBE cells overexpressing the mutated form of CFTR were treated with GM1 for 24 hours and/or with LDL for 48 hours, in the presence or not of 3 μM VX-661, 2 μM VX-445, and 5 μM VX-770 for 24 hours. Cells were then harvested, lysed, and analyzed for CFTR content by immunoblotting experiments.

As it can be appreciated from Figure 45, treatment of cells with Kaftrio in the presence of ganglioside GM1 increases the total amount of CFTR, including band-c and -b, with respect to cells treated only with the CFTR modulator. In turn, as observed before, LDL administration to cells together with Kaftrio strongly enhance CFTR correction, even more than GM1. Interestingly, the combined treatment of the two lipids with Kaftrio does not show an additive effect in the rescue of the F508del-CFTR with regards for its treatment with LDL and Kaftrio.

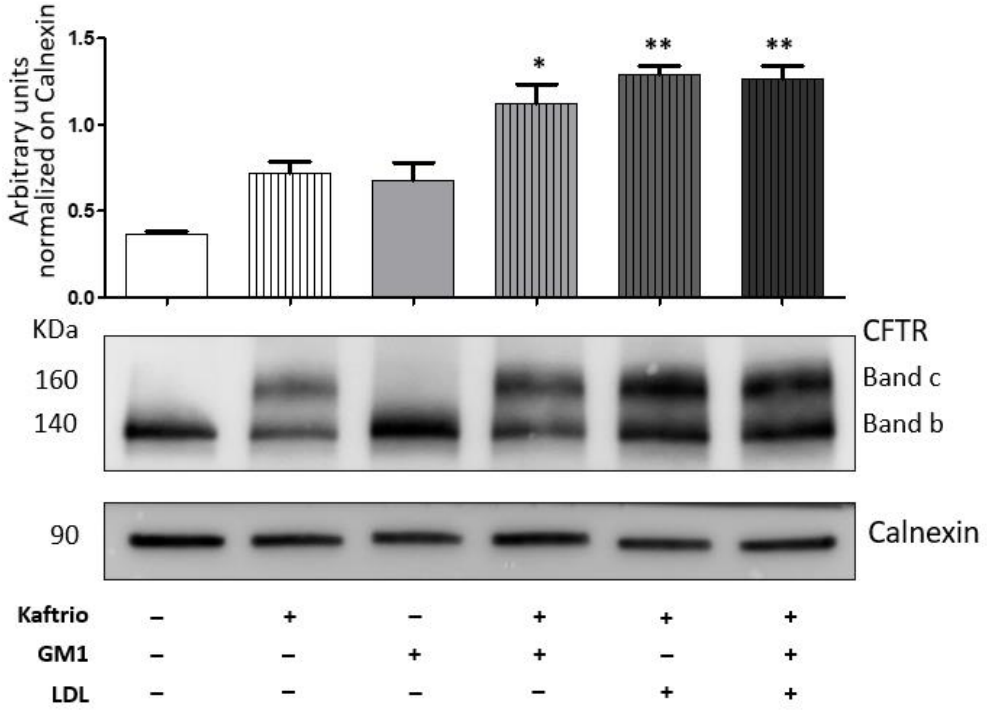

Figure 45. Effect of GM1 or/and LDL on the rescue of F508del-CFTR in cells treated with Kaftrio.

CFBE cells overexpressing F508del-CFTR were treated with 50 μM GM1 or/and 400 μg/ml LDL, in the presence or not of Kaftrio (3μM VX-661, 2μM VX-445, 5μM VX-770) for 24 hours. The figure reports a representative Western Blot against CFTR, and its quantification. Calnexin was used as a loading control. Densitometric analyses were performed using the ImageJ software. Data are presented in the graph as ratio of the expression of band-c and -b, normalized on Calnexin. *p<0,05, **p<0.01 vs Kaftrio.

Since I have previously observed that the molecular species of GM1 ganglioside with shorter acyl chains, in particular GM1 C4 and C10, have a significant impact in increasing the band-c of CFTR at the PM level (Figure 34), I decided to evaluate the effect of their combined administration with LDL on the expression of F508del-CFTR.

Thereupon, F508del CFBE cells were treated either for 24 hours with GM1 C4 or C10, or with LDL for 48 hours, with or without Kaftrio for the last 24 hours. Subsequently, cell lysates were assessed for the maturation of F508del-CFTR (Figure 46). As it was expected, treatment with either GM1 C4, GM1 C10 or LDL alone is not able to recover the mature form of CFTR. However, exogenous administration of the molecular species of GM1 ganglioside significantly increases the content of CFTR in cells treated with Kaftrio with reference to Kaftrio treatment alone. In addition, LDL enhance the efficacy of the CFTR modulator in the rescue of the mutated protein, even having a stronger effect than the molecular species of GM1. Nevertheless, the concurrent administration of the two lipids, while enhancing CFTR maturation compared to Kaftrio treatment alone, exhibits only a discernible tendency with respect to the combination of LDL and Kaftrio.

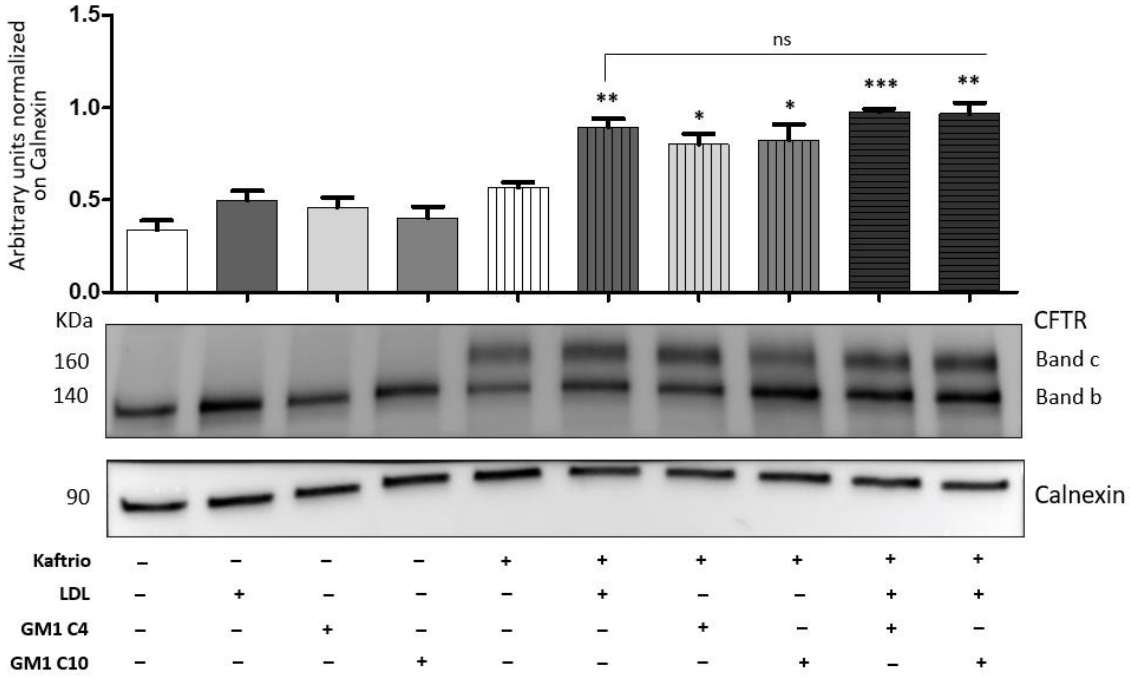

Figure 46. Effect of the molecular species of GM1 and LDL on the rescue of F508del-CFTR in cells treated with Kaftrio.

CFBE cells overexpressing F508del-CFTR were treated either with 50 μM GM1 C4 or GM1 C10, or 400 μg/ml LDL, in the presence or not of Kaftrio (3μM VX-661, 2μM VX-445, 5μM VX-770) in the last 24 hours. The figure reports a representative Western Blot against CFTR, and its quantification. Calnexin was used as a loading control. Densitometric analyses were performed using the ImageJ software. Data are presented in the graph as ratio of the expression of band-c and -b, normalized on Calnexin. *p<0.05, **p<0.005, ***p<0,001 vs Kaftrio. Ns = not significative.

Based on this evidence, I nevertheless proceeded with the biotinylation of the cell surface proteins to isolate the CFTR and evaluate the possible additive effect of GM1 C4/C10 and LDL administration to Kaftrio at the PM level, as performed previously. Hence, F508del CFBE cells were treated either for 24 hours with GM1 C4 or C10, or with LDL for 48 hours, in the presence or not of Kaftrio. The day after cells were incubated with EZ-Link™ Sulfo-NHS-Biotin for 30 minutes at 4°C, then they were harvested, lysed and PM proteins were precipitated using streptavidin conjugated magnetic beads. Consequently, samples of the lysates (PNS – post nuclear supernatant), intracellular proteins (SAP – supernatant after precipitation) and proteins associated with the PM (P60 – precipitate obtained at 60°C) were analysed with Western Blot (figures 47-49, respectively).

First of all, by verifying the presence of the PM markers in the P60 fraction, and their absence in the SAP, as well as the occurrence of intracellular proteins, I evaluated the quality of the biotinylation procedure. As seen in Figure 47, E-cadherin was present in the precipitate (P60), whereas GAPDH were detectable only in SAP suggesting a high efficacy in the precipitation of PM proteins, under all tested conditions. Moreover, Caveolin-1, a protein associated with lipid rafts, is afresh found at the PM confirming the preservation of these lipid microdomains throughout the biotinylation procedure.

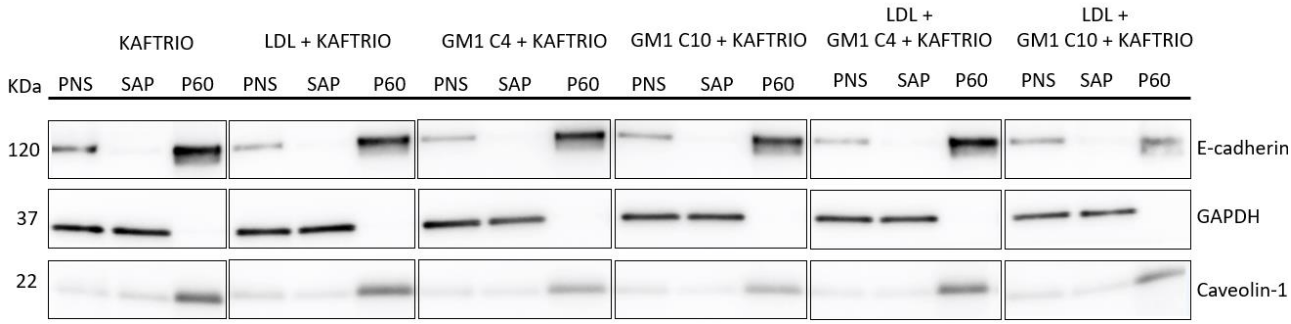

Figure 47. Quality control of the isolation of PM proteins of F508del CFBE cells treated with Kaftrio in the presence of the molecular species of GM1 and LDL.

Representative Western Blot against E-cadherin, GAPDH and Caveolin-1. CFBE cells overexpressing the F508del-CFTR were treated either with 50 μM GM1 C4 or GM1 C10, or 400 μg/ml LDL, in the presence or not of Kaftrio (3μM VX-661, 2μM VX-445, 5μM VX-770) in the last 24 hours. After treatment, cell surface proteins were biotinylated, then cells were lysed in microdomain preserving conditions. Consequently, post nuclear supernatant (PNS) was subjected to precipitation with streptavidin-conjugated beads to isolate cell surface proteins within the precipitate (P60) from intracellular proteins (SAP - supernatant after precipitation). Ratio 1:1 for PNS and SAP, and 1:6 for PNS/SAP and P60.

Secondly, I evaluated the pattern of the biotinylated proteins in all the conditions by incubation of the membranes with HRP-conjugated streptavidin (Figure 48). In the P60 fraction, proteins of the cell surface can be observed, whereas in the SAP they are not present. Therefore, I can confirm that the biotinylation procedure allowed the isolation of almost 100% of the PM proteins without the contamination of intracellular components.

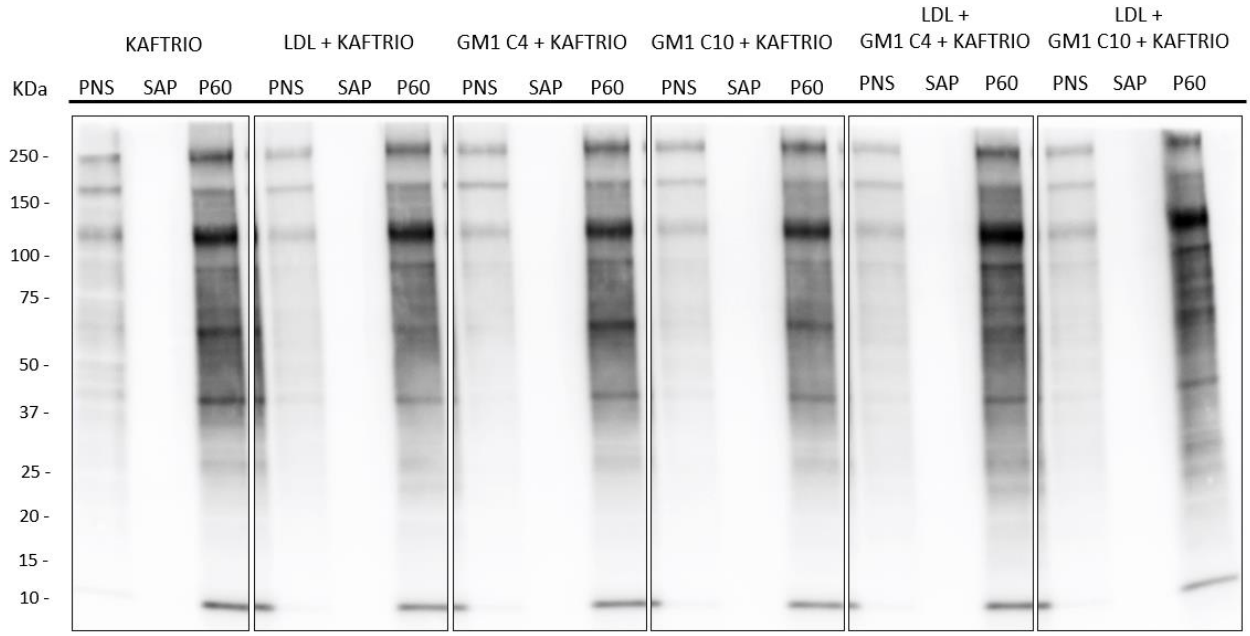

Figure 48. Pattern of the biotinylated proteins in F508del CFBE cells treated with Kaftrio in the presence of the molecular species of GM1 and LDL.

The figure shows a Western Blot about the biotinylated, cell surface proteins. CFBE cells overexpressing the F508del-CFTR were treated either with 50 μM GM1 C4 or GM1 C10, or 400 μg/ml LDL, in the presence or not of Kaftrio (3μM VX-661, 2μM VX-445, 5μM VX-770) in the last 24 hours After treatment, cell surface proteins were biotinylated, then cells were lysed in microdomain preserving conditions. Consequently, the post nuclear supernatant (PNS) was subjected to precipitation with streptavidin-conjugated beads. Aliquots of each condition were tested by immunoblotting incubating the membranes with HRP-conjugated streptavidin. SAP (supernatant after precipitation), P60 (precipitate obtained at 60°C). Ratio 1:1 for PNS and SAP, and 1:6 for PNS/SAP and P60.

Last, but not least, I evaluated the maturation and stabilization of F508del-CFTR at the PM level (Figure 49). As already discovered, LDL administration, when used together with Kaftrio, remarkably increases the content of the band-c of CFTR associated with the cell surface with respect to cells treated only with Kaftrio. On the contrary, I did not observe an additive effect neither of the molecular species of GM1 to Kaftrio, nor of the combination of the GM1 C4 or C10 and LDL to Kaftrio when analyzing the band-c in the P60 fraction. In addition, the presence of NHERF-1 in the precipitate indicates that the isolation of the CFTR interactome was successful.

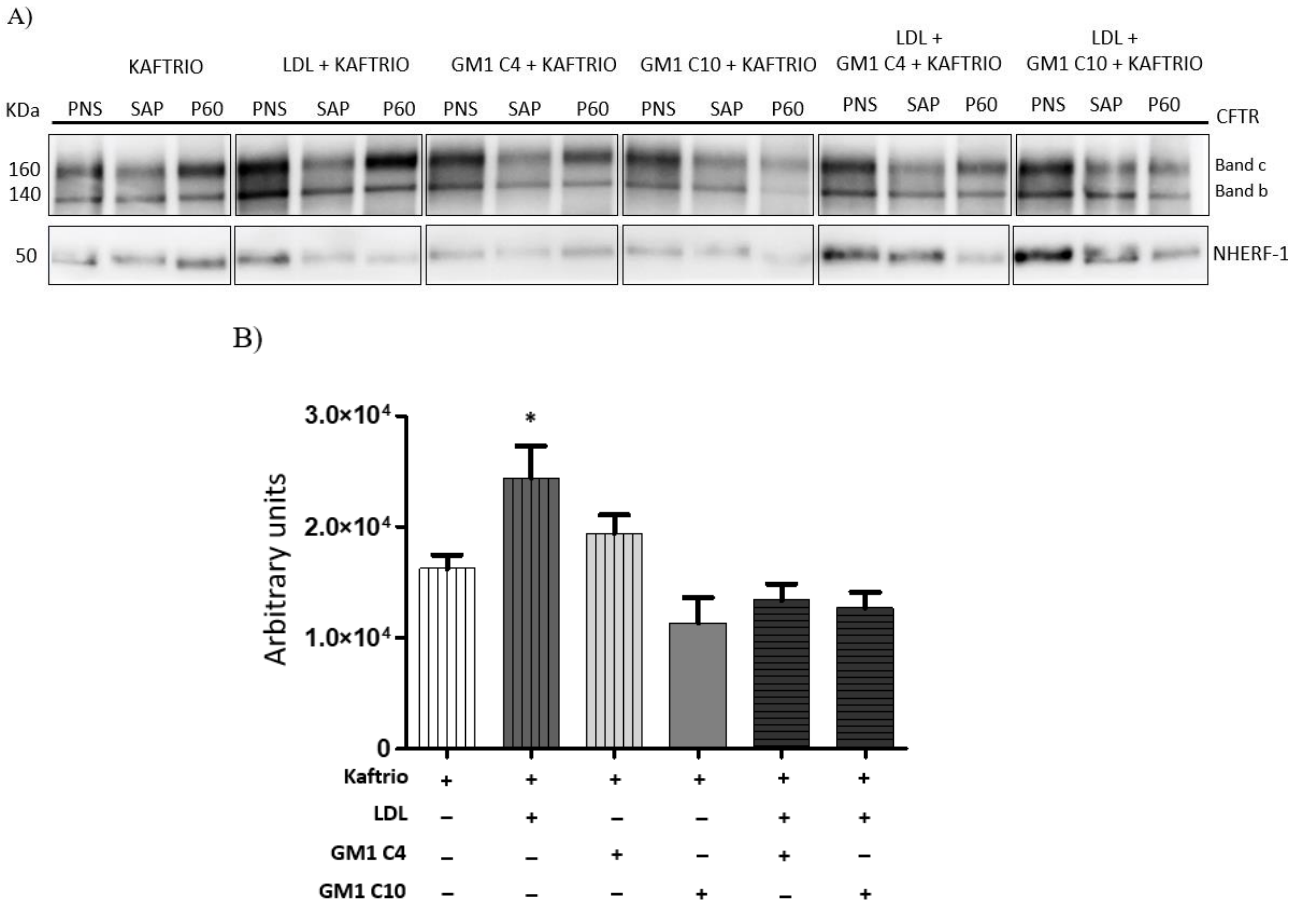

Figure 49. Effect of the molecular species of GM1 and/or LDL administration on the expression of CFTR at the PM level in F508del CFBE cells treated with Kaftrio.

Representative Western Blot against NHERF-1 and CFTR (A) and its quantification (B). F508del CFBE cells were treated either with 50 μM GM1 C4 or GM1 C10, or 400 μg/ml LDL, in the presence or not of Kaftrio (3μM VX-661, 2μM VX-445, 5μM VX-770) in the last 24 hours. After treatment, cell surface proteins were biotinylated, then cells were lysed in microdomain preserving conditions. Consequently, post nuclear supernatant (PNS) was subjected to precipitation with streptavidin-conjugated beads to isolate cell surface proteins within the precipitate (P60). (SAP - supernatant after precipitation). Data are presented as arbitrary units of the precipitated band-c of CFTR considering all conditions. *p<0,05 vs Kaftrio. Ratio 1:1 for PNS and SAP, and 1:6 for PNS/SAP and P60.

DISCUSSION

Multiple lines of evidence highlight the active involvement of lipids, particularly sphingolipids and cholesterol, in various aspects of cystic fibrosis. Indeed, altered sphingolipid metabolism in CF bronchial epithelial cells contributes to a high pro-inflammatory state, severe inflammatory responses, and increased susceptibility to bacterial infections, characteristic features of CF patients [63, 75]. Ceramide, a specific sphingolipid, is implicated in recurrent infections and chronic inflammation, influencing cell death, bacterial binding, and the release of inflammatory mediators, leading to the onset of the CF lung disease [200, 206, 207]. Additionally, certain glycosphingolipids (GSLs), like asialo-GM1 and asialo-GM2, serve as receptors for bacterial binding, further complicating the disease pathology [202].

CFTR, positioned at the apical membrane of epithelial cells, is associated with lipid rafts that are specific portions of the PM enriched in saturated lipids, sphingolipids, and cholesterol that organize macromolecular complexes crucial for cell signaling control. In fact, studies revealed a direct relationship between CFTR expression and plasma membrane lipid levels in human bronchial epithelial cells. On the one hand, it was reported that the lack of CFTR in the PM correlates with reduced levels of GM1 ganglioside, affecting cell migration and β1-integrin signaling, supported by a defect in wound healing in CF patients [42, 43]. On the other hand, distinct populations of CFTR within the PM were observed showing differential dynamics, mostly depending on cholesterol concentration. One, that is in clusters displaying confinement in lipid rafts and another, being diffusely distributed along the PM [44-46].

Given the current understanding that a proper PM microenvironment, involving a selected pattern of proteins and lipids, is crucial for maintaining the stability and functionality of CFTR, emerging therapies for CF must not only focus on rescuing the mutated channel but also on restoring its interactome, addressing both protein and lipid composition to ensure comprehensive therapeutic efficacy. The introduction of the CFTR-modulator combinatory therapy Orkambi in 2015 for CF patients with homozygous F508del mutation was aimed to restore the function of the mutated channel. Despite initial benefits, chronic treatment with Orkambi yielded modest and limited effects on lung function [121, 122]. Studies proved that VX-770, the potentiator of Orkambi, negatively impacted the rescue effect of VX-809 on F508del-CFTR, destabilizing the mature form of the protein at the PM [123]. Notably, Orkambi induced a decrease in GM1 content in F508del CFBE cells, however, exogenous administration of this lipid alongside modulators increased the cellular levels and channel activity of the mature form of F508del-CFTR [43]. The latest CFTR-modulator Kaftrio, administrable to around 90% of CF patients carrying the F508del mutation at least in one allele, shows significant improvements in the quality of life [133-135]. Although Kaftrio contains VX-770, its destabilizing

effect is mitigated by the presence of two correctors, VX-661 and VX-445, offering a promising therapeutic approach for CF.

Based on these findings and assumptions, in my PhD project first, I evaluated the effect of Kaftrio treatment on the lipid composition of WT and F508del CFBE bronchial epithelial cells to see whether it provokes alterations. In fact, administration of the three modulators led to a significant reduction in the levels of LacCer both in cells overexpressing the mutated CFTR and in WT CFBE cells, in which its levels are higher in general. In addition, I observed that regarding the gangliosides, in the cell line with the mutated protein the levels of GM3 are notably higher, and the levels of GM2 and GM1 are significantly lower with respect to the WT CFBE cell line. Treatment with Kaftrio formulation resulted in some modifications, such as the content of GM1 and GD1a increased in F508del CFBE cells, as the content of GT1b, which increased considerably also in cells overexpressing WT-CFTR. The changes in the lipid composition of cells upon administration of the modulators were actually attributable to the potentiator VX-770, as confirmed by the analysis of the effect of the single components of Kaftrio. The alterations in the lipid pattern are most probably due to alterations in the activity of important lysosomal glycohydrolytic and biosynthetic enzymes involved in the sphingolipid metabolism, as a result of Kaftrio treatment. Indeed, the activity of the non-lysosomal β-glucocerebroside (NLGase) showed a significant increase, while the activity of β-hexosaminidase and β-galactosidase was reduced in F508del CFBE cells, as was the activity of GCase. The difference in the effect of Kaftrio on lysosomal GCase activity compared to plasma membrane associated NLGase could be explained by the distinct direct influence of modulators on the enzyme when it is associated with lysosomes or the cell surface. Furthermore, the pharmacological treatment induced alterations in the activity of two key enzymes involved in the SL metabolism. On one hand, the GM3 synthase, which is responsible for the formation of GM3 from LacCer, and on the other, the sialidase Neu3, which leads to the formation of GM1 or LacCer, removing sialic acid residues. I found that the level of GM3 synthase is elevated, instead, the level of sialidase Neu3 is decreased in F508del CFBE cells with respect to the WT CFBE cell line. However, upon treatment with Kaftrio, I observed an increase in the activity of the GM3 synthase in F508del CFBE cells, and a decrease the in activity of the sialidase in both WT and F508del CFBE cells. These results further support my findings about the increased content of GM1 and GD1a of treated mutated cells, whereas the reduced content of LacCer of both cell lines, and could explain the differences between the lipid composition of these two cell lines.

As I have already mentioned before, administration of GM1, most likely by reorganizing the lipid environment of the protein, increased the maturation of F508del-CFTR and its channel activity in CF cells treated with Orkambi [43]. In case of Kaftrio, I have seen that this drug, unlike Orkambi,

increases the GM1 ganglioside level in F508del CFBE cells. However, to verify whether GM1 administration, also in case of CF cells treated with Kaftrio, has an additional effect in ameliorating the stability of the mutated protein, in my PhD project I addressed this aspect. Therefore, I treated F508del CFBE cells with the components of Kaftrio and observed that Kaftrio itself has a better efficacy in rescuing the F508del-CFTR, as the destabilizing effect of the VX-770 is less significant. What's more, GM1 administration appears to further increase the efficiency of modulators on the recovery of the mature form of CFTR, also when the protein is at the cell surface. In addition, for what concerns the molecular species of GM1, I could verify that those with shorter acyl chains were found to be highly effective in improving the PM stability of the rescued mutated CFTR. In fact, administration of GM1 with shorter acyl chains (GM1 C4 and C10), at the same concentration used before for the mixture of GM1 molecular species, significantly contributed to the maturation and stability of the mutated protein rescued by correctors. This enhanced effect is likely attributed to a greater cellular uptake of GM1 molecules. Indeed, gangliosides, like any amphiphilic molecule, tend to aggregate in aqueous solutions, forming small, ellipsoidal micelles. These micelles are typically in equilibrium with free monomers, with a critical micellar concentration (c.m.c.) ranging from 10^{-5}M to 10^{-9} M. C.m.c. indicates the concentration at which the molecules, in this case the gangliosides, initiate the organization into micelles. The c.m.c. of a ganglioside solution varies depending on, for example, the structure of ceramide. In particular, shorter fatty acid lengths correspond to higher c.m.c., and higher c.m.c. values result in a greater presence of monomers in the solution [217]. As only monomers integrate into the PM, operating at an equal concentration (50 µM of GM1) with ganglioside molecular species having shorter acyl chains would result in a higher quantity of monomers in the solution. Consequently, this leads to increased cellular uptake of GM1 C4 and C10 by cells. This observation could explain the promising results obtained by the administration of GM1 molecular species with shorter acyl chains in stabilizing the mutated-rescued protein at the cell surface. On the other hand, it is also important to notice that the ceramide portion of the ganglioside has a fundamental role for the observed effect, since oligo-GM1, consisting of only the oligosaccharide part of GM1, has no consequences on the maturation of F508del-CFTR (data not shown). In addition, I obtained similar results to GM1 administration also after administering Liga20, a lyso-derivative of GM1, to mutated CFBE cells. Liga20 contains the lipid moiety N-dichloroacetylsphingosine as the hydrophobic portion of the sphingolipid, and studies have revealed that the c.m.c. of this lysoGM1 is more dense than that of GM1 [218]. Therefore, its properties contribute to decreasing the probability of molecular self-aggregation, leading to an enhanced insertion into the lipid bilayer.

Furthermore, I also confirmed the effect of GM1 on the stability of mutated CFTR at the cell surface while using the protein synthesis inhibitor cycloheximide (CHX) during *P. aeruginosa* infection. Indeed, GM1 reduced the negative effect of VX-770 on the PM stability of F508del-CFTR, corrected by the use of VX-661 and VX-445, at all of the analyzed time points after CHX administration, even in the presence of PAO1, suggesting a protective effect of this ganglioside.

As previously stated, for the stability and function of the CFTR at the PM level the formation of a proper microenvironment with the involvement of both proteins and lipids is of necessity. Apart from the SLs, the other lipid whose presence is fundamental in the macromolecular complex is the cholesterol. In the literature, there are contradictory opinion about the level of cholesterol in CF bronchial epithelial cells, with some saying it is deceased, and some that it is increased. However, cholesterol and CFTR were found to exhibit reciprocal interaction regarding protein confinement in lipid rafts, and dynamics [45, 46]. Therefore, as for the last part of my PhD studies, I primarily wanted to analyze the alterations in the cellular cholesterol content upon the F508del mutation, if any, also following the treatment of cells with Kaftrio. In fact, I have demonstrated that the level of cholesterol is decreased in CF cells expressing the mutated form of CFTR with respect to WT-CFTR cells, and that Kaftrio reduces its level ulteriorly in both cell lines. Based on this evidence, next, I investigated whether restoring the lipid composition of the CFTR microdomain by exogenous administration of cholesterol could ameliorate the effectiveness of Kaftrio on rescuing F508del-CFTR. With the aim to deliver cholesterol to the cells, I have chosen a physiological vehicle consisting in the use of lipoproteins, in particular low-density lipoprotein (LDL), as LDL is known to carry the majority of cholesterol in the circulation. To decide at what concentration would it be optimal to add LDL to the cells, I considered the following evidence: in a healthy population, LDL-cholesterol typically circulates within the range of 100-130 mg/dl. However, in CF patients, this value is significantly decreased, approximately 60-70 mg/dl. In addition, the level of triacylglycerol lipase in CFBE cells is notably low, indicating a diminished capacity to hydrolyze triglycerides, essential components of the lipoprotein. Therefore, to mitigate potential toxic effects of cholesterol and triglycerides on CFBE cells, I have experimented with using a lower LDL concentration as opposed to concentrations within the general range, and performed cell vitality assays. I have treated F508del CFBE cells with LDL both for 24 and 48 hours, and I did not observe any significant toxic effect at 400 µg/ml final concentration. Afterwards, conducting Western Blot analysis, I found that LDL-cholesterol administration alone does not have any significant effect in the F508del-CFTR rescue. However, it seems to improve the trafficking of the immature form of the protein, as the levels of the band-b of F508del-CFTR are increased upon LDL administration. I also repeated the experiment in presence of treatment with the components of Kaftrio and I observed, similarly for the results with GM1, an

increase in the expression of the mature form of CFTR, revealing an additive effect of cholesterol to Kaftrio on the maturation of the rescued-mutated protein. Moreover, LDL strongly emphasizes the CFTR correction regarding both forms of the protein also at the PM level, even in a more significant way than GM1 before, suggesting its direct involvement in the mechanisms that favor the trafficking of F508del-CFTR toward the cell surface. Unfortunately, I did not notice an accumulative adjuvant effect on the recovery of the protein at the cell surface when administering GM1 and/or its molecular species together with LDL, only a tendency to it.

Taken together, we could say that understanding the lipid profile and enzyme activities of CF cells may provide insights into potential therapeutic targets to improve the overall health of individuals with cystic fibrosis. Moreover, these results indicate that exogenous administration of either GM1 and its molecular species, or cholesterol to F508del CFBE cells could restore the properties of the PM similar to those in case of WT-CFTR, allowing the establishment of proper physiological working conditions for the correctors to rescue the mutated protein, also in the presence of PAO1 infection.

CONCLUSION

Multiple findings for CFTR interactome focus on the protein side, whereas there is only few information on the role of lipids. The data obtained during my PhD studies could open a new scenario related to the CFTR-PM interactome, indicating that only a proper coordination between lipids and specific proteins could create a PM microenvironment that is able to host the CFTR and ensure its stability and function. Moreover, this experimental evidence contributes to the comprehension of secondary mechanisms of action of Kaftrio treatment.

The pursuit of innovative therapies continues to shape a new era for CF patients, emphasizing the need for sustained research and development in the field. Therefore, in the time of CFTR modulators, modifications of the SL pattern or the cholesterol content could represent an important adjuvant approach to further stabilize the rescued mutated channel at the cell surface. In addition, the study of the adverse effects of the modulators on the CFTR PM stability remains a high priority and could be useful to better address new therapeutic strategies for CF patients.

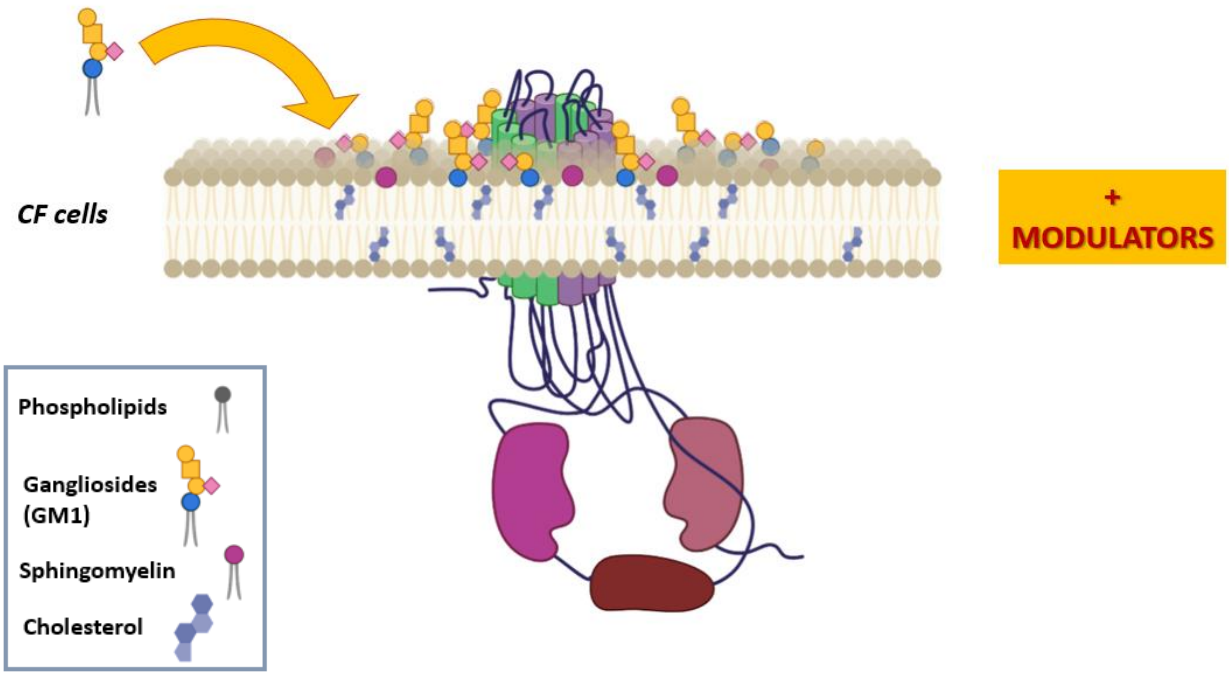

Figure 50. Image illustrating how the introduction of ganglioside GM1/cholesterol to the plasma membrane of bronchial epithelial cells carrying the F508del mutation can improve PM stability of mutated CFTR in the presence of CFTR modulators. Image from [137].

BIBLIOGRAPHY

1. O'Sullivan BP, Freedman SD. Cystic fibrosis. Lancet 2009;373:1891-904.
2. Billet, A., Jia, Y., Jensen, T., Riordan, J.R. and Hanrahan, J.W. Regulation of the cystic fibrosis transmembrane conductance regulator anion channel by tyrosine phosphorylation. FASEB J. 2015, 29, 3945-53.
3. Elborn JS, Prescott RJ, Stack BH, et al. Elective versus symptomatic antibiotic treatment in cystic fibrosis patients with chronic Pseudomonas infection of the lungs. Thorax 2000;55:355-8.
4. Tsui LC, Dorfman R. The cystic fibrosis gene: a molecular genetic perspective. Cold Spring Harbor perspectives in medicine 2013;3:a009472.
5. Zielenski J, Tsui LC. Cystic fibrosis: genotypic and phenotypic variations. Annu Rev Genet. 1995;29:777-807.
6. Ellsworth RE, Jamison DC, Touchman JW, et al. Comparative genomic sequence analysis of the human and mouse cystic fibrosis transmembrane conductance regulator genes. Proceedings of the National Academy of Sciences of the United States of America 2000;97:1172-7.
7. Rommens JM, Iannuzzi MC, Kerem B, et al. Identification of the cystic fibrosis gene: Chromosome walking and jumping. Science. 1989a. 245: 1059–1065
8. Xie J, Drumm ML, Ma J, Davis PB. Intracellular loop between transmembrane segments IV and V of cystic fibrosis transmembrane conductance regulator is involved in regulation of chloride channel conductance state. J Biol Chem. 1995 270: 28084–28091
9. Trezise AE, Chambers JA, Wardle CJ, Gould S, Harris A. Expression of the cystic fibrosis gene in human foetal tissues. Human molecular genetics 1993;2:213-8.
10. Stoltz DA, Meyerholz DK, Welsh MJ. Origins of cystic fibrosis lung disease. The New England journal of medicine 2015;372:351-62.
11. McCarthy VA, Harris A. The CFTR gene and regulation of its expression. Pediatric pulmonology 2005;40:1-8.
12. Tizzano EF, Buchwald M. CFTR expression and organ damage in cystic fibrosis. Annals of internal medicine. 1995;123:305-8.
13. Gillen AE, Harris A. Transcriptional regulation of CFTR gene expression. Front Biosci (Elite Ed). 2012;4:587-92.
14. Yoshimura K, Nakamura H, Trapnell BC, et al. The cystic fibrosis gene has a "housekeeping"-type promoter and is expressed at low levels in cells of epithelial origin. The Journal of biological chemistry. 1991;266:9140-4.
15. Higgins CF. ABC transporters: from microorganisms to man. Annu Rev Cell Biol. 1992;8:67-113.
16. Dean M, Allikmets R. Complete characterization of the human ABC gene family. Journal of bioenergetics and biomembranes. 2001;33:475-9.
17. Hunt JF, Wang C, Ford RC. Cystic fibrosis transmembrane conductance regulator (ABCC7) structure. Cold Spring Harbor perspectives in medicine. 2013;3:a009514.
18. Moran O. On the structural organization of the intracellular domains of CFTR. The international journal of biochemistry & cell biology. 2014;52:7-14.
19. Farinha CM, Canato S. From the endoplasmic reticulum to the plasma membrane: mechanisms of CFTR folding and trafficking. Cell Mol Life Sci. 2017 Jan;74(1):39-55
20. Nagel G. Differential function of the two nucleotide binding domains on cystic fibrosis transmembrane conductance regulator. Biochim Biophys Acta. 1999 Dec 6;1461(2):263-74.
21. Anderson MP, Sheppard DN, Berger HA, Welsh MJ. Chloride channels in the apical membrane of normal and cystic fibrosis airway and intestinal epithelia. The American journal of physiology 1992;263:L1-14.

22. Choi JY, Lee MG, Ko S, Muallem S. Cl(-)-dependent HCO3- transport by cystic fibrosis transmembrane conductance regulator. JOP : Journal of the pancreas 2001;2:243-6.
23. Choi JY, Muallem D, Kiselyov K, Lee MG, Thomas PJ, Muallem S. Aberrant CFTR-dependent HCO3- transport in mutations associated with cystic fibrosis. Nature 2001;410:94-7.
24. Cant N, Pollock N, Ford RC. CFTR structure and cystic fibrosis. The international journal of biochemistry & cell biology 2014;52:15-25.
25. Higgins CF, Linton KJ. The ATP switch model for ABC transporters. Nat Struct Mol Biol. 2004 Oct;11(10):918-26.
26. Riordan JR, Rommens JM, Kerem B, et al. Identification of the cystic fibrosis gene: cloning and characterization of complementary DNA. Science. 1989 Sep 8;245(4922):1066-73. Erratum in: Science 1989 Sep 29;245(4925):1437.
27. Jia Y, Mathews CJ, Hanrahan JW. Phosphorylation by protein kinase C is required for acute activation of cystic fibrosis transmembrane conductance regulator by protein kinase A. J Biol Chem. 1997 Feb 21;272(8):4978-84
28. Vaandrager AB, Tilly BC, Smolenski A, et al. cGMP stimulation of cystic fibrosis transmembrane conductance regulator Cl- channels co-expressed with cGMP-dependent protein kinase type II but not type Ibeta. J Biol Chem. 1997 Feb 14;272(7):4195-200.
29. Bozoky Z, Ahmadi S, Milman T, et al. Synergy of cAMP and calcium signaling pathways in CFTR regulation. Proceedings of the National Academy of Sciences of the United States of America 2017;114:E2086-E95.
30. Callebaut I, Chong PA, Forman-Kay JD. CFTR structure. Journal of cystic fibrosis : official journal of the European Cystic Fibrosis Society 2018;17:S5-S8.
31. Bozoky Z, Krzeminski M, Muhandiram R, et al. Regulatory R region of the CFTR chloride channel is a dynamic integrator of phospho-dependent intra- and intermolecular interactions. Proc Natl Acad Sci U S A. 2013 Nov 19;110(47):E4427-36.
32. Pranke IM, Sermet-Gaudelus I. Biosynthesis of cystic fibrosis transmembrane conductance regulator. The international journal of biochemistry & cell biology. 2014;52:26-38.
33. Kleizen B, van Vlijmen T, de Jonge HR, Braakman I. Folding of CFTR is predominantly cotranslational. Mol Cell. 2005 Oct 28;20(2):277-87.
34. Gentzsch M, Chang XB, Cui L, et al Endocytic trafficking routes of wild type and DeltaF508 cystic fibrosis transmembrane conductance regulator. Mol Biol Cell. 2004 Jun;15(6):2684-96. Epub 2004 Apr 9.
35. Okiyoneda T, Lukacs GL. Cell surface dynamics of CFTR: the ins and outs. Biochim Biophys Acta. 2007 Apr;1773(4):476-9. Epub 2007 Jan 19.
36. Csanády L, Chan KW, Nairn AC, Gadsby DC. Functional roles of nonconserved structural segments in CFTR's NH2-terminal nucleotide binding domain. J Gen Physiol. 2005 Jan;125(1):43-55. Epub 2004 Dec 13.
37. Dulhanty AM, Riordan JR. A two-domain model for the R domain of the cystic fibrosis transmembrane conductance regulator based on sequence similarities. FEBS Lett. 1994 Apr 25;343(2):109-14.
38. Farinha CM, Miller E, McCarty N. Protein and lipid interactions - Modulating CFTR trafficking and rescue. Journal of cystic fibrosis : official journal of the European Cystic Fibrosis Society 2018;17:S9-S13.
39. Farinha CM, Matos P. Rab GTPases regulate the trafficking of channels and transporters - a focus on cystic fibrosis. Small GTPases 2018;9:136-44.
40. Lobo MJ, Amaral MD, Zaccolo M, Farinha CM. EPAC1 activation by cAMP stabilizes CFTR at the membrane by promoting its interaction with NHERF1. J Cell Sci. 2016; 129: 2599-2612.

41. Aureli M, Schiumarini D, Loberto N, et al. Unravelling the role of sphingolipids in cystic fibrosis lung disease, Chem. Phys. Lipids, 2016; 200, 94–103.
42. Itokazu Y, Pagano RE, Schroeder AS, et al. Reduced GM1 ganglioside in CFTR-deficient human airway cells results in decreased beta1-integrin signaling and delayed wound repair. American journal of physiology Cell physiology 2014;306:C819-30.
43. Mancini G, Loberto N, Olioso D, et al . GM1 as Adjuvant of Innovative Therapies for Cystic Fibrosis Disease, Int J Mol Sci, 2020, Jun 24;21(12):4486.
44. Abu-Arish A, Pandžić E, Kim D, et al. Agonists that stimulate secretion promote the recruitment of CFTR into membrane lipid microdomains. J Gen Physiol. 2019 Jun 3;151(6):834-849.
45. Abu-Arish A, Pandzic E, Goepp J, et al. Cholesterol modulates CFTR confinement in the plasma membrane of primary epithelial cells. Biophys J 2015;109:85-94.
46. Cui G, Cottrill KA, Strickland KM, Mashburn SA, Koval M, McCarty NA. Alteration of Membrane Cholesterol Content Plays a Key Role in Regulation of Cystic Fibrosis Transmembrane Conductance Regulator Channel Activity. Front Physiol. 2021 Jun 7;12:652513.
47. Cystic fibrosis statistics. Cystic Fibrosis News Today. Accessed January 9, 2024.
48. Guo J, Garratt A, Hill A. Worldwide rates of diagnosis and effective treatment for cystic fibrosis. J Cyst Fibros. 2022 May;21(3):456-462.
49. Scotet V, L'Hostis C, Férec C. The Changing Epidemiology of Cystic Fibrosis: Incidence, Survival and Impact of the CFTR Gene Discovery. Genes (Basel). 2020 May 26;11(6):589.
50. Cystic fibrosis: frequency. MedlinePlus. Updated July 6, 2021. Accessed January 9, 2024.
51. De Boeck K, Wilschanski M, Castellani C, et al. Cystic fibrosis: terminology and diagnostic algorithms. Thorax 2006;61:627-35.
52. De Boeck, K. Cystic fibrosis in the year 2020: A disease with a new face. Acta Paediatr. 2020; 109, 893-899.
53. Veit G, Avramescu RG, Chiang AN, , et al. From CFTR biology toward combinatorial pharmacotherapy: expanded classification of cystic fibrosis mutations. Molecular biology of the cell 2016;27:424-33.
54. Fanen P, Wohlhuter-Haddad A, Hinzpeter A. Genetics of cystic fibrosis: CFTR mutation classifications toward genotype-based CF therapies. The international journal of biochemistry & cell biology. 2014;52:94-102.
55. Haardt M, Benharouga M, Lechardeur D, Kartner N, Lukacs GL. C-terminal truncations destabilize the cystic fibrosis transmembrane conductance regulator without impairing its biogenesis. A novel class of mutation. The Journal of biological chemistry 1999;274:21873-7
56. Silvis MR, Picciano JA, Bertrand C, Weixel K, Bridges RJ, Bradbury NA. A mutation in the cystic fibrosis transmembrane conductance regulator generates a novel internalization sequence and enhances endocytic rates. The Journal of biological chemistry 2003;278:11554-60.
57. De Boeck K, Amaral MD. Progress in therapies for cystic fibrosis. Lancet Respir Med. 2016 Aug;4(8):662-67. Epub 2016 Apr 1.
58. Chen Q, Shen Y, Zheng J. A review of cystic fibrosis: Basic and clinical aspects. Animal Model Exp Med. 2021 Sep 16;4(3):220-232.
59. Boat TF. The future of pediatric research. The Journal of pediatrics 2007;151:S21-7
60. Cutting GR. Cystic fibrosis genetics: from molecular understanding to clinical application. Nat Rev Genet. 2015 Jan;16(1):45-56. Epub 2014 Nov 18.
61. Cantin AM, Hartl D, Konstan MW, Chmiel JF. Inflammation in cystic fibrosis lung disease: Pathogenesi137333333333s and therapy. Journal of cystic fibrosis: official journal of the European Cystic Fibrosis Society 2015;14:419-30.

62. Chmiel JF, Berger M, Konstan MW. The role of inflammation in the pathophysiology of CF lung disease. Clin Rev Allergy Immunol. 2002;23(1):5-27.
63. Becker KA, Riethmuller J, Luth A, Doring G, Kleuser B, Gulbins E. Acid sphingomyelinase inhibitors normalize pulmonary ceramide and inflammation in cystic fibrosis. Am J Respir Cell Mol Biol 2010;42:716-24.
64. Boucher RC. Cystic fibrosis: a disease of vulnerability to airway surface dehydration. Trends in molecular medicine 2007;13:231-40.
65. Perez-Vilar J, Boucher RC. Reevaluating gel-forming mucins' roles in cystic fibrosis lung disease. Free radical biology & medicine 2004;37:1564-77.
66. Perez-Vilar J, Randell SH, Boucher RC. C-Mannosylation of MUC5AC and MUC5B Cys subdomains. Glycobiology 2004;14:325-37.
67. Nichols DP, Chmiel JF. Inflammation and its genesis in cystic fibrosis. Pediatric pulmonology 2015;50 Suppl 40:S39-56.
68. Hoegger MJ, Fischer AJ, McMenimen JD, et al. Impaired mucus detachment disrupts mucociliary transport in a piglet model of cystic fibrosis. Science 2014;345:818-22.
69. Coakley RD, Grubb BR, Paradiso AM, et al. Abnormal surface liquid pH regulation by cultured cystic fibrosis bronchial epithelium. Proceedings of the National Academy of Sciences of the United States of America 2003;100:16083-8.
70. Song Y, Salinas D, Nielson DW, Verkman AS. Hyperacidity of secreted fluid from submucosal glands in early cystic fibrosis. Am J Physiol Cell Physiol. 2006 Mar;290(3):C741-9.
71. Welsh MJ, Smith JJ. cAMP stimulation of HCO3- secretion across airway epithelia. JOP : Journal of the pancreas 2001;2:291-3.
72. Poulsen JH, Fischer H, Illek B, Machen TE. Bicarbonate conductance and pH regulatory capability of cystic fibrosis transmembrane conductance regulator. Proceedings of the National Academy of Sciences of the United States of America 1994;91:5340-4.
73. De Lisle RC. Pass the bicarb: the importance of HCO3- for mucin release. The Journal of clinical investigation 2009;119:2535-7.
74. Boucher RC. An overview of the pathogenesis of cystic fibrosis lung disease. Advanced drug delivery reviews 2002;54:1359-71
75. Becker KA, Riethmüller J, Zhang Y, Gulbins E. The role of sphingolipids and ceramide in pulmonary in cystic fibrosis. Open Respir Med J. 2010 Mar 30;4:39-47.
76. Grassmé H, Jendrossek V, Riehle A, et al. Host defense against Pseudomonas aeruginosa requires ceramide-rich membrane rafts. Nat Med. 2003 Mar;9(3):322-30.
77. Kumar S, Tana A, Shankar A. Cystic fibrosis--what are the prospects for a cure? Eur J Intern Med. 2014 Nov;25(9):803-7.
78. National Herat, Lung and Blood Institute. Cystic Fibrosis. Treatment. Last updated on November 21, 2023. Acessed January 12, 2024.
79. Esposito C, Kamper M, Trentacoste J, Galvin S, Pfister H, Wang J. Advances in the Cystic Fibrosis Drug Development Pipeline. Life (Basel). 2023 Aug 30;13(9):1835.
80. Mogayzel PJ, Naureckas ET, Robinson KA, et al. Cystic Fibrosis Pulmonary Guidelines Chronic Medications for Maintenance of Lung Health. Am J Resp Crit Care 2013;187:680-9.
81. Hector A, Kirn T, Ralhan A, Graepler-Mainka U, et al. Microbial colonization and lung function in adolescents with cystic fibrosis. J Cyst Fibros. 2016 May;15(3):340-9.
82. Konstan MW, Wagener JS, et al. Scientific Advisory Group and Investigators and Coordinators of Epidemiologic Study of Cystic Fibrosis. Clinical use of dornase alpha is associated with a slower rate of FEV1 decline in cystic fibrosis. Pediatr Pulmonol. 2011 Jun;46(6):545-53.

83. Bilton D, Daviskas E, Anderson SD, et al. B301 Investigators. Phase 3 randomized study of the efficacy and safety of inhaled dry powder mannitol for the symptomatic treatment of non-cystic fibrosis bronchiectasis. Chest. 2013 Jul;144(1):215-225.
84. De Boeck K, Amaral MD. Progress in therapies for cystic fibrosis. Lancet Respir Med. 2016 Aug;4(8):662-674. Epub 2016 Apr 1.
85. Lands LC, Stanojevic S. Oral non-steroidal anti-inflammatory drug therapy for lung disease in cystic fibrosis. The Cochrane database of systematic reviews 2016;4:CD001505.
86. Balfour-Lynn IM, Welch K. Inhaled corticosteroids for cystic fibrosis. The Cochrane database of systematic reviews 2014:CD001915.
87. Hraiech S, Brégeon F, Rolain JM. Bacteriophage-based therapy in cystic fibrosis-associated Pseudomonas aeruginosa infections: rationale and current status. Drug Des Devel Ther. 2015 Jul 16;9:3653-63.
88. Cafora M, Brix A, Forti F, Briani F, Pistocchi A. Studying Bacteriophage Efficacy Using a Zebrafish Model. Methods Mol Biol. 2024;2734:151-169.
89. Suh GA, Lodise TP, Tamma PD, Knisely JM, et al. Antibacterial Resistance Leadership Group. Considerations for the Use of Phage Therapy in Clinical Practice. Antimicrob Agents Chemother. 2022 Mar 15;66(3):e0207121.
90. Martínez-Gallardo MJ, Villicaña C, Yocupicio-Monroy M, Alcaraz-Estrada SL, León-Félix J. Current knowledge in the use of bacteriophages to combat infections caused by Pseudomonas aeruginosa in cystic fibrosis. Folia Microbiol (Praha). 2023 Feb;68(1):1-16. Huang W, Smith
91. AT, Korotun M, Iacono A, Wang J. Lung Transplantation in a New Era in the Field of Cystic Fibrosis. Life (Basel). 2023 Jul 21;13(7):1600.
92. Sellers ZM. Pancreatic complications in children with cystic fibrosis. Curr Opin Pediatr. 2020 Oct;32(5):661-667.
93. Freswick PN, Reid EK, Mascarenhas MR. Pancreatic Enzyme Replacement Therapy in Cystic Fibrosis. Nutrients. 2022 Mar 23;14(7):1341
94. Dana J, Debray D, Beaufrère A, Hillaire S, et al. Cystic fibrosis-related liver disease: Clinical presentations, diagnostic and monitoring approaches in the era of CFTR modulator therapies. J Hepatol. 2022 Feb;76(2):420-434.
95. Costaguta G, Patey N, Álvarez F. Cystic fibrosis liver disease in children - A review of our current understanding. Arch Argent Pediatr. 2023 Aug 1;121(4):e202202905. Epub 2023 Mar.
96. Cystic Fibrosis Foundation. Available online: https://www.cff.org/press-releases/2019-10/cystic-fibrosis-foundation-launches-500-million-path-cure (accessed on 13 January 2024).
97. Alton E, Armstrong DK, Ashby D, et al. Repeated nebulisation of non-viral CFTR gene therapy in patients with cystic fibrosis: a randomised, double-blind, placebo-controlled, phase 2b trial. The Lancet Respiratory medicine 2015;3:684-91.
98. Crawford DK, Mullenders J, Pott J, Boj SF, Landskroner-Eiger S, Goddeeris MM. Targeting G542X CFTR nonsense alleles with ELX-02 restores CFTR function in human-derived intestinal organoids. J Cyst Fibros. 2021 May;20(3):436-442.
99. ClinicalTrials.gov. Available online: https://clinicaltrials.gov/ct2/show/NCT04135495 (13 January 2024).
100. Rowe SM, Zuckerman JB, Dorgan D, Lascano J, et atl. Inhaled mRNA therapy for treatment of cystic fibrosis: Interim results of a randomized, double-blind, placebo-controlled phase 1/2 clinical study. J Cyst Fibros. 2023 Jul;22(4):656-664. Epub 2023 Apr 29.
101. Maule G, Arosio D, Cereseto A. Gene Therapy for Cystic Fibrosis: Progress and Challenges of Genome Editing. Int J Mol Sci. 2020 May 30;21(11):3903.

102. König J, Schreiber R, Voelcker T, Mall M, Kunzelmann K. The cystic fibrosis transmembrane conductance regulator (CFTR) inhibits ENaC through an increase in the intracellular Cl- concentration. EMBO Rep. 2001 Nov;2(11):1047-51.
103. Hirsh AJ, Zhang J, Zamurs A, et al. Pharmacological properties of N-(3,5-diamino-6-chloropyrazine-2-carbonyl)-N'-4-[4-(2,3-dihydroxypropoxy)phenyl]butyl-guanidine ethanesulfonate (552-02), a novel epithelial sodium channel blocker with potential clinical efficacy for cystic fibrosis lung disease. J Pharmacol Exp Ther. 2008 Apr;325(1):77-88.
104. Tagalakis AD, Munye MM, Ivanova R, et al. Effective silencing of ENaC by siRNA delivered with epithelial-targeted nanocomplexes in human cystic fibrosis cells and in mouse lung. Thorax 2018, 73, 847–856
105. Galietta LJV. TMEM16A (ANO1) as a therapeutic target in cystic fibrosis. Curr Opin Pharmacol. 2022 Jun;64:102206. Epub 2022 Mar 29.
106. Pinto MC, Quaresma MC, Silva IAL, et al. Synergy in Cystic Fibrosis Therapies: Targeting SLC26A9. Int J Mol Sci. 2021 Dec 2;22(23):13064.
107. Clancy JP, Cotton CU, Donaldson SH, et al. CFTR modulator theratyping: Current status, gaps and future directions. J Cyst Fibros. 2019 Jan;18(1):22-34.
108. Drug Approval Package: Kalydeco (ivacaftor)". U.S. Food and Drug Administration (FDA). 13 March 2012.
109. Eckford PD, Li C, Ramjeesingh M, Bear CE. Cystic fibrosis transmembrane conductance regulator (CFTR) potentiator VX-770 (ivacaftor) opens the defective channel gate of mutant CFTR in a phosphorylation-dependent but ATP-independent manner. J Biol Chem. 2012 Oct 26;287(44):36639-49.
110. Ramsey BW, Davies J, McElvaney NG, et al. A CFTR potentiator in patients with cystic fibrosis and the G551D mutation. The New England journal of medicine 2011;365:1663-72.
111. Yu H, Burton B, Huang CJ, et al. Ivacaftor potentiation of multiple CFTR channels with gating mutations. Journal of cystic fibrosis : official journal of the European Cystic Fibrosis Society 2012;11:237-45.
112. De Boeck K, Munck A, Walker S, et al. Efficacy and safety of ivacaftor in patients with cystic fibrosis and a non-G551D gating mutation. J Cyst Fibros. 2014 Dec;13(6):674-80.
113. Cystic Fibrosis Foundation. Available online: https://www.cff.org/managing-cf/cftr-modulator-therapies (accessed on 13 January 2024).
114. Du K, Sharma M, Lukacs GL. The DeltaF508 cystic fibrosis mutation impairs domain-domain interactions and arrests post-translational folding of CFTR. Nature structural & molecular biology 2005;12:17-25.
115. Fiedorczuk K, Chen J. Mechanism of CFTR correction by type I folding correctors. Cell. 2022 Jan 6;185(1):158-168.e11.
116. Ren HY, Grove DE, De La Rosa O, et al. VX-809 corrects folding defects in cystic fibrosis transmembrane conductance regulator protein through action on membrane-spanning domain 1. Mol Biol Cell. 2013 Oct;24(19):3016-24.
117. Jones AM, Barry PJ. Lumacaftor/ivacaftor for patients homozygous for Phe508del-CFTR: should we curb our enthusiasm? Thorax. 2015 Jul;70(7):615-6.
118. Wainwright CE, Elborn JS, Ramsey BW, et al.; TRAFFIC Study Group; TRANSPORT Study Group. Lumacaftor-Ivacaftor in Patients with Cystic Fibrosis Homozygous for Phe508del CFTR. N Engl J Med. 2015 Jul 16;373(3):220-31.
119. Konstan MW, McKone EF, Moss RB, et al. Assessment of safety and efficacy of long-term treatment with combination lumacaftor and ivacaftor therapy in patients with cystic fibrosis homozygous for the F508del-CFTR mutation (PROGRESS): a phase 3, extension study. Lancet Respir Med. 2017 Feb;5(2):107-118.

120. Connett GJ. Lumacaftor-ivacaftor in the treatment of cystic fibrosis: design, development and place in therapy. Drug Des Devel Ther. 2019 Jul 19;13:2405-2412.
121. Cholon DM, Quinney NL, Fulcher ML, et al. Potentiator ivacaftor abrogates pharmacological correction of ΔF508 CFTR in cystic fibrosis. Sci Transl Med. 2014 Jul 23;6(246):246ra96.
122. Veit G, Avramescu RG, Perdomo D, et al. Some gating potentiators, including VX-770, diminish ΔF508-CFTR functional expression. Sci Transl Med. 2014 Jul 23;6(246):246ra97.
123. Chin S, Hung M, Won A, et al. Lipophilicity of the Cystic Fibrosis drug, Ivacaftor, and its destabilizing effect on the major CF-causing mutation: F508del. Molecular pharmacology 2018.
124. Tezacaftor/ivacaftor for cystic fibrosis. Aust Prescr. 2019 Oct;42(5):174-175. Epub 2019 Sep.
125. Southern KW, Murphy J, Sinha IP, Nevitt SJ. Corrector therapies (with or without potentiators) for people with cystic fibrosis with class II CFTR gene variants (most commonly F508del). Cochrane Database Syst Rev. 2020 Dec 17;12(12):CD010966. Update in: Cochrane Database Syst Rev. 2023 Nov 20;11:CD010966.
126. Taylor-Cousar JL, Munck A, McKone EF, et al. Tezacaftor-Ivacaftor in Patients with Cystic Fibrosis Homozygous for Phe508del. N Engl J Med. 2017 Nov 23;377(21):2013-2023.
127. Veit G, Roldan A, Hancock MA, et al. Allosteric folding correction of F508del and rare CFTR mutants by elexacaftor-tezacaftor-ivacaftor (Trikafta) combination. JCI Insight. 2020 Sep 17;5(18):e139983
128. Capurro V, Tomati V, Sondo E, Pedemonte N, et al. Partial Rescue of F508del-CFTR Stability and Trafficking Defects by Double Corrector Treatment. Int J Mol Sci. 2021 May 17;22(10):5262.
129. Fiedorczuk K, Chen J. Molecular structures reveal synergistic rescue of Δ508 CFTR by Trikafta modulators. Science. 2022 Oct 21;378(6617):284-290.
130. Bongiorno R, Ludovico A, Moran O, Baroni D. Elexacaftor Mediates the Rescue of F508del CFTR Functional Expression Interacting with MSD2. Int J Mol Sci. 2023 Aug 16;24(16):12838.
131. Laselva O, Bartlett C, Gunawardena TNA, et al. Rescue of multiple class II CFTR mutations by elexacaftor+tezacaftor+ivacaftor mediated in part by the dual activities of elexacaftor as both corrector and potentiator. Eur Respir J. 2021 Jun 17;57(6):2002774.
132. Veit G, Vaccarin C, Lukacs GL. Elexacaftor co-potentiates the activity of F508del and gating mutants of CFTR. J Cyst Fibros. 2021 Sep;20(5):895-898.
133. Keating D, Marigowda G, Burr L, et al; VX16-445-001 Study Group. VX-445-Tezacaftor-Ivacaftor in Patients with Cystic Fibrosis and One or Two Phe508del Alleles. N Engl J Med. 2018 Oct 25;379(17):1612-1620.
134. Ridley K, Condren M. Elexacaftor-Tezacaftor-Ivacaftor: The First Triple-Combination Cystic Fibrosis Transmembrane Conductance Regulator Modulating Therapy. J Pediatr Pharmacol Ther. 2020;25(3):192-197.
135. Middleton PG, Mall MA, Dřevínek P, et al; VX17-445-102 Study Group. Elexacaftor-Tezacaftor-Ivacaftor for Cystic Fibrosis with a Single Phe508del Allele. N Engl J Med. 2019 Nov 7;381(19):1809-1819. Epub 2019 Oct 31.
136. Cystic Fibrosis Foundation. Patient Registry 2021 Annual Data Report; Cystic Fibrosis Foundation: Bethesda, MD, USA, 2021.
137. Dobi D, Loberto N, Bassi R, et al. Cross-talk between CFTR and sphingolipids in cystic fibrosis. FEBS Open Bio. 2023 Sep;13(9):1601-1614.
138. Degroote S, Wolthoorn J, van Meer G. The cell biology of glycosphingolipids. Seminars in cell & developmental biology 2004;15:375-87.
139. Futerman AH, Hannun YA. The complex life of simple sphingolipids. EMBO Rep 2004;5:777-82.

140. Hakomori S. Bifunctional role of glycosphingolipids. Modulators for transmembrane signaling and mediators for cellular interactions. The Journal of biological chemistry 1990;265:18713-6.
141. Huwiler A, Kolter T, Pfeilschifter J, Sandhoff K. Physiology and pathophysiology of sphingolipid metabolism and signaling. Biochimica et biophysica acta 2000;1485:63-99.
142. Sonnino S, Prinetti A, Mauri L, Chigorno V, Tettamanti G. Dynamic and structural properties of sphingolipids as driving forces for the formation of membrane domains. Chem. Rev. 2006;106, 2111–2125.
143. Carter HE, Glick FJ, Norris WP, Phillips GE. Biochemisrty of sphingolipides. III. Structure of sphingosine. J Biol Chem 1947;170: 285-94.
144. Merrill AH Jr. Sphingolipid and glycosphingolipid metabolic pathways in the era of sphingolipidomics. Chem Rev 2011;111:6387-422.
145. SVENNERHOLM L. THE GANGLIOSIDES. J Lipid Res. 1964 Apr;5:145-55.
146. Hakomori S. Glycosphingolipids in cellular interaction, differentiation, and oncogenesis. Annu. Rev. Biochem. 1981;50, 733–764.
147. Suchański J, Ugorski M. The biological role of sulfatides. Postepy Hig. Med. Dosw. (Online)2016; 70, 489–504.
148. Aureli M, Mauri L, Carsana EV, Dobi D, Breviario S, Lunghi G, Sonnino S. Gangliosides and Cell Surface Ganglioside Metabolic Enzymes in the Nervous System. Adv Neurobiol. 2023;29:305-332.
149. Merrill AH, Jr. De novo sphingolipid biosynthesis: a necessary, but dangerous, pathway. The Journal of biological chemistry 2002;277:25843-6.
150. Kolter T, Proia RL, Sandhoff K. Combinatorial ganglioside biosynthesis. The Journal of biological chemistry 2002;277:25859-62.
151. van Meer G, Lisman Q. Sphingolipid transport: rafts and translocators. The Journal of biological chemistry 2002;277:25855-8.
152. Stoffel W. Studies on the biosynthesis and degradation of sphingosine bases. Chem Phys Lipids. 1970 Oct;5(1):139-58.
153. Nagiec MM, Baltisberger JA, Wells GB, Lester RL, Dickson RC. The LCB2 gene of Saccharomyces and the related LCB1 gene encode subunits of serine palmitoyltransferase, the initial enzyme in sphingolipid synthesis. Proceedings of the National Academy of Sciences of the United States of America 1994;91:7899-902.
154. Sribney M. Enzymatic synthesis of ceramide. Biochim Biophys Acta. 1966 Dec 7;125(3):542-7.
155. Rother J, van Echten G, Schwarzmann G, Sandhoff K. Biosynthesis of sphingolipids: dihydroceramide and not sphinganine is desaturated by cultured cells. Biochem Biophys Res Commun 1992;189:14-20.
156. Geeraert L, Mannaerts GP, van Veldhoven PP. Conversion of dihydroceramide into ceramide: involvement of a desaturase. Biochem J 1997;327 (Pt 1):125-32.
157. Merrill AH, Jr., van Echten G, Wang E, Sandhoff K. Fumonisin B1 inhibits sphingosine (sphinganine) N-acyltransferase and de novo sphingolipid biosynthesis in cultured neurons in situ. The Journal of biological chemistry 1993;268:27299-306.
158. Merrill AH Jr, Wang E. Biosynthesis of long-chain (sphingoid) bases from serine by LM cells. Evidence for introduction of the 4-trans-double bond after de novo biosynthesis of N-acylsphinganine(s). J Biol Chem. 1986 Mar 15;261(8):3764-9. PMID: 3081509.
159. Tettamanti G, Bassi R, Viani P, Riboni L. Salvage pathways in glycosphingolipid metabolism. Biochimie. 2003 Mar-Apr;85(3-4):423-37.
160. Merrill AH, Jr., Jones DD. An update of the enzymology and regulation of sphingomyelin metabolism. Biochimica et biophysica acta 1990;1044:1-12.

161. Futerman AH, Stieger B, Hubbard AL, Pagano RE. Sphingomyelin synthesis in rat liver occurs predominantly at the cis and medial cisternae of the Golgi apparatus. The Journal of biological chemistry 1990;265:8650-7.
162. Prinetti A, Loberto N, Chigorno V, Sonnino S. Glycosphingolipid behaviour in complex membranes. Biochimica et biophysica acta 2009;1788:184-93.
163. Jeckel D, Karrenbauer A, Burger KN, van Meer G, Wieland F. Glucosylceramide is synthesized at the cytosolic surface of various Golgi subfractions. J Cell Biol 1992;117:259-67.
164. Warnock DE, Lutz MS, Blackburn WA, Young WW Jr, Baenziger JU. Transport of newly synthesized glucosylceramide to the plasma membrane by a non-Golgi pathway. Proc Natl Acad Sci U S A. 1994 Mar 29;91(7):2708-12.
165. Lannert H, Gorgas K, Meissner I, et al. Functional organization of the Golgi apparatus in glycosphingolipid biosynthesis. Lactosylceramide and subsequent glycosphingolipids are formed in the lumen of the late Golgi. J Biol Chem. 1998 Jan 30;273(5):2939-46.
166. Sundberg EL, Deng Y, Burd CG. Monitoring Sphingolipid Trafficking in Cells using Fluorescence Microscopy. Curr Protoc Cell Biol. 2019 Mar;82(1):e67.
167. Gault CR, Obeid LM, Hannun YA. An overview of sphingolipid metabolism: from synthesis to breakdown. Advances in experimental medicine and biology 2010;688:1-23.
168. Carter HE, Rothfus,J. A., Gigg, R. Biochemistry of the sphingolipids: XII. conversion of cerebrosides to ceramides and sphingosine; structure of Gaucher cerebroside. J Lipid Res 1961;2:228-34.
169. Bartke N, Hannun YA. Bioactive sphingolipids: metabolism and function. J Lipid Res 2009;50 Suppl:S91-6.
170. Kytzia HJ, Sandhoff K. Evidence for two different active sites on human beta-hexosaminidase A. Interaction of GM2 activator protein with beta-hexosaminidase A. The Journal of biological chemistry 1985;260:7568-72.
171. Fingerhut R, van der Horst GT, Verheijen FW, Conzelmann E. Degradation of gangliosides by the lysosomal sialidase requires an activator protein. Eur J Biochem 1992;208:623-9.
172. Zschoche A, Furst W, Schwarzmann G, Sanhoff K. Hydrolysis of lactosylceramide by human galactosylceramidase and GM1-beta-galactosidase in a detergent-free system and its stimulation by sphingolipid activator proteins, sap-B and sap-C. Activator proteins stimulate lactosylceramide hydrolysis. Eur J Biochem 1994;222:83-90.
173. Aureli M, Masilamani AP, Illuzzi G, et al. Activity of plasma membrane beta-galactosidase and beta-glucosidase. FEBS Lett. 2009 Aug 6;583(15):2469-73.
174. Spence MW. Sphingomyelinases. Adv Lipid Res 1993;26:3-23.
175. van Meer G, Voelker DR, Feigenson GW. Membrane lipids: where they are and how they behave. Nat Rev Mol Cell Biol 2008;9:112-24.
176. Aureli M, Loberto N, Bassi R, Ferraretto A, Perego S, Lanteri P, et al. Plasma membrane-associated glycohydrolases activation by extracellular acidification due to proton exchangers. Neurochem Res 2011;37:1296-307.
177. Mencarelli S, Cavalieri C, Magini A, et al. Identification of plasma membrane associated mature beta-hexosaminidase A, active towards GM2 ganglioside, in human fibroblasts. FEBS Lett. 2005 Oct 24;579(25):5501-6.
178. Miyagi T, Wada T, Yamaguchi K, Hata K, Shiozaki K. Plasma membrane-associated sialidase as a crucial regulator of transmembrane signalling. J Biochem. 2008 Sep;144(3):279-85.
179. Boot RG, Verhoek M, Donker-Koopman W, et al. Identification of the non-lysosomal glucosylceramidase as β-glucosidase 2. The Journal of biological chemistry 2007;282:1305-12.
180. Aureli M, Loberto N, Chigorno V, Prinetti A, Sonnino S. Remodeling of sphingolipids by plasma membrane associated enzymes. Neurochem Res. 2011 Sep;36(9):1636-44.

181. Hannun YA, Obeid LM. Principles of bioactive lipid signalling: lessons from sphingolipids. Nat Rev Mol Cell Biol 2008;9:139-50.
182. Ohanian J, Ohanian V. Sphingolipids in mammalian cell signalling. Cellular and molecular life sciences : CMLS 2001;58:2053-68.
183. Giussani P, Tringali C, Riboni L, Viani P, Venerando B. Sphingolipids: key regulators of apoptosis and pivotal players in cancer drug resistance. International journal of molecular sciences 2014;15:4356-92.
184. Lahiri S, Futerman AH. The metabolism and function of sphingolipids and glycosphingolipids. Cellular and molecular life sciences : CMLS 2007;64:2270-84.
185. Sonnino S, Prinetti A. Membrane domains and the "lipid raft" concept. Curr Med Chem. 2013;20(1):4-21.
186. Simons K, Sampaio JL. Membrane organization and lipid rafts. Cold Spring Harb Perspect Biol 2011;3:a004697.
187. Grassi S, Giussani P, Mauri L, et al. Lipid rafts and neurodegeneration: structural and functional roles in physiologic aging and neurodegenerative diseases. J Lipid Res. 2020 May;61(5):636-654.
188. Thomas CM, Smart EJ. Caveolae structure and function. J Cell Mol Med. 2008 Jun;12(3):796-809.
189. Ouweneel AB, Thomas MJ, Sorci-Thomas MG. The ins and outs of lipid rafts: functions in intracellular cholesterol homeostasis, microparticles, and cell membranes: Thematic Review Series: Biology of Lipid Rafts. J Lipid Res. 2020 May;61(5):676-686.
190. Craig M, Yarrarapu SNS, Dimri M. Biochemistry, Cholesterol. 2023 Aug 8. In: StatPearls [Internet]. Treasure Island (FL): StatPearls Publishing; 2023 Jan.
191. Maxfield FR, Menon AK. Intracellular sterol transport and distribution. Curr Opin Cell Biol. 2006 Aug;18(4):379-85.
192. McMahon HT, Boucrot E. Membrane curvature at a glance. J Cell Sci. 2015 Mar 15;128(6):1065-70.
193. Arenas F, Garcia-Ruiz C, Fernandez-Checa JC. Intracellular Cholesterol Trafficking and Impact in Neurodegeneration. Front Mol Neurosci. 2017 Nov 17;10:382.
194. Goldstein JL, Anderson RG, Brown MS. Receptor-mediated endocytosis and the cellular uptake of low density lipoprotein. Ciba Found Symp. 1982;(92):77-95
195. Mesmin B, Antonny B, Drin G. Insights into the mechanisms of sterol transport between organelles. Cell Mol Life Sci. 2013 Sep;70(18):3405-21.
196. Mansson JE, Fredman P, Bigner DD, Molin K, Rosengren B, Friedman HS, et al. Characterization of new gangliosides of the lactotetraose series in murine xenografts of a human glioma cell line. FEBS Lett 1986;201:109-13.
197. Mansson JE, Mo HQ, Egge H, Svennerholm L. Trisialosyllactosylceramide (GT3) is a ganglioside of human lung. FEBS Lett 1986;196:259-62.
198. Seitz AP, Grassme H, Edwards MJ, Pewzner-Jung Y, Gulbins E. Ceramide and sphingosine in pulmonary infections. Biol Chem 2015;396:611-20.
199. Grassme H, Jekle A, Riehle A, et al. CD95 signaling via ceramide-rich membrane rafts. J Biol Chem. 2001 Jun 8;276(23):20589-96.
200. Teichgraber V, Ulrich M, Endlich N, et al. Ceramide accumulation mediates inflammation, cell death and infection susceptibility in cystic fibrosis. Nat Med 2008;14:382-91.
201. Bezzerri V, Borgatti M, Finotti A, et al. Mapping the transcriptional machinery of the IL-8 gene in human bronchial epithelial cells. J Immunol. 2011 Dec 1;187(11):6069-81.

202. Aman AT, Fraser S, Merritt EA, et al. A mutant cholera toxin B subunit that binds GM1-ganglioside but lacks immunomodulatory or toxic activity. Proc Natl Acad Sci U S A. 2001 Jul 17;98(15):8536-41.
203. Guilbault C, Wojewodka G, Saeed Z, et al. Cystic fibrosis fatty acid imbalance is linked to ceramide deficiency and corrected by fenretinide. Am J Respir Cell Mol Biol 2009;41:100-6.
204. Guilbault C, De Sanctis JB, Wojewodka G, et al. Fenretinide corrects newly found ceramide deficiency in cystic fibrosis. Am J Respir Cell Mol Biol 2008;38:47-56.
205. Vilela RM, Lands LC, Chan HM, Azadi B, Kubow S. High hydrostatic pressure enhances whey protein digestibility to generate whey peptides that improve glutathione status in CFTR-deficient lung epithelial cells. Mol Nutr Food Res 2006;50:1013-29.
206. Brodlie M, McKean MC, Johnson GE, et el. Ceramide is increased in the lower airway epithelium of people with advanced cystic fibrosis lung disease. Am J Respir Crit Care Med. 2010 Aug 1;182(3):369-75.
207. Becker KA, Riethmüller J, Seitz AP, et el. Sphingolipids as targets for inhalation treatment of cystic fibrosis. Adv Drug Deliv Rev. 2018 Aug;133:66-75.
208. Hamai H, Keyserman F, Quittell LM, Worgall TS. Defective CFTR increases synthesis and mass of sphingolipids that modulate membrane composition and lipid signaling. J Lipid Res 2009;50:1101-8.
209. Prior IA, Harding A, Yan J, Sluimer J, Parton RG, Hancock JF. GTP-dependent segregation of H-ras from lipid rafts is required for biological activity. Nature cell biology 2001;3:368-75.
210. Kowalski MP, Pier GB. Localization of cystic fibrosis transmembrane conductance regulator to lipid rafts of epithelial cells is required for Pseudomonas aeruginosa-induced cellular activation. J Immunol 2004;172:418-25.
211. Loberto N, Tebon M, Lampronti I, et al. GBA2-encoded β-glucosidase activity is involved in the inflammatory response to Pseudomonas aeruginosa. PLoS One. 2014 Aug 20;9(8):e104763.
212. Garić D, De Sanctis JB, Shah J, Dumut DC, Radzioch D. Biochemistry of very-long-chain and long-chain ceramides in cystic fibrosis and other diseases: The importance of side chain. Prog Lipid Res. 2019 Apr;74:130-144.
213. Trinh NT, Bardou O, Privé A, et al. Improvement of defective cystic fibrosis airway epithelial wound repair after CFTR rescue. Eur Respir J. 2012 Dec;40(6):1390-400.
214. Ramu Y, Xu Y, Lu Z. Inhibition of CFTR Cl- channel function caused by enzymatic hydrolysis of sphingomyelin. Proceedings of the National Academy of Sciences of the United States of America 2007;104:6448-53.
215. Rubino R, Bezzerri V, Favia M, et al A. Pseudomonas aeruginosa reduces the expression of CFTR via post-translational modification of NHERF1. Pflugers Arch. 2014 Dec;466(12):2269-78.
216. Chin S, Ramjeesingh M, Hung M, et al. Cholesterol Interaction Directly Enhances Intrinsic Activity of the Cystic Fibrosis Transmembrane Conductance Regulator (CFTR). Cells. 2019 Jul 31;8(8):804.
217. Chiricozzi E, Lunghi G, Di Biase E, et al. GM1 Ganglioside Is A Key Factor in Maintaining the Mammalian Neuronal Functions Avoiding Neurodegeneration. Int J Mol Sci. 2020 Jan 29;21(3):868.
218. Kharlamov A, Zivkovic I, Polo A, et al. LIGA20, a lyso derivative of ganglioside GM1, given orally after cortical thrombosis reduces infarct size and associated cognition deficit. Proc Natl Acad Sci U S A. 1994 Jul 5;91(14):6303-7.